

ISSN 1881-7831 Online ISSN 1881-784X

DD & T

Drug Discoveries & Therapeutics

Volume 18, Number 5
October, 2024



www.ddtjournal.com

DD & T

Drug Discoveries & Therapeutics



ISSN: 1881-7831
Online ISSN: 1881-784X
CODEN: DDTRBX
Issues/Year: 6
Language: English
Publisher: IACMHR Co., Ltd.

Drug Discoveries & Therapeutics is one of a series of peer-reviewed journals of the International Research and Cooperation Association for Bio & Socio-Sciences Advancement (IRCA-BSSA) Group. It is published bimonthly by the International Advancement Center for Medicine & Health Research Co., Ltd. (IACMHR Co., Ltd.) and supported by the IRCA-BSSA.

Drug Discoveries & Therapeutics publishes contributions in all fields of pharmaceutical and therapeutic research such as medicinal chemistry, pharmacology, pharmaceutical analysis, pharmaceuticals, pharmaceutical administration, and experimental and clinical studies of effects, mechanisms, or uses of various treatments. Studies in drug-related fields such as biology, biochemistry, physiology, microbiology, and immunology are also within the scope of this journal.

Drug Discoveries & Therapeutics publishes Original Articles, Brief Reports, Reviews, Policy Forum articles, Case Reports, Communications, Editorials, News, and Letters on all aspects of the field of pharmaceutical research. All contributions should seek to promote international collaboration in pharmaceutical science.

Editorial Board

International Field Chief Editors:

Fen-Er CHEN
Fudan University, Shanghai, China

Takashi KARAKO
National Center for Global Health and Medicine, Tokyo, Japan

Hongzhou LU
National Clinical Research Centre for Infectious Diseases, Shenzhen, Guangdong, China

Munehiro NAKATA
Tokai University, Hiratsuka, Japan

Sven SCHRÖDER
University Medical Center Hamburg Eppendorf (UKE), Hamburg, Germany

Kazuhiisa SEKIMIZU
Teikyo University, Tokyo, Japan

Corklin R. STEINHART
CAN Community Health, FL, USA

Associate Editors:

Nobuyoshi AKIMITSU
The University of Tokyo, Tokyo, Japan

Feihu CHEN
Anhui Medical University, Hefei, Anhui, China

Jianjun GAO
Qingdao University, Qingdao, Shandong, China

Hiroshi HAMAMOTO
Teikyo University, Tokyo, Japan

Chikara KAITO
Okayama University, Okayama, Japan

Gagan KAUSHAL
Jefferson College of Pharmacy, Philadelphia, PA, USA

Xiao-Kang LI
National Research Institute for Child Health and Development, Tokyo, Japan

Yasuhiko MATSUMOTO
Meiji Pharmaceutical University, Tokyo, Japan

Atsushi MIYASHITA
Teikyo University, Tokyo, Japan

Masahiro MURAKAMI
Osaka Ohtani University, Osaka, Japan

Tomofumi SANTA
The University of Tokyo, Tokyo, Japan

Tianqiang SONG
Tianjin Medical University, Tianjin, China

Sanjay K. SRIVASTAVA
Texas Tech University Health Sciences Center, Abilene, TX, USA

Hongbin SUN
China Pharmaceutical University, Nanjing, Jiangsu, China

Fengshan WANG
Shandong University, Jinan, Shandong, China.

Proofreaders:

Curtis BENTLEY
Roswell, GA, USA
Thomas R. LEBON
Los Angeles, CA, USA

Editorial and Head Office:

Pearl City Koishikawa 603,
2-4-5 Kasuga, Bunkyo-ku,
Tokyo 112-0003, Japan
E-mail: office@ddtjournal.com

Drug Discoveries & Therapeutics

Editorial and Head Office

Pearl City Koishikawa 603, 2-4-5 Kasuga, Bunkyo-ku,
Tokyo 112-0003, Japan

E-mail: office@ddtjournal.com
URL: www.ddtjournal.com

Editorial Board Members

Alex ALMASAN (Cleveland, OH)	Youcai HU (Beijing)	Sridhar MANI (Bronx, NY)	Yong XU (Guangzhou, Guangdong)
John K. BUOLAMWINI (Memphis, TN)	Yu HUANG (Hong Kong)	Tohru MIZUSHIMA (Tokyo)	Bing YAN (Ji'nan, Shandong)
Jianping CAO (Shanghai)	Zhangjian HUANG (Nanjing, Jiangsu)	Jasmin MONPARA (Philadelphia, PA)	Chunyan YAN (Guangzhou, Guangdong)
Shousong CAO (Buffalo, NY)	Amrit B. KARMARKAR (Karad, Maharashtra)	Yoshinobu NAKANISHI (Kanazawa, Ishikawa)	Xiao-Long YANG (Chongqing)
Jang-Yang CHANG (Tainan)	Toshiaki KATADA (Tokyo)	Siriporn OKONOGI (Chiang Mai)	Yun YEN (Duarte, CA)
Zhe-Sheng CHEN (Queens, NY)	Ibrahim S. KHATTAB (Kuwait)	Weisan PAN (Shenyang, Liaoning)	Yongmei YIN (Tianjin)
Zilin CHEN (Wuhan, Hubei)	Shiroh KISHIOKA (Wakayama, Wakayama)	Chan Hum PARK (Eumseong)	Yasuko YOKOTA (Tokyo)
Xiaolan CUI (Beijing)	Robert Kam-Ming KO (Hong Kong)	Rakesh P. PATEL (Mehsana, Gujarat)	Yun YOU (Beijing)
Saphala DHITAL (Clemens, SC)	Nobuyuki KOBAYASHI (Nagasaki, Nagasaki)	Shivanand P. PUTHLI (Mumbai, Maharashtra)	Rongmin YU (Guangzhou, Guangdong)
Shaofeng DUAN (Lawrence, KS)	Toshiro KONISHI (Tokyo)	Shafiqur RAHMAN (Brookings, SD)	Tao YU (Qingdao, Shandong)
Hao FANG (Ji'nan, Shandong)	Peixiang LAN (Wuhan, Hubei)	Gary K. SCHWARTZ (New York, NY)	Guangxi ZHAI (Ji'nan, Shandong)
Marcus L. FORREST (Lawrence, KS)	Chun-Guang LI (Melbourne)	Luqing SHANG (Tianjin)	Liangren ZHANG (Beijing)
Tomoko FUJIYUKI (Tokyo)	Minyong LI (Ji'nan, Shandong)	Yuemao SHEN (Ji'nan, Shandong)	Lining ZHANG (Ji'nan, Shandong)
Takeshi FUKUSHIMA (Funabashi, Chiba)	Xun LI (Ji'nan, Shandong)	Rong SHI (Shanghai)	Na ZHANG (Ji'nan, Shandong)
Harald HAMACHER (Tübingen, Baden-Württemberg)	Dongfei LIU (Nanjing, Jiangsu)	Chandan M. THOMAS (Bradenton, FL)	Ruiwen ZHANG (Houston, TX)
Kenji HAMASE (Fukuoka, Fukuoka)	Jian LIU (Hefei, Anhui)	Michihisa TOHDA (Sugitani, Toyama)	Xiu-Mei ZHANG (Ji'nan, Shandong)
Junqing HAN (Ji'nan, Shandong)	Jikai LIU (Wuhan, Hubei)	Li TONG (Xining, Qinghai)	Xuebo ZHANG (Baltimore, MD)
Xiaojiang HAO (Kunming, Yunnan)	Jing LIU (Beijing)	Murat TURKOGLU (Istanbul)	Yingjie ZHANG (Ji'nan, Shandong)
Kiyoshi HASEGAWA (Tokyo)	Xinyong LIU (Ji'nan, Shandong)	Hui WANG (Shanghai)	Yongxiang ZHANG (Beijing)
Waseem HASSAN (Rio de Janeiro)	Yuxiu LIU (Nanjing, Jiangsu)	Quanxing WANG (Shanghai)	Haibing ZHOU (Wuhan, Hubei)
Langchong HE (Xi'an, Shaanxi)	Hongxiang LOU (Jinan, Shandong)	Stephen G. WARD (Bath)	Jian-hua ZHU (Guangzhou, Guangdong)
Rodney J. Y. HO (Seattle, WA)	Hai-Bin LUO (Haikou, Hainan)	Zhun WEI (Qingdao, Shandong)	(As of October 2022)
Hsing-Pang HSIEH (Zhunan, Miaoli)	Xingyuan MA (Shanghai)	Tao XU (Qingdao, Shandong)	
Yongzhou HU (Hangzhou, Zhejiang)	Ken-ichi MAFUNE (Tokyo)	Yuhong XU (Shanghai)	

Review

- 269-276 **Novel and emerging therapeutics for antimicrobial resistance: A brief review.**
Raja Amir Hassan Kuchay

Original Article

- 277-282 **General selection criteria for safety and patient benefit [XIII]: Comparing the formulation characteristics of brand-name and generic bifonazole creams.**
Ken-ichi Shimokawa, Natsuki Ichimura, Marika Nozawa, Mitsuru Nozawa, Yuko Wada Imanaka, Fumiyoshi Ishii
- 283-289 **Mitotic abnormalities and spindle assembly checkpoint inactivation in a cell model of Shwachman-Diamond syndrome with mutations in the Shwachman-Bodian-Diamond syndrome gene, 258+2T > C.**
Yukihiro Sera, Tsuneo Imanaka, Yusuke Iguchi, Masafumi Yamaguchi
- 290-295 **Histopathological analysis of filament formation of *Nocardia farcinica* in a silkworm infection model.**
Koki Iwata, Mizuho Sato, Shoko Yoshida, Hiroo Wada, Kazuhisa Sekimizu, Mitsuhiro Okazaki
- 296-302 **Astaxanthin compound nutrient improved insulin resistance, hormone levels, embryo quality and pregnancy outcomes in polycystic ovary syndrome patients undergoing *in vitro* fertilization/intracytoplasmic sperm injection.**
Xiayan Fu, Wenli Cao, Feijun Ye, Jialu Bei, Yan Du, Ling Wang

Brief Report

- 303-307 **Electrolytic-reduction ion water protects keratinocytes from hydrogen peroxide through radical scavenging activity and induction of AQP3 expression.**
Hiroyuki Yamamoto, Tokuko Takajo, Ami Tsuchibuchi, Kaho Makuta, Toshiyuki Yamada, Mitsuo Ikeda, Yoshinao Okajima, Masahiro Okajima
- 308-313 **Panax notoginseng root extract induces nuclear translocation of CRTCL1 and *Bdnf* mRNA expression in cortical neurons.**
Shunsuke Shimizu, Aoi Nakano, Daisuke Ihara, Hironori Nakayama, Michiko Jo, Kazufumi Toume, Katsuko Komatsu, Naotoshi Shibahara, Masaaki Tsuda, Mamoru Fukuchi, Akiko Tabuchi
- 314-318 **Padding the seat of a wheelchair reduces ischial pressure and improves sitting comfort.**
Yoshiyuki Yoshikawa, Kiyo Sasaki, Kyoko Nagayoshi, Kenta Nagai, Yuki Aoyama, Shuto Takita, Teppei Wada, Yoshinori Kitade

Letter to the Editor

- 319-322** **A stroke patient with persistently intermittent fever treated with gabapentin: A clinical case.**
Jingjie Huang, Bangqi Wu, Yupei Cheng, Chaoran Wang
- 323-324** **Effect of switching from dulaglutide to tirzepatide on blood glucose and renal function.**
Atsushi Ishimura, Hiroyoshi Kumakura

Novel and emerging therapeutics for antimicrobial resistance: A brief review

Raja Amir Hassan Kuchay*

Department of Biotechnology, Baba Ghulam Shah Badshah University, Rajouri, J&K, India.

SUMMARY A pandemic known as anti-microbial resistance (AMR) poses a challenge to contemporary medicine. To stop AMR's rise and quick worldwide spread, urgent multisectoral intervention is needed. This review will provide insight on new and developing treatment approaches for AMR. Future therapy options may be made possible by the development of novel drugs that make use of developments in "omics" technology, artificial intelligence, and machine learning. Vaccines, immunoconjugates, antimicrobial peptides, monoclonal antibodies, and nanoparticles may also be intriguing options for treating AMR in the future. Combination therapy may potentially prove to be a successful strategy for combating AMR. To lessen the impact of AMR, ideas like drug repurposing, antibiotic stewardship, and the one health approach may be helpful.

Keywords anti-microbial resistance, mechanisms, drugs, therapeutics, FDA approved, monoclonal antibodies, anti-microbial peptides, AMR vaccines

1. Introduction

Antibiotics, widely used to treat diseases in both humans and animals, are hailed as the greatest medical discovery of the 20th century. Global antibiotic usage increased by 46% between 2000 and 2018, according to a new analysis that provided longitudinal estimates for human antibiotic consumption across 204 nations (1). However, rising levels of antimicrobial resistance (AMR) globally pose a danger to the beneficial health effects of antibiotics. AMR has become one of the main public health issues of the twenty-first century, posing a threat to the efficient prevention and treatment of a growing variety of microbial illnesses (2). The relationship between spread of AMR and antibiotic use is well documented (3). Additionally, it has been predicted that AMR would be the primary cause of death worldwide by 2050 due to the declining effectiveness of existing antibiotics and the dearth of novel antibiotics available on the market (4). It is concerning to note that AMR caused 1.27 million fatalities globally in 2019 alone, more than HIV and malaria combined (1). In addition to its direct effects on human health, AMR is linked to a substantial worldwide financial burden because of rising hospitalization and medication-related healthcare expenses (5).

Recognizing the seriousness of the situation, the World Health Organization (WHO) drafted the Global Action Plan (GAP) on AMR, which was approved at

the 68th World Health Assembly in May 2015 (6,7). This was followed by National action plans (NAPs) by many countries. The World Health Assembly recently called on member states to support and encourage basic, applied, and implementation research on infection prevention and control, diagnostic tools, vaccines, therapeutics, and antimicrobial stewardship through cooperation with academia, the private sector, and civil society in its 77th resolution on accelerating national and global responses to AMR (8,9). Furthermore, a key dimension to overcome AMR is ensuring that the world has a sustainable supply of antimicrobials. To this end, there is an urgent need to replace drugs rendered useless by the emergence of resistance by new therapeutics. This review will focus on new and emerging therapeutic options to combat AMR.

2. AMR mechanisms

Bacteria can develop acquired or innate antibiotic resistance (10). The intrinsic resistance characteristic, which is uniformly shared within a bacterial species, is unrelated to horizontal gene transfer and unaffected by prior antibiotic exposure (11). Intrinsic resistance might help bacteria survive an antibiotic through evolution (like changing their structure or components). Intrinsic resistance, for instance, might result from the natural activity of efflux pumps and decreased permeability

of the outer membrane, such as the lipopolysaccharide (LPS) in gram-negative bacteria (11,12). Acquisition of genetic material through horizontal gene transfer (HGT) including transformation, transposition, and conjugation or a new genetic mutation can lead to acquired resistance (11,13). AMR mechanisms include limiting uptake of a drug, modifying a drug target, inactivating a drug and active drug efflux (11,14). Figure 1 represents some AMR mechanisms and some novel and emerging options to tackle AMR.

Antibiotic uptake may be hampered by modifications in the permeability of the outer membrane or by the presence of porins, a subclass of transmembrane pore-forming outer membrane proteins (OMPs) (11,14). Drug uptake may be restricted by a reduction in the number of porins or mutations that alter the porin channel's selectivity (11). AMR, especially carbapenem resistance, is significantly influenced by outer-membrane remodeling, a key characteristic of many bacterial pathogens (15). Recently, the five-protein β -barrel assembly machine (BAM) complex, which is essential for the synthesis of outer membrane proteins in gram-negative bacteria, has become a viable target for drug development (16,17).

The antibiotic's low potency may result from changes to the drug target that prevent it from binding (11,13). Antimicrobial treatments may target several different parts of the bacterial cell, and the bacteria may alter

many of these targets to make them resistant to the medications. β -lactam antibiotics target penicillin-binding proteins (PBPs), which are necessary for the bacterial cell wall to form (18). The quantity of drug binding to that target will be affected by an increase in PBPs with reduced drug binding ability or a decrease in PBPs with normal drug binding (11). Compared to sensitive strains, AMR strains frequently feature chimeric high molecular mass PBPs (HMM PBPs) (19). The analysis of 26,465 *S. pyogenes* genome sequences revealed that amino acid alterations in PBP1a, 1b, 2a, and 2x resulted in decreased susceptibility to β -lactams (19,20). The *vanA* gene cluster on the transposon *Tn1546*, which is commonly found on plasmids, can give vancomycin resistance by altering the structure of peptidoglycan precursors, which reduces vancomycin's binding capacity (21). A 44-bp deletion in the *vanHAX* promoter region that permits the production of *vanHAX* was linked to an enhanced *vanA* plasmid copy number in a study on vancomycin variable enterococci with resistant phenotype (22).

Drug inactivation leading to AMR can be achieved by actual degradation of the drug, or by transfer of a chemical group to the drug (11). Modified existing bacterial enzyme can interact with an antibiotic making it inactive towards bacteria (14). The common structural element of all β -lactam antibiotics, including penicillins, cephalosporins, carbapenems, and monobactams, is the amide bond in the β -lactam ring, which is hydrolyzed by

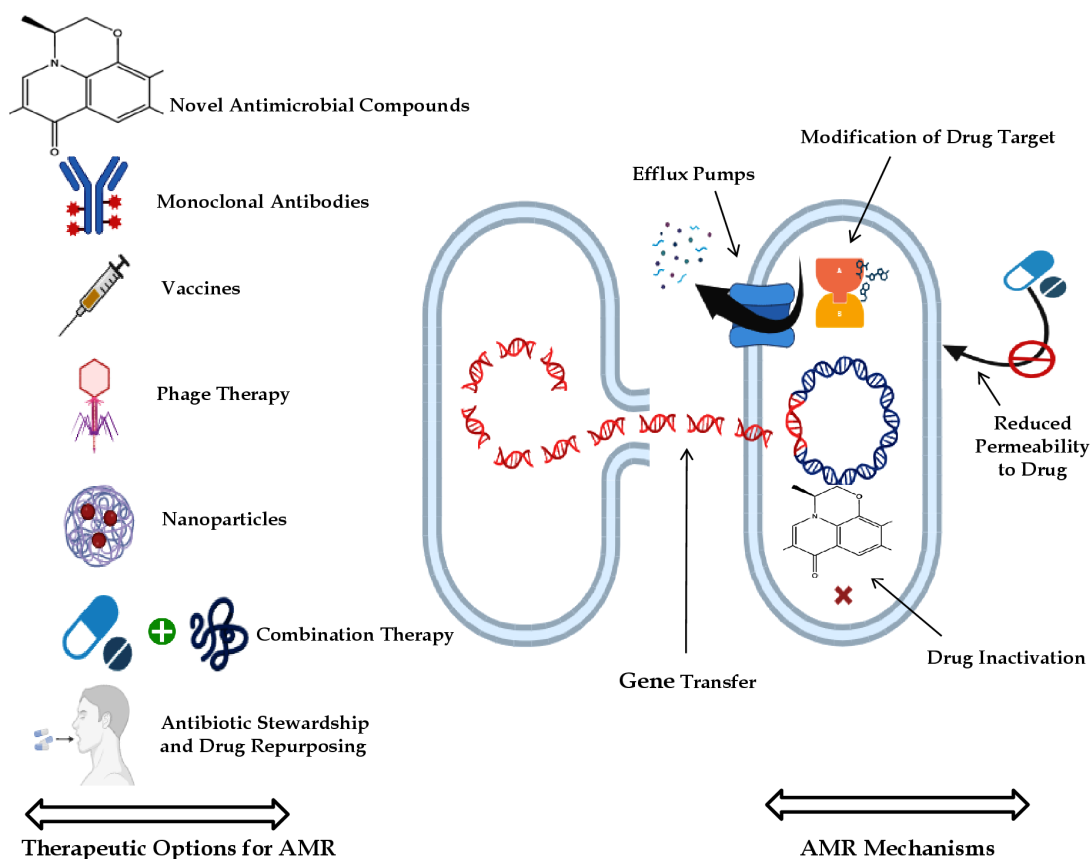


Figure 1. AMR mechanisms and some novel and emerging options to tackle AMR.

β -lactamases, a superfamily of hydrolyzing enzymes with over 2,000 members, rendering them ineffective (23). Aminoglycoside-modifying enzymes (AMEs) catalyze enzymatic modification of aminoglycoside antibiotics leading to their inactivation. AME-encoding genes were found in 48 out of 619 clinical isolates of *P. aeruginosa* in a recent study using bioinformatics analysis. The most prevalent of these genes were *ant(2')-Ia* and *aac(6')-Ib3*, which are linked to tobramycin and gentamicin resistance (24). Macrolide phosphotransferases (MPHs) are enzymes that add a phosphate to the 2'-OH group of macrolides thereby modifying and inactivating them (25). Macrolides interact with 23S rRNA at the A2058 residue within the nascent peptide exit tunnel around the peptidyl transferase center to inhibit protein synthesis (25). The substitution of 23s rRNA in the A2058 or A2059 positions leads to macrolide resistance in both Enterobacteriaceae and gram-positive isolates alike (26).

Efflux pumps decrease the intracellular concentration of drugs and function at the frontline to protect bacteria against antimicrobials (27). Efflux transporters are mainly categorized five superfamilies: ATP-Binding Cassette (ABC) superfamily, Multidrug and Toxic Compound Extrusion (MATE) superfamily, Major Facilitator Superfamily (MFS), Resistance Nodulation and Cell Division (RND) superfamily, and Small Multidrug Resistance (SMR) superfamily (27). The tripartite complex MacAB-TolC efflux pump, an ABC-type transporter that has been extensively explored in gram-negative bacteria, actively extrudes macrolides and polypeptide virulence factors that are driven by the ATPase MacB (27). The efflux of cationic dyes, including the efflux of fluoroquinolone medications, is facilitated by the MATE efflux family, which uses the Na^+ gradient as its energy source (27). In gram-positive microorganism, MFS family is the largest characterized family of transporters with 12 or 14 transmembrane segments (27). MFS pumps like Lde and NorA in *Listeria monocytogenes* and NorA in *Staphylococcus aureus* extrude hydrophilic fluoroquinolones like norfloxacin and ciprofloxacin (27). In many gram negative bacteria, substrate efflux via substrate/ H^+ antiport mechanism is catalyzed by RND efflux family members (27). Pumps like MexAB-OprM in *P. aeruginosa*, AcrAB-TolC in *E. coli*, OqxAB in *K. pneumoniae* and AdeABC in *A. baumannii* are some examples of RND superfamily pumps (27). Energized by the proton-motive force (H^+), SMR efflux family are hydrophobic, efflux mainly lipophilic cations having a narrow substrate range (27). The SMR superfamily member EmrE protein, which is found in *E. coli* and *P. aeruginosa*, detects and facilitates the extrusion of harmful poly-aromatic chemicals (27).

3. Novel and emerging therapeutics for AMR

In the light of above information, it is imperative to look for new therapeutics to combat AMR. Some

emerging options include monoclonal antibodies (mAbs), antimicrobial peptides (AMPs), novel antibiotic compounds, phage therapy, vaccines, combination drug therapy and nanoparticles to name a few. Many mAbs against bacteria have entered clinical trial but only few have succeeded (28,29). Obiltoximab and raxibacumab against *Bacillus anthracis*, actoxumab and bezlotoxumab against *Clostridium difficile*, edobacumab and nebacumab against *Escherichia coli*, aurograb against *Staphylococcus aureus* are few important examples (28,29). Bezlotoxumab has recently obtained FDA approval for preventing recurrent *Clostridium difficile* infections, while obiltoximab and raxibacumab for the treatment of inhalational anthrax (30,31). Being distinct from conventional small-molecule antibiotics, mechanisms of action of mAbs is less prone to drug resistance. AMPs are peptide sequences linked to biological action that typically contain 10–60 amino acid residues and lack any particular consensus amino acid patterns (32,33). Dalbavancin, daptomycin, telavancin, telaprevir, bacitracin and polymyxins are some examples of AMP approved by FDA (34). Phage therapy, an alternative therapy to combat bacterial infections has also been extensively investigated (35). Phage therapy registered clinical trials seek to exploit the bacteriocidal activity of lytic phages. Furthermore, focus on the ability of phages to disrupt biofilms is also under consideration (36). List of some novel and emerging therapeutics to treat AMR is given in Table 1.

Zoliflodacin, a compound based on a new benzisoxazole scaffold containing the pyrimidinetrione spirocyclic pharmacophore is in phase III trial since 2019 for the treatment of multidrug-resistant *N. gonorrhoeae* (37,38). Ridinilazole, a bis-benzimidazoles class of synthetic antibiotic has been reported to have rapid bactericidal activity and is in phase II trial for effective clinical response in the eradication of *C. difficile* compared to vancomycin (39). Recently, a new potential combination therapy to combat AMR by targeting two key bacterial enzymes involved in resistance was published (40). Triple combination of meropenem (MEM), a novel metallo- β -lactamase (MBL) inhibitor (indole-2-carboxylate 58 (InC58), and a serine- β -lactamase (SBL) inhibitor (avibactam (AVI) showed a much wider spectrum of activity against different carbapenemase-producing bacteria, revealing a new strategy to combat β -lactamase-mediated AMR (40). Ceftolozane-tazobactam (C-T) and ceftazidime-avibactam (CAZ-AVI) are two novel antimicrobials that retain activity against resistant *Pseudomonas aeruginosa* (41-43).

Carbon-based nanoparticles (NPs) including carbon quantum dots (CDots), nanotubes and 2-D materials, including graphene have been proven to be effective with their bactericidal action against *Klebsiella oxytoca*, *Pseudomonas aeruginosa* and *Staphylococcus epidermidis* (44). 2,2-(ethylenedioxy)bis(ethylamine)

Table 1. List of some novel AMPs, mAbs and antibiotics (approved/clinical trials) for AMR

Drug Name	Type	Phase	Bacterial Species/Clinical Target	Reference
Dalbavancin	AMP [†]	FDA Approved	Methicillin-resistant <i>Staphylococcus aureus</i>	(47,48,49,51)
Raxibacumab	mAb*	FDA Approved	<i>Bacillus anthracis</i>	(51,52,53,54)
Obiltoximab	mAb	FDA Approved	<i>Bacillus anthracis</i>	(51,52,53)
Bezlotoxumab	mAb	FDA Approved	<i>Clostridium difficile</i>	(51,52,54)
Polymyxins	AMP	FDA Approved	Drug resistant <i>Enterobacteriales</i> , <i>Acinetobacter baumannii</i> and <i>Pseudomonas aeruginosa</i>	(55)
TNP-2092	Antibiotic	Phase 2	Bacterial skin infection	(60)
Edobacumab	mAb	Phase 3	<i>Escherichia coli</i>	(52)
Tefibazumab	mAb	Phase 2	<i>Staphylococcus aureus</i>	(52)
Aurograb	mAb	Phase 3	<i>Staphylococcus aureus</i>	(52)
Oritavancin	AMP	FDA Approved	Gram-positive bacteria	(52, 56,57)
Telavancin	AMP	FDA Approved	<i>Staphylococcus aureus</i> and other gram-positive bacteria	(52, 58)
Afabicin	Antibiotic	Phase 2	Bacterial skin infection	(59,60)
Benapenem	Antibiotic	Phase 2	Anti-Bacterial	(60)
Cefiderocol	Antibiotic	FDA Approved	Gram-negative bacteria	(59,60)
Zoliflodacin	Antibiotic	Phase 3	Gram-negative bacteria	(59,60)
Levonadifloxacin	Antibiotic	Phase 3	MRSA	(60)
Sulopenem	Antibiotic	Phase 3	Anti-Bacterial	(60)
Gepotidacin	Antibiotic	Phase 3	Gram-negative bacteria	(59,60)
Ceftobiprole	Antibiotic	Phase 3	MRSA	(61)
Imipenem	Antibiotic	FDA Approved	Anti-Bacterial	(62)
Pretomanid	Antibiotic	FDA Approved	Anti-Bacterial	(62)
Lefamulin	Antibiotic	FDA Approved	Anti-Bacterial	(62)
Cefilavancin	Antibiotic	Phase 3	Bacterial skin infections	(62)
LTX-109	AMP	Phase 2	MRSA	(63)
Surotomycin	AMP	Phase 3	<i>Clostridium difficile</i>	(63)
Murepavadin	AMP	Phase 3	<i>P. aeruginosa</i>	(63)
Opebacan	AMP	Phase 2	Meningococcal infections	(63)
Plazomicin	Antibiotic	FDA Approved	Enterobacteriaceae infections	(62)
Sarecycline	Antibiotic	FDA Approved	Anti-Bacterial	(62)
Eravacycline	Antibiotic	FDA Approved	Anti-Bacterial	(62)
XOMA-629	AMP	Phase 2	Endotoxins of gram-negative bacteria	(63)
Novarifyn	AMP	Phase 1	Bacterial infection	(63)
AMP PL-18	AMP	Phase 1	Bacterial vaginosis	(63)
Omiganan	AMP	Phase 3	<i>Staphylococcus</i> species	(63)
Salvecin	mAb	Phase 2	<i>Staphylococcus aureus</i>	(52)
MEDI4893	mAb	Phase 2	<i>Staphylococcus aureus</i>	(52)
MAB-T88	mAb	Phase 2	<i>Escherichia coli</i>	(52)
Brilacidin	AMP	Phase 2	Broad spectrum antibacterial therapy	(63)

[†]Anti-Microbial Peptide; *Monoclonal Antibody.

carbon quantum dots (EDA-CDots) were reported to be effective and treatment at 0.1 mg/mL for 1 h reduced 3.26 logs of viable cells (44). PEI₆₀₀-CDots and PEI₁₂₀₀-CDots treatment at 0.1 mg/mL for 1 h reduced > 7 logs and 1.82 logs viable cells, respectively (45). Potential effectiveness of CuO NPs against biofilms has been recently demonstrated in many microorganism groups (44). Recently, TiO₂ NPs were reported to be effective against MRSA (46). After 12 hours of incubation, it was shown that the most effective dose was 2 mM TiO₂ nanoparticles, however the combination of erythromycin and 3 mM TiO₂ nanoparticles was more efficient and considerably reduced the MIC of erythromycin to 2–16 mg/L (46). List of some novel and emerging therapeutics to treat AMR is given in Table 1 and Table 2.

Combination therapy, the concurrent use of multiple antimicrobials in clinical practice has been successfully used to prevent resistance evolving during the treatment of diseases like tuberculosis and HIV

(64,65). In a report on laboratory evolution of *E. coli*, three pairwise combinations of antibiotics that included amikacin, chloramphenicol and enoxacin significantly suppressed the resistance acquisition (66). Zheng *et al.* (2018) reported that vancomycin in combination with beta lactams: piperacillin-tazobactam, cefazolin, and meropenem effectively prevented the development of vancomycin intermediate *S. aureus* (67).

Four vaccine candidates in phase 3 clinical trials against *M. tuberculosis* were recently identified in a paper that offered insight into mapping vaccination options against pathogens prioritized owing to AMR. Phase 3 trials for VPM1002, GamTBvac, MTBVAC, and Immuvac are presently underway. Immuvac is a therapeutic vaccine that employs a heat-killed *Mycobacterium indicus pranii* and is undergoing a phase 3 trial in India; MTBVAC is a live attenuated *M. tuberculosis* candidate; and VPM1002 is a preventive recombinant BCG vaccine (68). ExPEC9V, a nine-

Table 2. List of some emerging vaccines, nanoparticles (NPs) and combination therapies for AMR

Drug Name	Type	Clinical Target	Reference
ZnONPs	Nanoparticles	Fungal feet infection	(74)
FeONPs	Nanoparticles	Anti-biofilm treatment	(74)
PLGANPs	Nanoparticles	<i>E. fecalis</i> infections	(74)
Tridecaptin B + rifamycin	Combination Therapy	<i>A. baumannii</i>	(75,63)
Nisin + Colistin	Combination Therapy	<i>Pseudomonas</i> biofilms	(76,63)
Ranaxetin + Endopeptidase lysostaphin	Combination Therapy	<i>S. aureus</i> (MRSA)	(76,63)
Lactoferricin + Ciprofloxacin+ Ceftazidime	Combination Therapy	<i>P. aeruginosa</i>	(76,63)
Gad-1+ Kanamycin+ Ciprofloxacin	Combination Therapy	<i>P. aeruginosa</i>	(77,63)
Ceftolozane + tazobactam	Combination Therapy	Bacterial infections	(78)
Ceftazidime + avibactam	Combination Therapy	Bacterial infection	(78)
Meropenem + vaborbactam	Combination Therapy	Bacterial infection	(78)
ETVAX/dmLT	Vaccine	Enterotoxigenic <i>E coli</i>	(68)
GlycoShig3	Vaccine	<i>S flexneri</i>	(68)
WRSS2/WRSS3	Vaccine	<i>Shigella sonnei</i>	(68)
iCVD1000	Vaccine	<i>S Typhi</i>	(68)
KlebV4	Vaccine	<i>K pneumoniae</i>	(68)
Bexsero	Vaccine	<i>N gonorrhoeae</i>	(68)
PF-06425090	Vaccine	<i>C difficile</i>	(68)
ExPEC9V	Vaccine	Extra-intestinal pathogenic <i>E coli</i>	(68)
H56:IC31	Vaccine	<i>M tuberculosis</i>	(68)
VPM1002	Vaccine	<i>M tuberculosis</i>	(68)
GamTBvac	Vaccine	<i>M tuberculosis</i>	(68)
MTBVAC	Vaccine	<i>M tuberculosis</i>	(68)
Immuvac	Vaccine	<i>M tuberculosis</i>	(68)
FmOC + Phenylalanine	Combination Therapy	<i>S.aureus</i> and <i>P. aeruginosa</i>	(79,80)
Fosfomycin + Colistin	Combination Therapy	<i>E.coli</i> , <i>K. pneumoniae</i>	(79,81)
NAC + Ciprofloxacin	Combination Therapy	<i>P.aeruginosa</i>	(79,82)
Light Stimuli Responsive Therapy	Combination Therapy	<i>E.coli</i> , <i>E.cloacae</i> , <i>S.aureus</i>	(79,83)

valent-O-polysaccharide conjugate vaccine is currently in a phase 3 clinical trial against extraintestinal pathogenic *E. coli* (68). PF-06425090 is a recombinant toxin vaccine targeting *C. difficile*, consisting of genetically and chemically detoxified TcdA and TcdB toxins (68). For *Klebsiella pneumoniae*, a tetravalent bioconjugated vaccine candidate, KlebV4, is being assessed with and without the AS03 adjuvant in a phase 1/2 trial (68). Besides these, next generation approach, CRISPR-Cas9 antimicrobials, nanoparticle based strategies, artificial intelligence (AI) approaches also offer as potential options to tackle AMR in future (69-71).

4. Conclusions

AMR's emergence poses a serious threat to global public health, requiring the creation of novel antibiotics and multifaceted approaches to effectively combat it. An attempt was made to educate researchers and physicians about new and developing treatments for AMR in this review article. While creating novel antimicrobials is a crucial part of treating AMR, other viable future solutions to address AMR include enhancing surveillance systems, repurposing current medications, antibiotic stewardship, and one health approach (72). Additionally, new synergistic drug interactions to combat AMR can be found with the aid of machine learning (ML) algorithms that are being used to predict and create innovative treatments (73). By using AI and ML, it is possible

to take use of the potential to create new medicine combinations to control the growth of AMR. Because AMR affects people all around the world and crosses national borders, international cooperation is essential to combating its worldwide scope. Governments, international organizations, and stakeholders must encourage worldwide collaboration on AMR in order to share best practices, harmonize regulations, and coordinate efforts to successfully combat AMR.

Acknowledgements

Author is thankful to Mr. Komal Adab and Ms. Sherub Ayub for their timely inputs.

Funding: None.

Conflict of Interest: The author has no conflicts of interest to disclose.

References

- Browne AJ, Chipeta MG, Haines-Woodhouse G, et al. Global antibiotic consumption and usage in humans, 2000-18: a spatial modelling study. *Lancet Planet Health*. 2021; 5:e893-e904.
- Prestinaci F, Pezzotti P, Pantosti A. Antimicrobial resistance: a global multifaceted phenomenon. *Pathog Glob Health*. 2015; 109:309-318.
- Llor C, Bjerrum L. Antimicrobial resistance: risk

- associated with antibiotic overuse and initiatives to reduce the problem. *Ther Adv Drug Saf*. 2014; 5:229-241.
4. Dadgostar P. Antimicrobial resistance: Implications and costs. *Infect Drug Resist*. 2019; 12:3903-3910.
 5. Poudel AN, Zhu S, Cooper N, Little P, Tarrant C, Hickman M, Yao G. The economic burden of antibiotic resistance: A systematic review and meta-analysis. *PLoS One*. 2023; 18:e0285170.
 6. World Health Organization. Global action plan on antimicrobial resistance. Geneva 2015. Available from: <https://www.who.int/antimicrobial-resistance/global-action-plan/en/>
 7. World Health Assembly. Global action plan on antimicrobial resistance 2015. Available from: https://apps.who.int/gb/ebwha/pdf_files/WHA68/A68_R7-en.pdf.
 8. WHO Seventy-seventh World Health Assembly agenda item 11.8 Antimicrobial resistance: accelerating national and global responses 2024. Available from: https://apps.who.int/gb/ebwha/pdf_files/WHA77/A77_ACONF1-en.pdf
 9. Bertagnolio S, Dobрева Z, Centner CM, et al. WHO global research priorities for antimicrobial resistance in human health. *Lancet Microbe*. 2024:100902.
 10. Habboush Y, Guzman N. Antibiotic Resistance. In: *StatPearls*. StatPearls Publishing, Treasure Island (FL), 2023.
 11. Reygaert WC. An overview of the antimicrobial resistance mechanisms of bacteria. *AIMS Microbiol*. 2018; 4:482-501.
 12. Cox G, Wright GD. Intrinsic antibiotic resistance: mechanisms, origins, challenges and solutions. *Int J Med Microbiol*. 2013; 303:287-292.
 13. Davies J, Davies D. Origins and evolution of antibiotic resistance. *Microbiol Mol Biol Rev*. 2010; 74:417-433.
 14. Annunziato G. Strategies to overcome antimicrobial resistance (AMR) making use of non-essential target inhibitors: A review. *Int J Mol Sci*. 2019; 20:5844.
 15. Rosas NC, Lithgow T. Targeting bacterial outer-membrane remodelling to impact antimicrobial drug resistance. *Trends Microbiol*. 2022; 30:544-552.
 16. Hart EM, Mitchell AM, Konovalova A, et al. A small-molecule inhibitor of BamA impervious to efflux and the outer membrane permeability barrier. *Proc Natl Acad Sci U S A*. 2019; 116:21748-21757.
 17. Yoshihara E, Kakizoe H, Umezawa K, Wakamatsu K, Asai S. Antimicrobial activity of the BAM complex-targeting peptides against multidrug-resistant gram-negative bacteria. *bioRxiv*. 2024:2024-04.
 18. Hunashal Y, Kumar GS, Choy MS, D'Andréa ÉD, Da Silva Santiago A, Schoenle MV, Desbonnet C, Arthur M, Rice LB, Page R, Peti W. Molecular basis of β -lactam antibiotic resistance of ESKAPE bacterium *E. faecium* Penicillin Binding Protein PBP5. *Nat Commun*. 2023; 14:4268.
 19. Yu D, Guo D, Zheng Y, Yang Y. A review of penicillin binding protein and group A *Streptococcus* with reduced- β -lactam susceptibility. *Front Cell Infect Microbiol*. 2023; 13:1117160.
 20. Beres SB, Zhu L, Pruitt L, Olsen RJ, Faili A, Kayal S, Musser JM. Integrative reverse genetic analysis identifies polymorphisms contributing to decreased antimicrobial agent susceptibility in *Streptococcus pyogenes*. *mBio*. 2022; 13:e0361821.
 21. Arredondo-Alonso S, Top J, Corander J, Willems RJL, Schürch AC. Mode and dynamics of vanA-type vancomycin resistance dissemination in Dutch hospitals. *Genome Med*. 2021; 13:9.
 22. Wagner TM, Janice J, Schulz M, Ballard SA, da Silva AG, Coombs GW, Daley DA, Pang S, Mowlaboccus S, Stinear T, Hegstad K, Howden BP, Sundsfjord A. Reversible vancomycin susceptibility within emerging ST1421 *Enterococcus faecium* strains is associated with rearranged vanA-gene clusters and increased vanA plasmid copy number. *Int J Antimicrob Agents*. 2023; 62:106849.
 23. Egorov AM, Ulyashova MM, Rubtsova MY. Bacterial enzymes and antibiotic resistance. *Acta Naturae*. 2018; 10:33-48.
 24. Thacharodi A, Lamont IL. Aminoglycoside-modifying enzymes are sufficient to make *Pseudomonas aeruginosa* clinically resistant to key antibiotics. *Antibiotics (Basel)*. 2022; 11:884.
 25. Amdan NAN, Shahruzamri NA, Hashim R, Jamil NM. Understanding the evolution of macrolides resistance: A mini review. *J Glob Antimicrob Resist*. 2024; 38:368-375.
 26. Golkar T, Zieliński M, Berghuis AM. Look and outlook on enzyme-mediated macrolide resistance. *Front Microbiol*. 2018; 9:1942.
 27. Huang L, Wu C, Gao H, Xu C, Dai M, Huang L, Hao H, Wang X, Cheng G. Bacterial multidrug efflux pumps at the frontline of antimicrobial resistance: An overview. *Antibiotics (Basel)*. 2022; 11:520.
 28. Chen HC, Pan YL, Chen Y, Yang TH, Hsu ET, Huang YT, Chiang MH. Monoclonal antibodies as a therapeutic strategy against multidrug-resistant bacterial infections in a post-COVID-19 Era. *Life (Basel)*. 2024; 14:246.
 29. McConnell MJ. Where are we with monoclonal antibodies for multidrug-resistant infections? *Drug Discov Today*. 2019; 24:1132-1138.
 30. Navalkele BD, Chopra T. Bezlotoxumab: an emerging monoclonal antibody therapy for prevention of recurrent *Clostridium difficile* infection. *Biologics*. 2018; 12:11-21.
 31. Gerding DN, Kelly CP, Rahav G, Lee C, Dubberke ER, Kumar PN, Yacyszyn B, Kao D, Eves K, Ellison MC, Hanson ME, Guris D, Dorr MB. Bezlotoxumab for prevention of recurrent *Clostridium difficile* infection in patients at increased risk for recurrence. *Clin Infect Dis*. 2018; 67:649-656.
 32. Lopes BS, Hanafiah A, Nachimuthu R, Muthupandian S, Md Nesran ZN, Patil S. The role of antimicrobial peptides as antimicrobial and antibiofilm agents in tackling the silent pandemic of antimicrobial resistance. *Molecules*. 2022; 27:2995.
 33. Garvey M. Antimicrobial peptides demonstrate activity against resistant bacterial pathogens. *Infect Dis Rep*. 2023; 15:454-469.
 34. Ji S, An F, Zhang T, Lou M, Guo J, Liu K, Zhu Y, Wu J, Wu R. Antimicrobial peptides: An alternative to traditional antibiotics. *Eur J Med Chem*. 2024; 265:116072.
 35. Strathdee SA, Hatfull GF, Mutalik VK, Schooley RT. Phage therapy: From biological mechanisms to future directions. *Cell*. 2023; 186:17-31.
 36. Harper DR, Parracho HM, Walker J, Sharp R, Hughes G, Werthén M, Lehman S, Morales S. Bacteriophages and biofilms. *Antibiotics*. 2014; 3:270-284.
 37. Terreni M, Taccani M, Pregnolato M. New Antibiotics for multidrug-resistant bacterial strains: Latest research developments and future perspectives. *Molecules*. 2021; 26:2671.
 38. Bradford PA, Miller AA, O'Donnell J, Mueller JP. Zoliflodacin: An oral spiropyrimidinetrione antibiotic for

- the treatment of *Neisseria gonorrhoeae*, including multi-drug-resistant isolates. *ACS Infect Dis.* 2020; 6:1332-1345.
39. Cho JC, Crotty MP, Pardo J. Ridinilazole: a novel antimicrobial for *Clostridium difficile* infection. *Ann Gastroenterol.* 2019; 32:134-140.
 40. Ling Z, Farley AJ, Lankapalli A, Zhang Y, Premchand-Branker S, Cook K, Baran A, Gray-Hammerton C, Rubio CO, Suna E, Mathias J. The triple combination of meropenem, avibactam, and a metallo- β -lactamase inhibitor optimizes antibacterial coverage against different β -lactamase producers. *Engineering.* 2024; 38:124-132.
 41. Shi Z, Zhang J, Tian L, Xin L, Liang C, Ren X, Li M. A comprehensive overview of the antibiotics approved in the last two decades: Retrospects and prospects. *Molecules.* 2023; 28:1762.
 42. Gabrielyan L, Hakobyan L, Hovhannisyanyan A, Trchounian A. Effects of iron oxide (Fe_3O_4) nanoparticles on *Escherichia coli* antibiotic-resistant strains. *J Appl Microbiol.* 2019; 126:1108-1116.
 43. Almangour TA, Ghonem L, Alassiri D, Aljurbua A, Al Musawa M, Alharbi A, Almohaizeie A, Almuhsen S, Alghaith J, Damfu N, Aljefri D, Alfahad W, Khormi Y, Alanazi MQ, Alsowaida YS. Ceftolozane-tazobactam versus ceftazidime-avibactam for the treatment of infections caused by multidrug-resistant *Pseudomonas aeruginosa*: a multicenter cohort study. *Antimicrob Agents Chemother.* 2023; 67:e0040523.
 44. Makabenta JMV, Nabawy A, Li CH, Schmidt-Malan S, Patel R, Rotello VM. Nanomaterial-based therapeutics for antibiotic-resistant bacterial infections. *Nat Rev Microbiol.* 2021; 19:23-36.
 45. Abu Rabe DI, Al Awak MM, Yang F, Okonjo PA, Dong X, Teisl LR, Wang P, Tang Y, Pan N, Sun YP, Yang L. The dominant role of surface functionalization in carbon dots' photo-activated antibacterial activity. *Int J Nanomedicine.* 2019; 14:2655-2665.
 46. Ullah K, Khan SA, Mannan A, Khan R, Murtaza G, Yameen MA. Enhancing the antibacterial activity of erythromycin with titanium dioxide nanoparticles against MRSA. *Curr Pharm Biotechnol.* 2020; 21:948-954.
 47. Tegethoff JI, Teitelbaum I, Kiser TH. Rapid and effective treatment of peritonitis in peritoneal dialysis patients with intravenous dalbavancin. *Am J Case Rep.* 2024; 25:e942755.
 48. Lange A, Thunberg U, Söderquist B. Ototoxicity associated with extended dalbavancin treatment for a shoulder prosthetic joint infection. *BMC Infect Dis.* 2023; 23:706.
 49. Zhang G, Zhang N, Xu J, Yang T, Yin H, Cai Y. Efficacy and safety of vancomycin for the treatment of *Staphylococcus aureus* bacteraemia: a systematic review and meta-analysis. *Int J Antimicrob Agents.* 2023; 62:106946.
 50. Bucataru C, Ciobanasu C. Antimicrobial peptides: Opportunities and challenges in overcoming resistance. *Microbiol Res.* 2024; 286:127822.
 51. La Guidara C, Adamo R, Sala C, Micoli F. Vaccines and monoclonal antibodies as alternative strategies to antibiotics to fight antimicrobial resistance. *Int J Mol Sci.* 2024; 25:5487.
 52. Troisi M, Marini E, Abbiento V, Stazzoni S, Andreano E, Rappuoli R. A new dawn for monoclonal antibodies against antimicrobial resistant bacteria. *Front Microbiol.* 2022; 13:1080059.
 53. Tsai CW, Morris S. Approval of raxibacumab for the treatment of inhalation anthrax under the US Food and Drug Administration "Animal Rule". *Front Microbiol.* 2015; 6:1320.
 54. Wilcox MH, Gerding DN, Poxton IR, Kelly C, Nathan R, Birch T, Cornely OA, Rahav G, Bouza E, Lee C, Jenkin G. Bezlotoxumab for prevention of recurrent *Clostridium difficile* infection. *N Engl J Med.* 2017; 376:305-317.
 55. Ledger EVK, Sabnis A, Edwards AM. Polymyxin and lipopeptide antibiotics: membrane-targeting drugs of last resort. *Microbiology (Reading).* 2022; 168:001136.
 56. Texidor WM, Miller MA, Molina KC, Krsak M, Calvert B, Hart C, Storer M, Fish DN. Oritavancin as sequential therapy for Gram-positive bloodstream infections. *BMC Infect Dis.* 2024; 24:127.
 57. Baiardi G, Cameran Caviglia M, Piras F, Sacco F, Prinapori R, Cristina ML, Mattioli F, Sartini M, Pontali E. The clinical efficacy of multidose oritavancin: A systematic review. *Antibiotics (Basel).* 2023; 12:1498.
 58. Lampejo T. Dalbavancin and telavancin in the treatment of infective endocarditis: a literature review. *Int J Antimicrob Agents.* 2020; 56:106072.
 59. Kanj SS, Bassetti M, Kiratisin P, Rodrigues C, Villegas MV, Yu Y, van Duin D. Clinical data from studies involving novel antibiotics to treat multidrug-resistant Gram-negative bacterial infections. *Int J Antimicrob Agents.* 2022; 60:106633.
 60. Parmanik A, Das S, Kar B, Bose A, Dwivedi GR, Pandey MM. Current treatment strategies against multidrug-resistant bacteria: A review. *Curr Microbiol.* 2022; 79:388.
 61. Paukner S, Goldberg L, Alexander E, Das AF, Heinrich S, Patel P, Moran GJ, Sandrock C, File Jr TM, Vidal JE, Waites KB. Pooled microbiological findings and efficacy outcomes by pathogen in adults with community-acquired bacterial pneumonia from the Lefamulin Evaluation Against Pneumonia (LEAP) 1 and LEAP 2 phase 3 trials of lefamulin versus moxifloxacin. *J Glob Antimicrob Resist.* 2022; 29:434-443.
 62. Andrei S, Droc G, Stefan G. FDA approved antibacterial drugs: 2018-2019. *Discoveries (Craiova).* 2019; 7:e102.
 63. Mba IE, Nweze EI. Antimicrobial peptides therapy: An emerging alternative for treating drug-resistant bacteria. *Yale J Biol Med.* 2022; 95:445-463.
 64. Woods RJ, Read AF. Combination antimicrobial therapy to manage resistance. *Evol Med Public Health.* 2023; 11:185-186.
 65. Garza-Cervantes JA, León-Buitimea A. Editorial: Synergistic combinatorial treatments to overcome antibiotic resistance. *Front Cell Infect Microbiol.* 2024; 14:1369264.
 66. Suzuki S, Horinouchi T, Furusawa C. Acceleration and suppression of resistance development by antibiotic combinations. *BMC Genomics.* 2017; 18:328.
 67. Zheng X, Berti AD, McCrone S, Roch M, Rosato AE, Rose WE, Chen B. Combination antibiotic exposure selectively alters the development of vancomycin intermediate resistance in *Staphylococcus aureus*. *Antimicrob Agents Chemother.* 2018; 62:e02100-17.
 68. Frost I, Sati H, Garcia-Vello P, Hasso-Agopsowicz M, Lienhardt C, Gigante V, Beyer P. The role of bacterial vaccines in the fight against antimicrobial resistance: an analysis of the preclinical and clinical development pipeline. *Lancet Microbe.* 2023; 4:e113-e125.
 69. Rabaan AA, Alhumaid S, Mutair AA, et al. Application of artificial intelligence in combating high antimicrobial resistance rates. *Antibiotics (Basel).* 2022; 11:784.

70. Bhandari V, Suresh A. Next-generation approaches needed to tackle antimicrobial resistance for the development of novel therapies against the deadly pathogens. *Front Pharmacol.* 2022; 13:838092.
71. Murugaiyan J, Kumar PA, Rao GS, *et al.* Progress in alternative strategies to combat antimicrobial resistance: Focus on antibiotics. *Antibiotics (Basel).* 2022; 11:200.
72. Ahmed SK, Hussein S, Qurbani K, Ibrahim RH, Fareeq A, Mahmood KA, Mohamed MG. Antimicrobial resistance: impacts, challenges, and future prospects. *J Med Surg Pub Health.* 2024; 2:100081.
73. Cantrell JM, Chung CH, Chandrasekaran S. Machine learning to design antimicrobial combination therapies: Promises and pitfalls. *Drug Discov Today.* 2022; 27:1639-1651.
74. Mondal SK, Chakraborty S, Manna S, Mandal SM. Antimicrobial nanoparticles: current landscape and future challenges. *RSC Pharm.* 2024; 1:388-402.
75. Jangra M, Raka V, Nandanwar H. *In vitro* evaluation of antimicrobial peptide tridecaptin M in combination with other antibiotics against multidrug resistant *Acinetobacter baumannii*. *Molecules.* 2020; 25:3255.
76. Jahangiri A, Neshani A, Mirhosseini SA, Ghazvini K, Zare H, Sedighian H. Synergistic effect of two antimicrobial peptides, Nisin and P10 with conventional antibiotics against extensively drug-resistant *Acinetobacter baumannii* and colistin-resistant *Pseudomonas aeruginosa* isolates. *Microb Pathog.* 2021; 150:104700.
77. Portelinha J, Angeles-Boza AM. The antimicrobial peptide Gad-1 clears *Pseudomonas aeruginosa* biofilms under cystic fibrosis conditions. *Chembiochem.* 2021; 22:1646-1655.
78. Lombardi A, Alagna L, Palomba E, Viero G, Tonizzo A, Mangioni D, Bandera A. New antibiotics against multidrug-resistant gram-negative bacteria in liver transplantation: Clinical perspectives, toxicity, and PK/PD properties. *Transpl Int.* 2024; 37:11692.
79. Bari AK, Belalekar TS, Poojary A, Rohra S. Combination drug strategies for biofilm eradication using synthetic and natural agents in KAPE pathogens. *Front Cell Infect Microbiol.* 2023; 13:1155699.
80. Singh H, Gahane A, Singh V, Ghosh S, Thakur A. Antibiofilm activity of Fmoc-phenylalanine against Gram-positive and Gram-negative bacterial biofilms. *J Antibiot (Tokyo).* 2021; 74:407-416.
81. Boncompagni SR, Micieli M, Di Maggio T, Aiezza N, Antonelli A, Giani T, Padoani G, Vailati S, Pallecchi L, Rossolini GM. Activity of fosfomycin/colistin combinations against planktonic and biofilm Gram-negative pathogens. *J Antimicrob Chemother.* 2022; 77:2199-2208.
82. Aiyer A, Manoharan A, Paino D, Farrell J, Whiteley GS, Kriel FH, Glasbey TO, Manos J, Das T. Disruption of biofilms and killing of *Burkholderia cenocepacia* from cystic fibrosis lung using an antioxidant-antibiotic combination therapy. *Int J Antimicrob Agents.* 2021; 58:106372.
83. Sikder A, Chaudhuri A, Mondal S, Singh NDP. Recent advances on stimuli-responsive combination therapy against multidrug-resistant bacteria and biofilm. *ACS Appl Bio Mater.* 2021; 4:4667-4683.

Received August 29, 2024; Revised October 18, 2024; Accepted October 23, 2024.

*Address correspondence to:

Raja Amir Hassan, Department of Biotechnology, Baba Ghulam Shah Badshah University, Rajouri, J&K, 185234, India.
E-mail: kuchay_bgsbu@yahoo.com

Released online in J-STAGE as advance publication October 27, 2024.

General selection criteria for safety and patient benefit [XIII]: Comparing the formulation characteristics of brand-name and generic bifonazole creams

Ken-ichi Shimokawa^{1,*}, Natsuki Ichimura¹, Marika Nozawa², Mitsuru Nozawa³, Yuko Wada Imanaka⁴, Fumiyoshi Ishii⁴

¹Department of Pharmaceutical Sciences, Meiji Pharmaceutical University, Tokyo, Japan;

²Ai-station Clinic, Tokyo, Japan;

³TH & C Co. Ltd., Kanagawa, Japan;

⁴Department of Self-medication and Health Care Sciences, Meiji Pharmaceutical University, Tokyo, Japan.

SUMMARY A comparative evaluation of the brand-name drug Mycospor and six generic drugs (IWAKI, Bifonol, F, YD, Sawai, and TEVA), all comprising a cream formulation containing the antifungal drug bifonazole, was performed based on physicochemical measurements. The pH of the various formulations was significantly higher for the generics Bifonol (pH 7.1), Sawai (pH 6.7), and TEVA (pH 7.3) and significantly lower for YD (pH 4.3) than for the brand-name drug Mycospor (pH 5.5). The viscosity of the various formulations was significantly higher for TEVA (25,011 mPa·s) versus Mycospor (22,376 mPa·s) and significantly lower for IWAKI, Bifonol, F, YD, and Sawai, with Bifonol (8,572 mPa·s) being particularly low. Considering the hysteresis loop area obtained for the shear rate vs. shear stress, which represents the thixotropic properties, and using the value of Mycospor as the reference for 100%, YD (179%), Sawai (557%), and TEVA (201%) showed significantly higher values. Furthermore, the membrane permeability of bifonazole at 24 hours was significantly higher for Bifonol (309 µg/mL) and F (182 µg/mL) and significantly lower for Sawai (124 µg/mL) and TEVA (92 µg/mL) than for Mycospor (153 µg/mL). Finally, optical micrographs showed that the dispersion of particles was similar in the various formulations, but the particles of F and TEVA were uniformly dispersed with a smaller particle size than the other formulations. Overall, significant differences were observed in the formulation characteristics between the brand-name drug and generic drugs, which were attributed to differences in the manufacturing process and the types of additives.

Keywords Brand-name drug, generic drug, cream, bifonazole, thixotropy

1. Introduction

In Japan, the overall national healthcare costs have recently been increasing each year, becoming a major social problem (1), and generic drugs are being promoted to reduce these healthcare costs (2). As of September 2023, the ratio of "generic drugs" to "brand-name drugs with generics + generic drugs" was 80.2%, but considering that the ratio was 79.0% in both 2021 and 2022, further increases are difficult to achieve (3). Therefore, as a new measure to increase the ratio, the "selective treatment of brand-name drugs (long-term listed drugs) with generic drugs" came into effect in October 2024 (4). This increases the patient's co-payment when a patient requests a prescription for a brand-

name drug for which a generic drug is available, which is intended to facilitate the transition to generic drugs. However, awareness of generic drugs among outpatients is low, and many patients are concerned about the side effects and efficacy of generic drugs (5). In addition, patients have different preferences when applying topical drugs. One study showed that some patients favored the topical solution that was "not sticky" and "smooth," while some patients reported that "other solutions are better," which were "sticky feeling" and "moist" (6). Notably, if pharmacists can inform patients regarding the sense of use characteristics for various products, then they can recommend generic drugs that meet patients' needs.

We have previously reported that the physicochemical

characterization of various dosage forms, mainly topicals with significant differences in the sense of use, including creams (7,8), ointments and lotions (9,10), ophthalmics (11,12), nasal sprays (13), and tapes (14-18), is necessary to help distinguish the formulations for patients and meet their needs. These reports suggest that differences in the formulation technology and additives used in the manufacturing process affect the sense of use and efficacy of each product among patients.

In this study, a comparative evaluation of brand-name and generic antifungal bifonazole-containing cream formulations was conducted to provide information that may assist patients in selecting the most appropriate product for their needs.

2. Materials and Methods

2.1. Materials

The brand-name bifonazole-containing cream (Mycospor[®] cream 1%) and the six generic versions used in this study are listed in Table 1.

2.2. pH measurement

The pH of each formulation was measured 10 times using a pH/°C meter designed for dairy and semi-solid foods (HI 99161N, Hanna Instruments Japan, Inc., Chiba, Japan).

2.3. Viscosity measurement

The viscosity of each formulation was measured using a TPE-100H cone-plate viscometer equipped with an integrated temperature control system (Toki Sangyo Co., Ltd., Tokyo, Japan). The measurement temperature was 25°C, the rotational speed of the cone plate (CORD-P1: 1°34' × R24) was set to 1 rpm, and the viscosity (Pa·s) after 90 seconds was recorded. The experiment was conducted 10 times for each formulation.

2.4. Thixotropy measurement

Thixotropy was measured using a TPE-100H cone-plate

viscometer with the CORD-04: 3° × R14 cone plate at a constant temperature of 25°C.

Step 1 was shear rate 2 (1/s), Step 2 was shear rate 4 (1/s), Step 3 was shear rate 10 (1/s), Step 4 was shear rate 20 (1/s), Step 5 was shear rate 40 (1/s), Step 6 was shear rate 100 (1/s), Step 7 was shear rate 200 (1/s), Step 8 was shear rate 100 (1/s), Step 9 was shear rate 40 (1/s), Step 10 was shear rate 20 (1/s), Step 11 was shear rate 10 (1/s), Step 12 was shear rate 4 (1/s), Step 13 was shear rate 2 (1/s), and the cone plate was rotated for 90 seconds during each step to obtain the shear stress (Pa). The loop area obtained from the viscosity curve of each formulation was calculated using Visco-chart software (Toki Sangyo Co., Ltd., Tokyo, Japan), and the relative area ratio (%) of the generic drug was compared using the loop area of the brand-name drug as the reference value of 100%.

2.5. Measurement of the membrane permeation volume

A vertical diffusion Franz cell (vertical palm cell) TP-8S (Biocom Systems, Inc., Fukuoka, Japan) was used for membrane permeation volume measurements, and the Strat-M[®] membrane designed for skin diffusion tests (Merck Ltd., Tokyo, Japan) was used as the membrane. The receptor solution used to fill the vertical diffusion Franz cell was a 1:1 ratio of phosphate buffer saline (pH 7.4) and acetonitrile. After the membrane was mounted in the vertical palm cell, various formulations (0.5 g) were applied to the membrane for measurement at 37°C. The volume of bifonazole that permeated the membrane after 1, 2, 4, 6, and 24 hours was determined by high-performance liquid chromatography (HPLC) using an LC-2000 Plus System (Japan Spectroscopic Corporation, Tokyo, Japan) equipped with an Inertsil ODS-3 column (4.6 × 150 mm, 5 μm; G.L. Science Corporation, Tokyo, Japan). The following HPLC conditions were used: column oven temperature of 40°C, wavelength of 254 nm, flow rate of 1.5 mL/min, analysis time of 4 min, uptake time of 3 min, and a mobile phase consisting of acetonitrile:0.12 M sodium acetate:methanol (84:15:1).

2.6. Visual observation by microscopy

Table 1. List of the creams evaluated in this study

Product name (Former product name)	Abbreviated name	Class	Company name	Lot number
Mycospor [®] cream 1%	Mycospor	brand name	Bayer Yakuhin, Ltd.	BJ35620
Bifonazol cream 1% "IWAKI" (Biconol [®] cream 1%)	IWAKI	generic	Iwaki Seiyaku Co., Ltd.	84065
Bifonol [®] cream 1%	Bifonol	generic	Toko Pharmaceutical Industries Co., Ltd.	B1101
Bifonazol cream 1% "F"	F	generic	Fuji Pharma Co., Ltd.	AA18A
Bifonazol cream 1% "YD"	YD	generic	Yoshindo Inc.	YAA-1
Bifonazol cream 1% "Sawai"	Sawai	generic	Sawai Pharmaceutical Co., Ltd.	17Z01
Bifonazol cream 1% "TAKEDA TEVA" (Bilmitin [®] cream 1%)	TEVA	generic	Teva Takeda Pharma Ltd.	CD011

Microscopic observation of the various formulations in the emulsification state was performed using a DMBA310 digital microscope (Shimadzu Rika Corporation, Tokyo, Japan) at 400× magnification. Motic Images Plus 2.2s software (Shimadzu Rika Corporation, Tokyo, Japan) was used to capture images.

2.7. Statistical analysis

The results of each pH measurement, viscosity measurement, flow curve loop area measurement, and membrane permeation volume measurement were tested for significance against the brand-name drug using Dunnett multiple comparison test (19). Significance levels are indicated on the graphs for each measurement result using * for $P \leq 0.05$ and ** for $P \leq 0.01$.

3. Results

3.1. pH measurement

The pH measurement results for the various formulations are shown in Figure 1. The generic drugs Bifonol (pH 7.1), Sawai (pH 6.7), and TEVA (pH 7.3) showed significantly higher values than Mycospor (pH 5.5), and YD (pH 4.3) showed significantly lower values.

3.2. Viscosity measurement

Figure 2 shows the viscosity measurement results for the various formulations. The viscosity of TEVA (25,011 Pa·s) was significantly higher than that of Mycospor (22,376 Pa·s), whereas IWAKI (15,301 Pa·s), Bifonol (8,572 Pa·s), F (15,050 Pa·s), YD (20,649 Pa·s), and Sawai (12,347 Pa·s) exhibited significantly lower values. Bifonol had particularly high flowability, with approximately 40% of the viscosity observed for Mycospor.

3.3. Thixotropy measurement

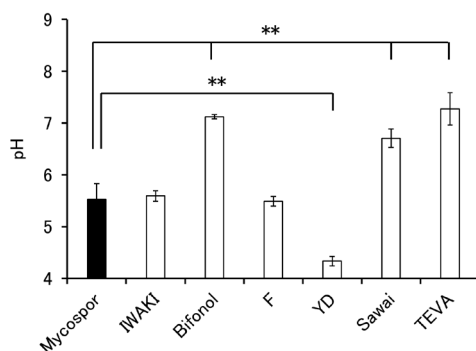


Figure 1. Comparison of pH among the various creams. ($n = 10$, vs. Mycospor, $**P < 0.01$, Dunnett-test) Black bar: brand-name drug, white bar: generic drugs.

For a dispersion system formulation, the viscosity curve may show hysteresis when the shear rate is reciprocated. This phenomenon is called thixotropy, and the magnitude of thixotropy is determined by measuring the hysteresis area. Therefore, Figure 3 shows the relationship between shear rate (1/s) and shear stress (Pa) obtained by cone-plate viscometry for the various formulations used in this experiment. The shear stress is lower for Bifonol (▲) and YD (○) than for Mycospor (●), whereas IWAKI (■), F (◆), Sawai (□), and TEVA (Δ) have higher shear stress, in that order.

The hysteresis loop areas for the various formulations are shown in Figure 4. The loop area of Mycospor (100%, the reference) was significantly lower than that of YD (179%), Sawai (557%), and TEVA (201%).

3.4. Measurement of the membrane permeation volume

The membrane permeation results at each time point are shown in Figure 5. Membrane permeation continually increased after 2, 4, 6, and 24 hours for all formulations. The permeated volume at 24 hours was significantly higher for F (182 μg/mL) and Bifonol (309 μg/mL) and significantly lower for Sawai (124 μg/mL) and TEVA (92 μg/mL) than that for Mycospor (153 μg/mL).

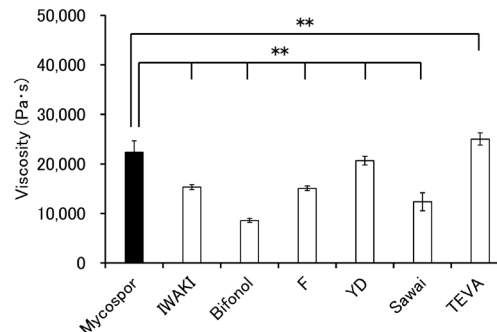


Figure 2. Comparison of viscosity among the various creams. ($n = 10$, vs. Mycospor, $**P < 0.01$, Dunnett-test) Black bar: brand-name drug, white bar: generic drugs.

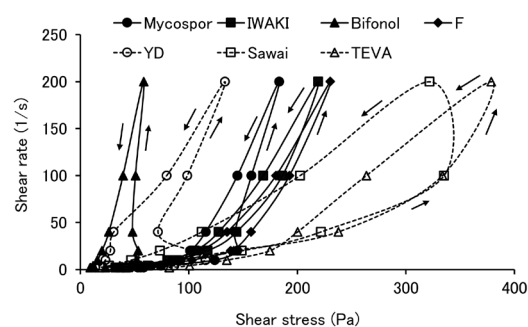


Figure 3. Comparison of thixotropy among the various creams. ($n = 10$) →: direction to strengthen shear stress, ←: direction to weaken shear stress.

3.5. Observation of each formulation in the dispersion state

Figure 6 shows the optical micrographs of each formulation in the dispersion state. Particles were dispersed in all formulations, but IWAKI and Bifonol had the same level of dispersion as Mycospor, YD and Sawai had the largest particles, and F and TEVA had the smallest particles.

4. Discussion

In this study, we comparatively evaluated the formulation characteristics of an antifungal brand-name bifonazole cream (Mycospor® cream 1%) and six generic creams by performing physicochemical measurements.

The pH was significantly higher for Bifonol (pH 7.1), Sawai (pH 6.7), and TEVA (pH 7.3) and significantly lower (pH 4.3) for YD than for Mycospor (pH 5.5) (Figure 1). In general, the pH of the healthy skin surface is reported to be slightly acidic (4.5-6.0) (20). However, Bifonol, Sawai, and TEVA may be less irritating to the skin because of their neutral pH range of 6.7 to 7.3. As an antifungal agent, the most common application sites are between the toes and on the soles, including the arch

and heel of the foot. Considering that epidermal damage may occur due to pruritus, a low pH may be irritating to the skin, especially in the interdigital area.

The viscosity is an indicator of comfort and is one of the most important factors when applying creams to the affected area. Generally, for ointments and creams, a higher viscosity results in a higher stickiness, and a lower viscosity results in a lower stickiness. The viscosity of TEVA was significantly higher than that of Mycospor, and the viscosities of IWAKI, Bifonol, F, YD, and Sawai were significantly lower (Figure 2). Based on these results, we believe that TEVA can be recommended for patients who do not mind stickiness when using cream formulations containing bifonazole, and Bifonol or Sawai, which have lower viscosity, can be recommended for patients who are concerned about stickiness. Furthermore, YD has a relatively similar viscosity to Mycospor, which may support a smoother changeover from the brand-name drug to the generic formulation.

Next, the hysteresis loop area (the area encompassed by the viscosity curves generated in the direction of the increasing (→) and decreasing (←) shear rate) was calculated for the various formulations (Figures 3 and 4). The larger the hysteresis loop area, the greater the thixotropy. Thixotropy is an indicator of the shear

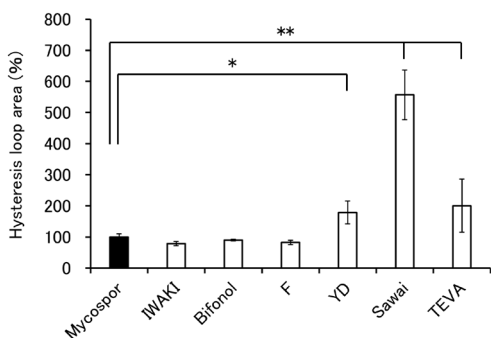


Figure 4. Comparison of hysteresis loop area (%) among the various creams. (n = 10, vs. Mycospor, *P < 0.05, **P < 0.01, Dunnett-test) Black bar: brand-name drug, white bar: generic drugs.

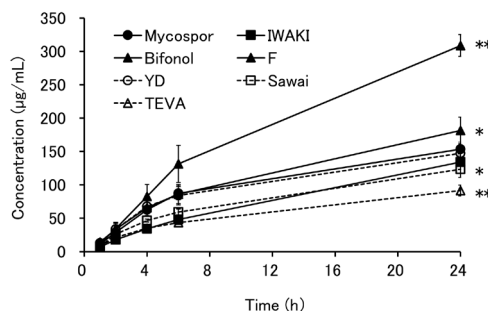


Figure 5. Comparison of membrane permeability of bifonazole after 24 hours among the various formulations. (n = 5, vs. Mycospor, *P < 0.05, **P < 0.01, Dunnett-test).

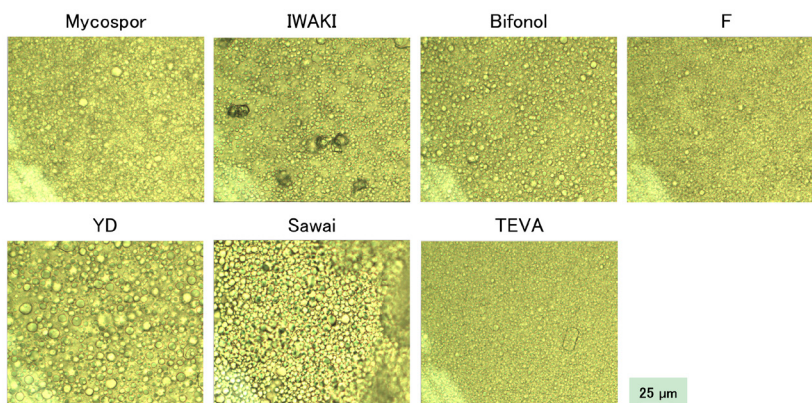


Figure 6. Optical micrographs of the various formulations (400×).

stress that is initially required during application with the fingers. Herein, we compared the formulations using the hysteresis loop area of Mycospor (●) as the reference (100%). Figure 3 shows that Bifonol (▲) and YD (○) have weaker shear stress values, with areas of 91% and 179%, respectively, indicating that they can be spread on the skin with relative ease. In contrast, Sawai (□) and TEVA (Δ) have higher shear stress values and hysteresis loop areas of 557% and 201%, respectively, indicating that they require relatively higher force when spreading them on the skin. These results indicate that the "usability" of Mycospor (●) significantly differed from that of the generic drugs. The formulations with relatively close shear stresses to Mycospor (●) were IWAKI (■) and TEVA (Δ), with loop areas of 79% and 82%, respectively. Therefore, recommending these two formulations may promote a smoother changeover from the brand-name drug to the generic drug.

The membrane permeability of bifonazole was measured for the different formulations using the Strat-M[®] membrane, an artificial membrane developed as a substitute for animal or human skin in permeability studies. Strat-M[®] is a multilayer membrane with varying permeability; the upper layer is a double layer of polyethersulfone and the lower layer has a polyolefin structure, which are used to predict the permeation of lipophilic and hydrophilic molecules (21). We found that the amount of permeation was significantly higher for Bifonol (309 μg/mL) and F (182 μg/mL) than Mycospor (153 μg/mL), whereas Sawai (124 μg/mL) and TEVA (92 μg/mL) showed significantly lower permeability. According to a questionnaire on generic drugs that was distributed among dermatologists in Kanagawa prefecture, Japan, "Some topicals with different substrates clearly have different efficacy" (22). Our results showed that there was approximately a 0.6- to 2-fold difference in permeation compared with Mycospor depending on the formulation, which is consistent with the opinion of the dermatologists, and this may be attributed to the different additives used in the formulations.

Microscopy showed that the dispersion of particles was similar among the various formulations (Figure 6). However, the F and TEVA particles were smaller and more uniformly dispersed than the Mycospor particles, and some YD and Sawai particles appeared to be crystals. The slight differences in dispersion and particle size may reflect the differences in viscosity, thixotropy, and membrane permeability, which may influence the sense of use.

Characteristic differences were observed among the bifonazole-containing cream formulations in terms of viscosity and thixotropy. Furthermore, the amount of drug permeation significantly differed among the formulations, suggesting that the permeation of the drug into the skin, as well as the effectiveness of the drug, is affected by the formulation.

In promoting the use of generic drugs, the differences in the sense of use and efficacy when switching from brand-name to generic drugs may lead to a decrease in adherence and therapeutic efficacy. Providing pharmacists with product-specific information may be critical in selecting or recommending drugs that meet the various needs of patients.

Acknowledgements

We are grateful to Mr. Daiki Shimada for his preliminary experiments and assistance in conducting this study.

Funding: None.

Conflict of Interest: The authors have no conflicts of interest to disclose.

References

1. "2021 national health care costs overview". Ministry of Health, Labor and Welfare. <https://www.mhlw.go.jp/toukei/saikin/hw/k-iryohi/21/dl/data.pdf> (accessed September 19, 2024). (in Japanese)
2. "Promotion of the use of generic medicines and biosimilars". Ministry of Health, Labor and Welfare. https://www.mhlw.go.jp/stf/seisakunitsuite/bunya/kenkou_iryohi/iryohi/kouhatsu-iyaku/index.html (accessed September 19, 2024). (in Japanese)
3. "Preliminary results of the 2023 pharmaceutical price survey (NHI)". Ministry of Health, Labor and Welfare. <https://www.mhlw.go.jp/content/000890776.pdf> (accessed September 19, 2024). (in Japanese)
4. "Selective treatment of original medicines (long-listed products) with generic medicines". https://www.mhlw.go.jp/stf/newpage_39830.html (accessed September 19, 2024). (in Japanese)
5. Yamamoto Y, Yamatani A, Funaki H, Horibe C. Investigation on the consciousness of drug costs and generic medicines for outpatients. *IRYO*. 2006; 60:459-464.
6. Tsunemi Y. Comparison of liranafate (Zefnart[®]) solution with other antifungal solutions with regard to comfort in topical use. *J New Rem Clin*. 2009; 58: 119-124.
7. Nozawa M, Goto M, Wada Y, Kumazawa M, Shimokawa K, Ishii F. Generic selection criteria for safety and patient benefit [VII]: Comparing the physicochemical and pharmaceutical properties of brand-name and generic terbinafine hydrochloride cream. *Drug Discov Ther*. 2018; 12:16-20.
8. Takata M, Wada Y, Iwasawa Y, Kumazawa M, Shimokawa K, Ishii F. Criteria for the selection of switch OTC drugs based on patient benefits, efficacy, and safety [II]: Comparing the physicochemical and pharmaceutical properties of brand-name and switch OTC terbinafine hydrochloride cream. *Drug Discov Ther*. 2018; 12:248-253.
9. Wada Y, Nozawa M, Goto M, Shimokawa K, Ishii F. Generic Selection Criteria for Safety and Patient Benefit [I] Comparing the original drugs and generic ones in pharmaceutical properties. *J Comm Pharm Sci*. 2014; 6:97-105. (in Japanese)

10. Nozawa M, Wada Y, Yamazaki N, Shimokawa K, Ishii F. Generic Selection Criteria for Safety and Patient Benefit [II] Physicochemical characteristics of original and generic drugs for three different difluprednate-containing preparations (ointment, cream, and lotion). *J Jpn Soc Comm Pharm.* 2014; 2:37-48. (in Japanese)
11. Wada Y, Nozawa M, Goto M, Shimokawa K, Ishii F. Generic selection criteria for safety and patient benefit [III] Comparing the pharmaceutical properties and patient usability of original and generic ophthalmic solutions containing timolol maleate. *J Jpn Soc Pharm Health Sci.* 2015; 41:394-403. (in Japanese)
12. Wada Y, Ami S, Nozawa M, Goto M, Shimokawa K, Ishii F. Generic selection criteria for safety and patient benefit [V]: Comparing the pharmaceutical properties and patient usability of original and generic nasal spray containing ketotifen fumarate. *Drug Discov Ther.* 2016; 10:88-92.
13. Goto M, Nozawa M, Wada Y, Shimokawa K, Ishii F. Generic selection criteria for safety and patient benefit [IX]: Evaluation of "feeling of use" of sodium hyaluronate eye drops using the Haptic Skill Logger (HapLog[®]) wearable sensor for evaluating haptic behaviors. *Drug Discov Ther.* 2020; 14:14-20.
14. Wada Y, Kihara M, Nozawa M, Shimokawa K, Ishii F. Generic Selection Criteria for Safety and Patient Benefit [IV] Physicochemical and pharmaceutical properties of brand-name and generic ketoprofen tapes. *Drug Discov Ther.* 2015; 9:229-233.
15. Wada Y, Takaoka Y, Nozawa M, Goto M, Shimokawa K, Ishii F. Generic selection criteria for safety and patient benefit [VI]: Comparing the physicochemical and pharmaceutical properties of brand-name, generic, and OTC felbinac tapes. *Drug Discov Ther.* 2016; 10:300-306.
16. Nozawa M, Goto M, Wada Y, Yotsukura K, Gannichida A, Ishii F, Shimokawa K. Generic selection criteria for safety and patient benefit [VIII]: Comparing the physicochemical and pharmaceutical properties of brand-name and generic diclofenac sodium tapes. *Drug Discov Ther.* 2019; 13: 50-156.
17. Nozawa M, Goto M, Wada Y, Ishii F, Shimokawa K. Generic selection criteria for safety and patient benefit [X]: Watervapor permeability and peel force properties of brand-name and generic ketoprofen tapes. *Drug Discov Ther.* 2021; 15:87-92.
18. Shimokawa K, Yotsukura K, Nozawa M, Wada Y, Ishii F. Generic selection criteria for safety and patient benefit [XII]: Comparing the physicochemical and pharmaceutical properties of brand-name and generic tulobuterol tape. *Drug Discov Ther.* 2023; 17: 409-414.
19. Yanai H. 4 Steps Excel Statistics (4rd Edition). OMS Publishing, Saitama Japan, 2015. (in Japanese)
20. Ponmozhi J, Dhinakaran S, Varga-Medveczky Z, Fónagy K, Anna Bors L, Iván K, Erdő F. Development of skin-on-a-chip platforms for different utilizations: factors to be considered. *Micromachines.* 2021; 12:294-318.
21. Mizoguchi M, Ohara K, Aiba Y, Takado T, Hino H, Matsunaga K, Watanabe S. The pH of the skin. In: *Encyclopedia of skin.* Asakura Bookstore, Tokyo, 2008; pp. 24. (in Japanese)
22. Takahashi A, Yuasa S, Inomoto T, Hamada Y, Iwasawa T, Ebara F, Kunishima T, Takeoka H, Tsukamoto M, Yamashita K, Yamamoto H, Yanagawa C, Kamata H, Kanamori A. Report of a questionnaire survey of dermatologists about generic drugs in kanagawa prefecture, Japan. *Jpn Phys Assoc.* 2023; 38:146-150.

Received September 23, 2024; Revised October 16, 2024; Accepted October 17, 2024.

**Address correspondence to:*

Ken-ichi Shimokawa, Department of Pharmaceutical Sciences, Meiji Pharmaceutical University, 2-522-1, Noshio, Kiyose, Tokyo 204-8588, Japan.
E-mail: kshimoka@my-pharm.ac.jp

Released online in J-STAGE as advance publication October 24, 2024.

Mitotic abnormalities and spindle assembly checkpoint inactivation in a cell model of Shwachman-Diamond syndrome with mutations in the Shwachman-Bodian-Diamond syndrome gene, 258+2T > C

Yukihiro Sera, Tsuneo Imanaka*, Yusuke Iguchi, Masafumi Yamaguchi

Laboratory of Physiological Chemistry, Faculty of Pharmaceutical Sciences, Hiroshima International University, Hiroshima, Japan.

SUMMARY Hematologic abnormalities are the most common symptoms of Shwachman-Diamond syndrome (SDS). The causative gene for SDS is the Shwachman-Bodian-Diamond syndrome (*SBDS*) gene; however, the function of SBDS and pathogenesis of each condition in SDS are largely unknown. SBDS is known to be localized at mitotic spindles and stabilizes microtubules. Previously, we demonstrated that SBDS is ubiquitinated and subsequently degraded in the mitotic phase, thereby accelerating mitotic progression. In this study, we examined mitosis in a myeloid cell model of SDS (SDS cells). 4',6-Diamidino-2-phenylindole (DAPI)-stained chromosome observation and cell cycle analysis of nocodazole-synchronized cells revealed that the SDS cells have abnormally rapid mitosis. In addition, many lagging chromosomes and micronuclei were detected. Moreover, the phosphorylation of threonine tyrosine kinase, the crucial kinase of the spindle assembly checkpoint (SAC), was suppressed. Chromosomal instability caused by SAC dysfunction may cause a variety of clinical conditions, including hematologic tumors in patients with SDS.

Keywords Shwachman-Diamond syndrome, mitosis, chromosomal instability, spindle assembly checkpoint

1. Introduction

Shwachman-Diamond syndrome (SDS) is an autosomal recessive inherited disorder characterized by bone marrow failure and exocrine pancreatic insufficiency (1). Neutropenia is present in almost all patients with SDS and can lead to serious infections, including sepsis. In addition, SDS is associated with other life-threatening complications such as myelodysplastic syndrome (MDS) and acute myeloid leukemia (AML) (2-4). Patients with SDS usually present in infancy and have an average life expectancy of 30-40 years; however, the life expectancy of patients with hematologic disorders, such as those aforementioned, is significantly shorter (5,6).

The causative gene for SDS is the highly conserved Shwachman-Bodian-Diamond syndrome (*SBDS*) gene on chromosome 7 (7). The most widely accepted function of SBDS is ribosome biogenesis and ribosomal RNA metabolism (8,9). In addition, SBDS is reportedly involved in several biological processes including cellular stress responses, proliferation, and differentiation (10-12). SBDS has also been implicated in mitosis. Austin *et al.* showed that SBDS localizes to mitotic

spindles and stabilizes microtubules (13). In addition, Orelio *et al.* showed the similar mitotic localization of SBDS, which may be associated with cell proliferation (14). Furthermore, we previously showed that SBDS colocalizes with ring finger protein 2 (RNF2) on centrosomal microtubules in the mitotic phase (M phase) and that the ubiquitination and degradation of SBDS by RNF2 accelerate mitotic progression (15,16). However, the precise role of SBDS remains unknown.

To elucidate the function of SBDS and the pathogenesis of SDS, we established a cell model of SDS harboring a common *SBDS* variant at intron 2, 258+2T > C, using a murine myeloid cell line (17). The mutation results in an aberrant splicing at position 251-252, which generates a premature termination codon in the mRNA of SBDS and consequently produces a truncated, non-functional protein. We examined the cell division process and found that mitosis was abnormally rapid in these cells. In addition, many lagging chromosomes and micronuclei were detected. Furthermore, the spindle assembly checkpoint (SAC), which is essential for proper chromosome segregation, was inactivated. As improper chromosome segregation is associated with DNA

damage, cell death, and tumor cell malignancy, failure of this mitotic checkpoint may be a key factor in various hematologic conditions such as neutropenia, AML, and MDS in patients with SDS.

2. Materials and Methods

2.1. Antibodies, reagents

Anti-SBDS antiserum was prepared as previously described (18). Anti-cyclin B1 antibody (sc-245) and anti-pituitary tumor-transforming gene (PTTG) antibody (sc-56207) were obtained from Santa Cruz Biotechnology (Dallas, TX, USA). Anti-threonine tyrosine kinase (TTK) (phospho Thr676) antibody was from Wuhan Huamei Biotech (CSB-PA060023; Wuhan, Hubei, China). Anti-TTK antibody was from Affinity Biosciences (DF6969; Cincinnati, OH, USA). Anti-phospho-Ser/Thr-Pro mitotic protein monoclonal 2 (MPM-2) antibody (anti-MPM-2 antibody) was from Sigma (05-368; St. Louis, MO, USA). Anti- α -tubulin antibody (017-25031) and anti- β -actin antibody (281-98721) were from Wako Chemicals (Osaka, Osaka, Japan). The secondary antibodies for immunofluorescence were anti-rabbit IgG-FITC (sc-2012; Santa Cruz Biotechnology) and anti-mouse IgG-rhodamine (55539; Cappel Laboratories, Malvern, PA, USA). Nocodazole (NCZ; 036-18371) was from Wako Chemicals.

2.2. Cell culture

32Dcl3 cells were cultured in Iscove's Modified Dulbecco's Medium supplemented with fetal bovine serum and WEHI-3b conditioned medium (16). 32Dcl3 cell model of SDS (SDS cells) was established as previously described (17). SDS cells were transfected with pcDNA3.1/Flag-SBDS *via* electroporation, as required. The synchronization of cells to the G2/M phase was achieved through the overnight culturing of cells in the presence of 100 ng/mL NCZ.

2.3. Immunofluorescence and chromosome staining

Cells were attached to a microscope slide and subsequently fixed, permeabilized, and stained in accordance with the previously described procedure (16). Images were obtained using the LSM800 confocal microscope (Carl Zeiss Microscopy, White Plains, NY, USA).

2.4. Cell cycle analysis

Cell cycle analysis was performed as previously described (16). In brief, DNA in fixed cells was stained with propidium iodide (Wako Chemicals). DNA content was measured using the FACSCalibur flow cytometer (BD Biosciences, Franklin Lakes, NJ, USA).

2.5. Immunoblotting

Cells were lysed in extraction buffer (20 mM Tris-HCl, pH 7.5, 150 mM NaCl, 1 mM EDTA, 100 μ M sodium orthovanadate, 1% NP-40, 2 μ M leupeptin, 2 μ M pepstatin A, 1 mM phenylmethylsulfonyl fluoride, 5 nM calyculin A). Lysates were centrifuged at 20,000 g for 15 min at 4°C to remove debris. The cell extract was denatured by heating to 55°C for 10 min in sodium dodecyl sulfate loading buffer (50 mM Tris-HCl, pH 6.8, 100 mM dithiothreitol, 2% sodium dodecyl sulfate, 0.1% bromophenol blue, 10% glycerol), separated by sodium dodecyl sulfate-polyacrylamide gel electrophoresis, and electrotransferred to polyvinylidene fluoride membranes. The membranes were blocked in 1% bovine serum albumin in tris-buffered saline with Tween 20 (200 mM NaCl, 20 mM Tris-HCl, 0.05% Tween 20, pH 7.5), and then incubated with primary antibodies followed by horseradish peroxidase-conjugated anti-immunoglobulin secondary antibodies.

2.6. Micronucleus assay

Cells were treated with 100 ng/mL NCZ for 16 h to induce micronuclei. The cells were deposited to a slide glass by centrifugation at 40 g for 5 min (StatSpin Cytofuge 2; StatSpin, Norwood, MA, USA). Cell fixation, permeabilization, and staining of chromosomes were performed as for immunofluorescence. Images were acquired on the LSM800 confocal microscope (Carl Zeiss Microscopy). Nuclei that are completely independent of the main nucleus and sufficiently small compared to the main nucleus were identified as micronuclei.

3. Results

3.1. Abnormally rapid M phase progression in SDS cells

We previously reported an association between SBDS degradation and mitotic progression (16). Therefore, we examined the mitotic progression of the myeloblastic 32Dcl3 cell model of SDS harboring a common pathogenic *SBDS* variant in both alleles at intron 2, 258+2T > C (SDS cells). Wild-type (WT) and SDS cells were synchronized at the G2/M phase by NCZ treatment and collected every 15 min during mitosis. Cell cycle progression was analyzed by chromosome observation and flow cytometry analysis of DNA content. The observation of 4',6-diamidino-2-phenylindole (DAPI)-stained chromosomes revealed that SDS cells transitioned to anaphase earlier than WT cells (Figure 1A). Following the removal of NCZ, 51% of SDS cells had progressed to anaphase after 30 min, compared to 26% of WT cells (Figure 1B). Although no significant differences were obtained because the degree of progression of the mitotic phase differed in each experiment, the observed

trend exhibited a consistent pattern across all three experiments (Figure S1, <https://www.ddtjournal.com/action/getSupplementalData.php?ID=218>). Consistent with this result, SDS cells transitioned to G1 phase faster than WT cells after NCZ removal (Figure 1C and Figure S2, <https://www.ddtjournal.com/action/getSupplementalData.php?ID=218>). These results demonstrated that SDS cells had an abnormally rapid mitosis.

Another notable finding was that SDS cells exhibited incomplete G2/M arrest when treated with NCZ. Most WT cells treated with 100 ng/mL NCZ for 16 h stopped at the G2/M phase and only 1.25% of cells leaked into the G1 phase, whereas 3.97% of SDS cells leaked into the G1 phase (Figure S3, <https://www.ddtjournal.com/action/getSupplementalData.php?ID=218>). In addition, at 24 h after NCZ removal, many WT cells remained in the G2/M phase, whereas most SDS cells had already returned to the normal cell cycle (Figure S2, <https://www.ddtjournal.com/action/getSupplementalData.php?ID=218>). These findings indicate a reduced sensitivity to NCZ in SDS cells.

3.2. Chromosomal instability in SDS cells

In the previous chromosome observation experiment, we observed lagging chromosomes. This finding prompted us to determine the frequency of lagging chromosomes in mitosis. It has been reported that the formation of lagging chromosomes is enhanced in cells released from NCZ treatment (19). Indeed, several lagging chromosomes were observed during the chromosome observation experiment. Briefly, WT and SDS cells were synchronized at the G2/M phase by treatment with 100 ng/mL NCZ for 13 h, and then released into fresh medium. To recover the anaphase cells, SDS cells were collected 30 min after release from the NCZ block, and WT cells were collected 15 min later. Then DAPI-stained chromosomes were observed together with immunostained microtubules (Figure 2A). Cells undergoing chromosome segregation were counted to determine the percentage of cells with lagging chromosomes. Lagging chromosomes were observed in about half of the anaphase SDS cells and were almost twice as frequent in SDS cells as in WT cells (Figure 2B). Chromosomal instability seems to be increased in SDS cells.

3.3. SAC inactivation in SDS cells

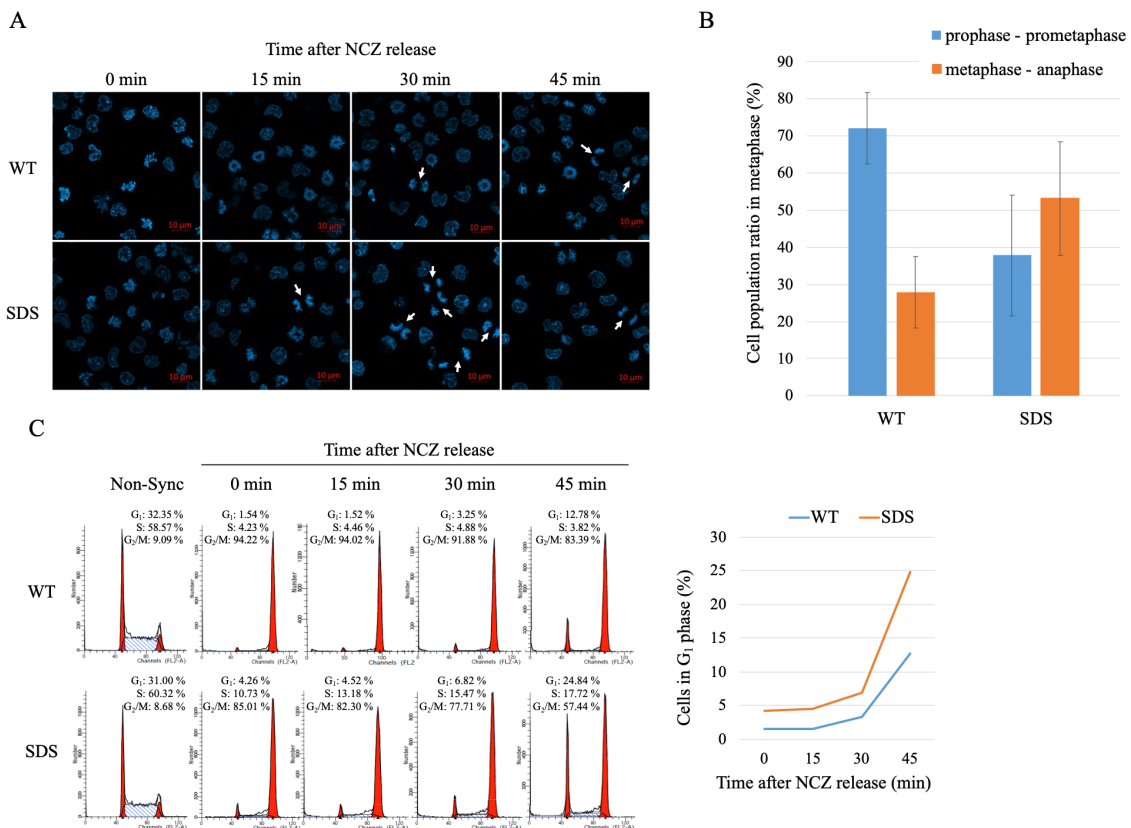


Figure 1. Abnormally rapid M phase progression in SDS cells. Cells were synchronized at the G2/M phase by treating with NCZ for 13 h, released into fresh medium, and harvested at the indicated time. (A) DAPI-stained chromosome observation. Prophase, in which chromosomes are cohesive; prometaphase, in which chromosomes are aligned in a ring; and anaphase, in which chromosomes are segregating (white arrows). (B) More than 50 mitotic cells were observed and the ratio of pre-metaphase to post-metaphase cells was calculated. The experiment was repeated three times. (C) Cell cycle analysis with propidium iodide. The percentage of cells transitioning from the M to G1 phase after NCZ removal was analyzed over time.

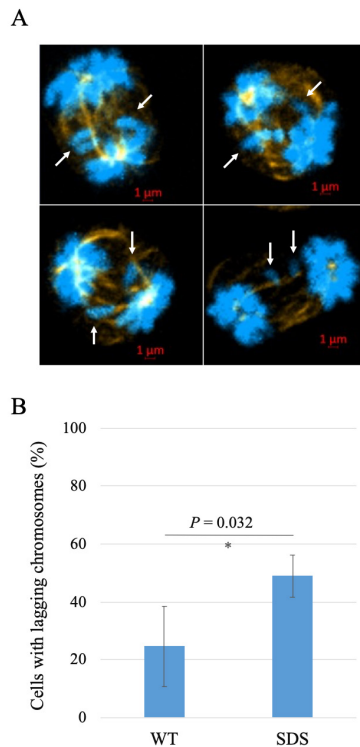


Figure 2. Increased frequency of NCZ-induced lagging chromosomes in SDS cells. (A) Lagging chromosomes (white arrows) detected in SDS cells after release from NCZ. (B) Approximately 50 anaphase cells were observed and the frequency of lagging chromosomes was calculated. The experiment was repeated three times.

NCZ, an inhibitor of microtubule polymerization, activates SAC and induces G2/M arrest in cells (20). The abnormally rapid mitosis, reduced sensitivity to NCZ, and especially, the increased number of lagging chromosomes led us to hypothesize that SAC may not be functioning properly in SDS cells. SAC monitors the attachment of spindle microtubules to kinetochores. Once the nuclear membrane disappears, the SAC leader kinase, TTK/monopolar spindle kinase 1, localizes to the kinetochore and is activated by autophosphorylation (21). Activated TTK on the unattached kinetochores phosphorylates a number of substrates and triggers the accumulation of SAC proteins, leading to formation of the mitotic checkpoint complex (MCC). MCC inhibits the anaphase-promoting complex/cyclosome (APC/C) E3 ubiquitin ligase. Once the SAC is satisfied, the APC/C is activated and initiates chromosome segregation through ubiquitination-mediated degradation of PTTG1/securin and cyclin B1 (22). First, we examined the activation of TTK in cells treated with NCZ. TTK phosphorylation was enhanced after NCZ treatment of WT cells, whereas it was drastically suppressed in SDS cells (Figure 3A). A similar trend was observed for the amounts of M phase-specific phosphoproteins recognized by the anti-MPM-2 antibody (Figure 3B). In addition, the substrates of APC/C, namely, PTTG1 and cyclin B1, were decreased from early mitosis in SDS cells (Figure 3C). These results suggest that SAC activation is attenuated in SDS cells.

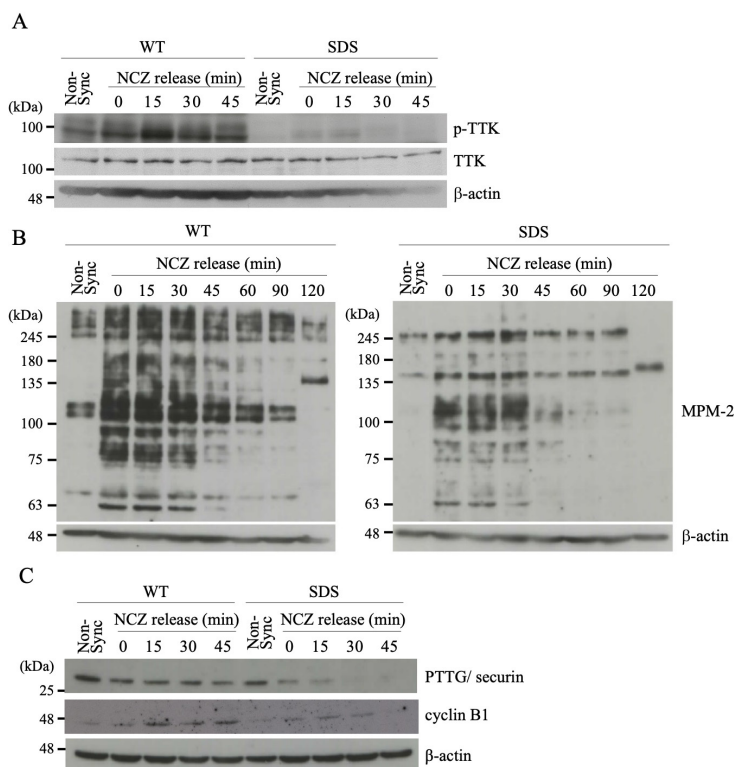


Figure 3. SAC inactivation in SDS cells. Cells were synchronized with NCZ treatment and harvested at the indicated time after release from NCZ. (A) Phosphorylated TTK, the master kinase in SAC, (B) a variety of mitosis-specific phosphoproteins detected by anti-MPM-2 antibody, and (C) PTTG/securin and cyclin B1, representative substrates of APC/C, were detected by immunoblotting.

3.4. SBDS required for SAC activation

SDS cells have mutations in the *SBDS* gene, resulting in a substantial reduction of SBDS protein expression. We overexpressed Flag-SBDS in SDS cells. Re-expression of SBDS in SDS cells increased the phosphorylation of TTK and other mitotic proteins upon NCZ treatment (Figure 4A). In addition, the abnormally rapid mitosis and reduced sensitivity to NCZ were improved (Figure 4B). Lagging chromosomes that are not incorporated into the main nucleus form micronuclei. In accordance with the observed increase in lagging chromosomes (Figure 2), the formation of micronuclei was also elevated in SDS cells, which was suppressed by the re-expression of SBDS in SDS cells (Figures 4C and 4D). These results indicate that SBDS is essential for proper functioning of the SAC. In addition, the mitotic localization of SBDS was examined in detail. The WT 32Dcl3 cells were harvested every 15 min after release from NCZ block and immunostained with the appropriate antibodies. Consistent with our report and others (13,14,16), SBDS was localized to the nucleolus in interphase and to the mitotic spindles in the M phase. The mitotic localization

was stronger from prometaphase to metaphase and weaker in anaphase (Figure S4, <https://www.ddtjournal.com/action/getSupplementalData.php?ID=218>). This change in SBDS localization coincides with the timing of SAC activation and inactivation, suggesting that SBDS coordinates with SAC activation.

4. Discussion

This is the first study to present evidence showing the inactivation of SAC in SBDS-downregulated cells and the involvement of SBDS in SAC activation. In 2008, localization of SBDS to the mitotic spindles and its contribution to the stabilization of the mitotic spindles were shown for the first time, but the contribution of SBDS to SAC was unclear as the cells lacking SBDS were arrested at the G2/M phase by treatment with NCZ, an activator of SAC (13). In our study, SDS cells with mutations in both *SBDS* alleles were also synchronized to the G2/M phase by NCZ treatment, but a fraction of the cells leaked into the G1 phase during G2/M arrest (Figure S3, <https://www.ddtjournal.com/action/getSupplementalData.php?ID=218>). In addition,

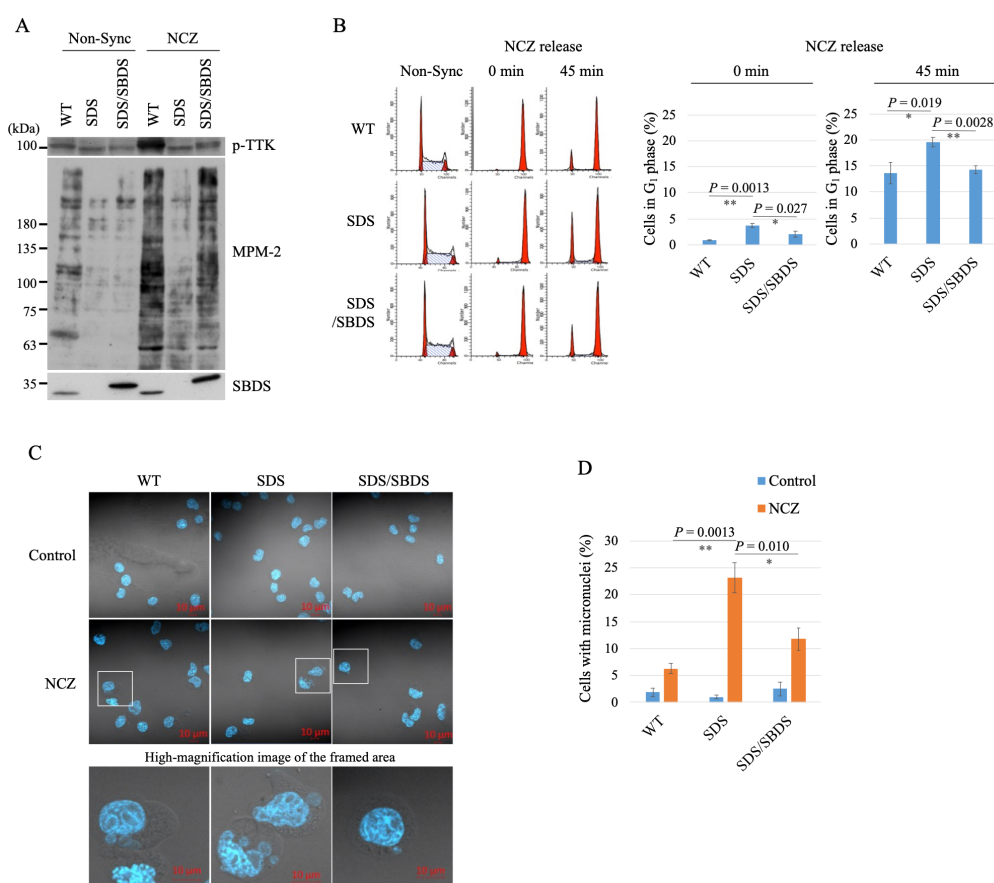


Figure 4. Re-expression of SBDS reactivates the SAC and normalizes mitosis in SDS cells. (A) Immunoblot analysis of phosphorylated TTK and mitosis-specific phosphoproteins detected by anti-MPM-2 antibody in WT, SDS, and SDS/SBDS cells. **(B)** Assessment of mitotic progression and NCZ sensitivity by cell cycle analysis. NCZ sensitivity was assessed by the percentage of cells that leaked into the G1 phase under G2/M arrest by NCZ treatment (NCZ release 0 min), and mitotic progression was assessed by the percentage of cells that transitioned to the G1 phase 45 min after release from NCZ block. **(C, D)** Evaluation of genomic instability by micronucleus assay. More than 100 cells were observed and the experiment was repeated three times.

after NCZ removal, the SDS cells immediately entered anaphase and then the G1 phase compared to WT cells (Figure 1). Furthermore, more lagging chromosomes were detected in the SDS cells (Figure 2). These results suggest that SAC, the surveillance mechanism to delay mitotic progression for accurate chromosome segregation, is not functioning properly in SDS cells. This is also supported by the fact that SDS cells returned to the normal cell cycle sooner than WT cells after NCZ removal (Figure S2, <https://www.ddtjournal.com/action/getSupplementalData.php?ID=218>). Indeed, the activation of TTK, the leader kinase of SAC, was suppressed in SDS cells (Figure 3A). These findings are consistent with the report that SAC inactivation through TTK inhibition significantly decreases the mitotic delay caused by NCZ treatment (23).

The SAC monitors microtubule attachment to the kinetochore and arrests the metaphase-anaphase transition until all microtubules have attached to the kinetochore (24). Therefore, an incomplete SAC leads to chromosome missegregation, which in turn leads to genomic instability and tumorigenesis. Mutations in SAC genes and alterations in the protein levels of SAC proteins have been reported in several human tumors including T-cell leukemia/lymphoma, B-cell lymphoma, and AML (25-27), which are often associated with SAC impairment, chromosomal instability, and even aneuploidy. Genomic instability has been found in primary bone marrow stromal cells derived from patients with SDS as well our established SDS cell model (13). In addition, hematologic malignancies such as AML and MDS are serious complications of SDS. SAC inactivation may contribute to genomic instability and tumorigenesis in SDS.

Most patients with SDS have variants of *SBDS*. The most common combination of mutations is 183-184TA>CT/ 258+2T>C (50%), followed by the 258+2T>C/ missense mutation (27.8%) (7). The mutations result in a decrease of SBDS protein. Although little is known about the function of SBDS, it is well known that SBDS is localized to the nucleolus for the assembly of mature ribosomes and ribosome biogenesis in the interphase. SBDS binds to microtubules and stabilizes the mitotic spindles in the M phase. In addition, here we revealed that SBDS is localized to the mitotic spindles, particularly in the prometaphase to metaphase interval, which is associated with the activation of SAC (Figure S4, <https://www.ddtjournal.com/action/getSupplementalData.php?ID=218>). SBDS may support the activation of SAC by stabilizing microtubules and inhibiting the initiation of chromosome segregation until all of the spindles are bound to the chromosomes. On the other hand, the interaction between SBDS and M phase-specific polo-like kinase 1 (PLK1)-interacting protein (MPLKIP) has been reported (28). PLK1, the mitotic binding partner of MPLKIP, is a kinase

that phosphorylates TTK and other SAC proteins to promote SAC signaling. SBDS may regulate PLK1 activity through the SBDS-MPLKIP-PLK1 interaction. At present, it is unclear whether there is a link between spindle stabilization and SAC activation.

In conclusion, we found that SAC does not function properly in SDS cells, resulting in chromosomal instability. Additionally, our results also suggest that SBDS contributes to SAC activation by some mechanism. Further studies focusing on this mitotic checkpoint, which is essential for chromosome stability, may help elucidate the pathogenesis of neutropenia, AML, and MDS, which are important pathological conditions in SDS. Our findings provide new perspectives for therapeutic drug development in SDS.

Funding: None.

Conflict of Interest: The authors have no conflicts of interest to disclose.

References

1. Shwachman H, Diamond LK, Oski FA, Khaw KT. The syndrome of pancreatic insufficiency and bone marrow dysfunction. *J Pediatr.* 1964; 65:645-663.
2. Woods WG, Roloff JS, Lukens JN, Krivit W. The occurrence of leukemia in patients with the Shwachman syndrome. *J Pediatr.* 1981; 99:425-428.
3. Dror Y, Squire J, Durie P, Freedman MH. Malignant myeloid transformation with isochromosome 7q in Shwachman-Diamond syndrome. *Leukemia.* 1998; 12:1591-1595.
4. Donadieu J, Leblanc T, Bader Meunier B, *et al.* Analysis of risk factors for myelodysplasias, leukemias and death from infection among patients with congenital neutropenia. Experience of the French Severe Chronic Neutropenia Study Group. *Haematologica.* 2005; 90:45-53.
5. Furutani E, Liu S, Galvin A, *et al.* Hematologic complications with age in Shwachman-Diamond syndrome. *Blood Adv.* 2022; 6:297-306.
6. Myers KC, Furutani E, Weller E, *et al.* Clinical features and outcomes of patients with Shwachman-Diamond syndrome and myelodysplastic syndrome or acute myeloid leukaemia: a multicentre, retrospective, cohort study. *Lancet Haematol.* 2020; 7:e238-e246.
7. Boocock GR, Morrison JA, Popovic M, Richards N, Ellis L, Durie PR, Rommens JM. Mutations in *SBDS* are associated with Shwachman-Diamond syndrome. *Nat Genet.* 2003; 33:97-101.
8. Ganapathi KA, Austin KM, Lee CS, Dias A, Malsch MM, Reed R, Shimamura A. The human Shwachman-Diamond syndrome protein, SBDS, associates with ribosomal RNA. *Blood.* 2007; 110:1458-1465.
9. Weis F, Giudice E, Churcher M, Jin L, Hilcenko C, Wong CC, Traynor D, Kay RR, Warren AJ. Mechanism of eIF6 release from the nascent 60S ribosomal subunit. *Nat Struct Mol Biol.* 2015; 22:914-919.
10. Rujkijyanont P, Watanabe K, Ambekar C, Wang H, Schimmer A, Beyene J, Dror Y. SBDS-deficient cells undergo accelerated apoptosis through the Fas-pathway.

- Haematologica. 2008; 93:363-371.
11. Nihrane A, Sezgin G, Dsilva S, Dellorusso P, Yamamoto K, Ellis SR, Liu JM. Depletion of the Shwachman-Diamond syndrome gene product, SBDS, leads to growth inhibition and increased expression of OPG and VEGF-A. *Blood Cells Mol Dis*. 2009; 42:85-91.
 12. Rawls AS, Gregory AD, Woloszynek JR, Liu F, Link DC. Lentiviral-mediated RNAi inhibition of Sbds in murine hematopoietic progenitors impairs their hematopoietic potential. *Blood*. 2007; 110:2414-2422.
 13. Austin KM, Gupta ML, Jr., Coats SA, Tulpule A, Mostoslavsky G, Balazs AB, Mulligan RC, Daley G, Pellman D, Shimamura A. Mitotic spindle destabilization and genomic instability in Shwachman-Diamond syndrome. *J Clin Invest*. 2008; 118:1511-1518.
 14. Orelia C, Verkuijlen P, Geissler J, van den Berg TK, Kuijpers TW. SBDS expression and localization at the mitotic spindle in human myeloid progenitors. *PLoS One*. 2009; 4:e7084.
 15. Sera Y, Sadoya M, Ichinose T, Matsuya S, Imanaka T, Yamaguchi M. SBDS interacts with RNF2 and is degraded through RNF2-dependent ubiquitination. *Biochem Biophys Res Commun*. 2022; 598:119-123.
 16. Sera Y, Imanaka T, Yamaguchi M. M phase-specific interaction between SBDS and RNF2 at the mitotic spindles regulates mitotic progression. *Biochem Biophys Res Commun*. 2023; 682:118-123.
 17. Sera Y, Yamamoto S, Mutou A, Koba S, Kurokawa Y, Imanaka T, Yamaguchi M. *SBDS* Gene mutation increases ROS production and causes DNA damage as well as oxidation of mitochondrial membranes in the murine myeloid cell line 32Dcl3. *Biol Pharm Bull*. 2024; 47:1376-1382.
 18. Yamaguchi M, Fujimura K, Toga H, Khwaja A, Okamura N, Chopra R. Shwachman-Diamond syndrome is not necessary for the terminal maturation of neutrophils but is important for maintaining viability of granulocyte precursors. *Exp Hematol*. 2007; 35:579-586.
 19. Cimini D, Tanzarella C, Degraffi F. Differences in malsegregation rates obtained by scoring ana-telophases or binucleate cells. *Mutagenesis*. 1999; 14:563-568.
 20. Hoyt MA, Totis L, Roberts BT. *S. cerevisiae* genes required for cell cycle arrest in response to loss of microtubule function. *Cell*. 1991; 66:507-517.
 21. Pachis ST, Kops G. Leader of the SAC: molecular mechanisms of Mps1/TTK regulation in mitosis. *Open Biol*. 2018; 8:180109.
 22. Thornton BR, Toczyski DP. Securin and B-cyclin/CDK are the only essential targets of the APC. *Nat Cell Biol*. 2003; 5:1090-1094.
 23. Novais-Cruz M, Alba Abad M, van IWF, Galjart N, Jeyaprakash AA, Maiato H, Ferras C. Mitotic progression, arrest, exit or death relies on centromere structural integrity, rather than de novo transcription. *Elife*. 2018; 7:e36898.
 24. McAinsh AD, Kops G. Principles and dynamics of spindle assembly checkpoint signalling. *Nat Rev Mol Cell Biol*. 2023; 24:543-559.
 25. Ohshima K, Haraoka S, Yoshioka S, Hamasaki M, Fujiki T, Suzumiya J, Kawasaki C, Kanda M, Kikuchi M. Mutation analysis of mitotic checkpoint genes (hBUB1 and hBUBR1) and microsatellite instability in adult T-cell leukemia/lymphoma. *Cancer Lett*. 2000; 158:141-150.
 26. Ru HY, Chen RL, Lu WC, Chen JH. hBUB1 defects in leukemia and lymphoma cells. *Oncogene*. 2002; 21:4673-4679.
 27. Schnerch D, Schmidts A, Follo M, Udi J, Felthaus J, Pfeifer D, Engelhardt M, Wasch R. BubR1 is frequently repressed in acute myeloid leukemia and its re-expression sensitizes cells to antimetabolic therapy. *Haematologica*. 2013; 98:1886-1895.
 28. Havugimana PC, Hart GT, Nepusz T, *et al*. A census of human soluble protein complexes. *Cell*. 2012; 150:1068-1081.
- Received October 2, 2024; Revised October 17, 2024; Accepted October 21, 2024.
- *Address correspondence to:*
Tsuneo Imanaka, Laboratory of Physiological Chemistry, Faculty of Pharmaceutical Sciences, Hiroshima International University, Hirokoshingai 5-1-1, Kure, 737-0112, Japan.
E-mail: imanaka@hirokoku-u.ac.jp
- Released online in J-STAGE as advance publication October 26, 2024.

Histopathological analysis of filament formation of *Nocardia farcinica* in a silkworm infection model

Koki Iwata^{1,2}, Mizuho Sato³, Shoko Yoshida³, Hiroo Wada⁴, Kazuhisa Sekimizu^{5,6}, Mitsuhiro Okazaki^{1,3,*}

¹ Graduate School of Clinical Technology, Tokyo University of Technology, Tokyo, Japan;

² Department of RNA Pathobiology and Therapeutics, Meiji Pharmaceutical University, Tokyo, Japan;

³ Department of Medical Technology, School of Health Sciences, Tokyo University of Technology, Tokyo, Japan;

⁴ Department of Public Health & Division of Medical Education, Juntendo University Graduate School of Medicine, Tokyo, Japan;

⁵ Drug Discoveries by Silkworm Models, Faculty of Pharma-Science, Teikyo University, Tokyo, Japan;

⁶ Genome Pharmaceuticals Institute, Tokyo, Japan.

SUMMARY The silkworm *Nocardia* infection model has been established as a useful animal model for screening the pathogenicity of *Nocardia* and evaluating the therapeutic effects of antimicrobial agents against *Nocardia* infection. No histopathological analysis of silkworms infected with *Nocardia farcinica* has yet been performed. In this study, we performed histological analyses on organs of silkworms infected with *N. farcinica*. One day after infection with *N. farcinica*, the organism developed a branching filamentous form from coccid cells in the hemolymph. In addition, we evaluated effective doses (ED₅₀) values by treating infected silkworms with amikacin 30 seconds and 24 hours after infection and found that the ED₅₀ values treated within 30 seconds and 24 hours after infection were 4.1 µg/larva and 5.6 µg/larva, respectively. Evaluation of treatment with amikacin against the infected silkworms was unaffected by the growth process form of *Nocardia*. These results suggest that the silkworm *Nocardia* infection model is a useful tool for evaluating the antimicrobial therapy in the growth process of the *N. farcinica*.

Keywords *Nocardia farcinica*, silkworm, filament, amikacin, infection

1. Introduction

Nocardia farcinica, a ubiquitous bacterial species in an environment such as soil organic material and water (1), is an important opportunistic pathogen, causing infections in the lung, blood, and central nervous system sites in immunocompromised patients (2,3). In addition, nocardial brain abscesses by *N. farcinica* rarely occur in healthy individuals (4). This organism is more likely to cause disseminated infection and higher mortality than other *Nocardia* species (5-7). The whole-genome sequencing identified virulence factors in the organism, including genes responsible for antimicrobial resistance and virulence (8,9). However, current research on pathogenesis and virulence using a mouse model on this organism is limited (10). In addition, although an antimicrobial susceptibility test is necessary for selecting antimicrobial agents for infection by *N. farcinica*, the correlation between the results of an *in vitro* antimicrobial susceptibility test and the *in vivo* response to antimicrobial therapy in patients with

Nocardia infection has not been adequately investigated (11). These problems are due to very few reports of experimental infections with this organism in a mouse model.

Animal experiments using mice and other mammalian models have contributed to the development of pathological analysis, drug discovery, and medicine related to human diseases (12). However, high costs and ethical considerations have been a hindrance to international experimentation with mammalian infections (13,14), so it is desirable to develop an experimental animal model that can serve as an alternative to mammals. For this purpose, invertebrate larvae, such as the Waxworm (*Galleria mellonella*), the Hornworm (*Manduca sexta*), and the cotton bollworm (*Helicoverpa armigera*) have attracted attention as alternative models for mice (13,15,16), and the silkworm (*Bombyx mori*) is one of non-mammalian animals (13).

Silkworms can be reared in a small space at low cost and used for experiments on large numbers of individuals, and they grow to a size that can be used for

experiments after about three weeks of rearing (13,17,18). Silkworm infection models have been established to date for various pathogenic microorganisms, including *Staphylococcus aureus*, *Pseudomonas aeruginosa*, and *Bacillus anthracis* (13,19), as well as *Aspergillus fumigatus* and *Cryptococcus neoformans* (20,21). A silkworm *Nocardia* infection model has been established for the evaluation of pathogenicity of *N. farcinica* (22). However, the focal area of *N. farcinica* in the silkworm *Nocardia* infection model is not identified. Histopathological analysis is a direct method of revealing the causal relationship between a lesion and its cause. Recently, those silkworm infection models have yielded to histopathological analyses, to identify and observe the focal site of infection (20,23,24), however, not with *N. farcinica*.

The aims of the present study were to observe the accumulation of *N. farcinica* in the hemolymph of infected silkworms using histopathological analysis, then to elucidate if changes in the filament morphology of the organism over time could be observed. We finally determined the utility of the silkworm *Nocardia* infection model, which may represent a potentially useful tool for studying the mechanisms of the growth process of *N. farcinica* in infected lesions.

2. Materials and Methods

2.1. Bacterial strain, culture condition, and adjustment of bacterial cell suspension

The *N. farcinica* TUTN006 strain was used in this study. This strain was stored at -80°C in a microbank tube (Iwaki & Co., Ltd., Tokyo, Japan) and cultured on a brain heart infusion agar plate (BHI, Eiken Chemical Co., Ltd., Tokyo, Japan) under CO₂ conditions at 37°C for 72 h. The colonies grown on the BHI agar plate were picked up using a 10 µg loop, suspended in sterile 1 mm glass beads (Fuji Manufacturing Co., Ltd., Tokyo, Japan) and 4 mL sterile saline (Otsuka Pharmaceutical Co., Ltd., Tokyo, Japan), and after 3 minutes of vortex and adjusted to OD₆₀₀=2.5~2.6 using a UVmini-1240 spectrophotometer (Shimadzu Co., Ltd., Kyoto, Japan). The bacterial cell suspension was diluted 100-fold using sterile saline, and used for silkworm infection experiments.

2.2. Silkworm rearing

Silkworm eggs were purchased from Ehime Sansyu Co. LTD (Ehime, Japan), disinfected, and reared at 27°C. The silkworms were fed Silkmate 2S (Katakura Industries Co., Ltd., Tokyo, Japan) until they developed the fifth molted larva. Fifth-instar larvae were fasting for 24 h and used for the infection experiment.

2.3. Silkworm infection experiment

An experimental protocol on producing silkworm infection models were described elsewhere (22). Briefly, either 50 µL bacterial cell suspension of *N. farcinica* TUTN006 cells (3.2×10^6 cells per larva) or saline (the control group) was administered to the silkworm hemolymph by injecting the silkworm dorsally using a 1 ml tuberculin syringe (Terumo Medical CO., Ltd., Tokyo, Japan). The amount of bacteria inoculated into silkworms was measured by plating the used bacterial cell suspension on the BHI agar plate. After inoculation, silkworms were reared in incubators at 25-27°C without feeding and observed over time.

2.4. Histopathological analysis

Silkworms were fixed at 15, 18, 24, 28 and 40 hours after inoculation of bacterial cell suspension. Tissue specimens of silkworms fixed in 10% neutral buffered formalin (Fujifilm Wako Pure Chemicals Co., Ltd., Osaka, Japan) were prepared according to standard pathology physiological techniques. Briefly, for fixation, silkworms were placed on ice in a state of suspended animation, wrapped in gauze as they were to prevent bending, and then immersed in 10% neutral buffered formalin for 72 hours while pinned to an eraser. After fixation was completed, silkworms were cut out by inserting a blade from the dorsal side and slicing them into rings. After paraffin embedding, sections were thinned to 3 µm thickness, pasted onto Super Frost (Matsunami Glass Industries Co., Ltd., Osaka, Japan), stretched at 50°C, and dried at 37°C. Each paraffin section was deparaffinized, de-xyleneated, and rinsed under running water, and then staining of each was performed. Hematoxylin-eosin (HE) staining was performed by staining with Carracci's hematoxylin for 7 minutes, fractionating and coloring with 1% hydrochloric alcohol, rinsing, passing through distilled water, staining with eosin for 3 minutes, dehydrating, permeabilizing, and encapsulation. The specimens were stained with Gram staining (Hucker) methods (Muto Chemical Co., Ltd., Tokyo, Japan), and sealed in xylene. After staining, each specimen was observed and photographed using an Olympus BX43 (Olympus Co., Ltd., Tokyo, Japan) and Olympus DP21 (Olympus Co., Ltd., Tokyo, Japan) optical microscope. For some specimens, the virtual slide scanner NanoZoomer (Hamamatsu Photonics K.K., Shizuoka, Japan) was used to convert the histopathology slides into image data.

2.5. Assessment of survival rates and ED₅₀ values in the infected silkworms to injection of amikacin at two points in time

The *N. farcinica* TUTN006 strain suspension (3.5×10^7 CFU/larva•g in 50 µL saline) was injected into the hemolymph of silkworms, followed by an injection of various amounts (1.0, 2.0, 4.1, 5.4, 8.1, 16.25, 43, 65

and 130 µg/larva) of amikacin (FUJIFILM Wako Pure Chemical CO., Ltd., Osaka, Japan) within 30 seconds and 24 hours (the reference group). Silkworms were kept without feeding in an incubator at 27°C. Each group had 20 silkworms. The survival rate of silkworms after infection was determined at 48 hours. Next, the ED₅₀ values were determined as the amount of amikacin of silkworms required for a 50% survival rate at 72 hours post-infection. To confirm the dilution concentrations of amikacin, the quality control strains used in this study include *Staphylococcus aureus* ATCC 29213 and *Escherichia coli* ATCC 25922.

3. Results

3.1. Histopathological analysis of the silkworm *Nocardia* infection model

No tissue damage was observed in the infected silkworms compared with non-infected controls (Figure 1). In the HE stained tissue specimen of the silkworms with infection, bacteria were found in the hemolymph, and showed filamentous branching bacilli (Figure 1). The formation of filament morphology of the bacterium indicated that the bacterium had established and grown in the hemolymph. The location of the filament morphology of the bacterium was mainly around the fat body in the hemolymph, not in the muscular and capsular cell layer of the mid-gut, and no invasion into the fat body tissue was observed.

Next, we analyzed the histopathological finding of the silkworms infected with *N. farcinica* TUTN006 at various time points. Gram staining of thin sections showed the Gram-positive, filamentous branching bacilli and beaded structure at 15-40 hours after inoculation with the bacterial cell suspension, whereas none of the control silkworms. Compared to druse at 15 hours (Figure 1d), the size of druse was observed to grow over time more than twice with growing filamentation (Figures 1e-h). In addition, bacterial cells surrounded a granule-like mass, which disappeared over time.

3.2. Effect of different time amikacin inoculation on silkworm survival

Silkworms in the reference group, which was inoculated with bacterial cell suspension alone, started to die at 48 hours after inoculation, and all the silkworms died after 72 hours, whereas all the silkworms in the sterile saline (control) and amikacin inoculation groups survived (Figure 2). These results indicate that the effect of administration of bacterial cell suspension alone on the survival of silkworms tended to increase with time after 48 hours, while that of amikacin alone did not.

Next, we evaluated silkworm survival rates by inoculating infected silkworms with amikacin within 30 seconds and 24 hours (Figure 2). In the group of silkworms inoculated with amikacin 24 hours later, mortality increased predominantly at high amikacin concentrations (more over 16.5 µ/mL).

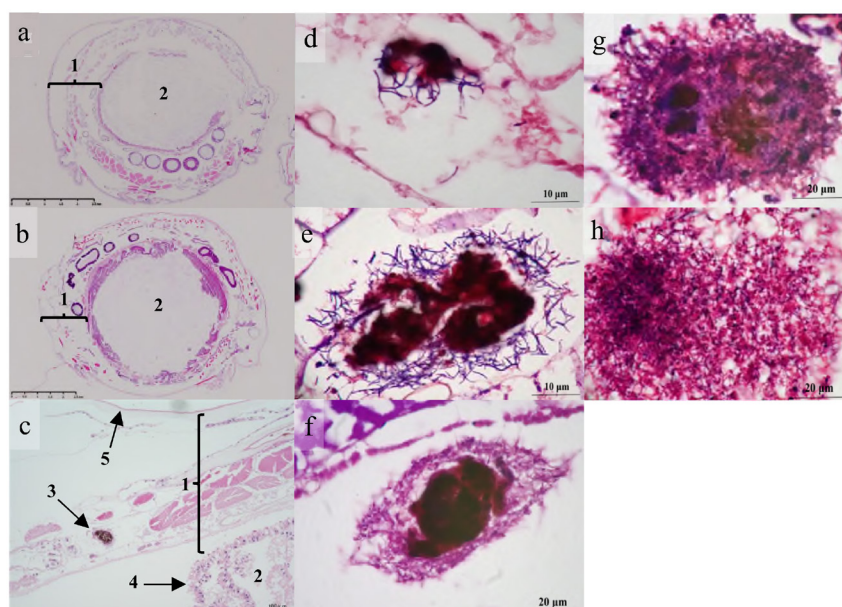


Figure 1. Histopathological analysis. Hematoxylin-eosin staining (100× magnification) was shown non-infected with *N. farcinica* TUTN006 strain (control, a) and infected with *N. farcinica* TUTN006 strain (b). (1) Hemolymph. (2) Gut lumen. No tissue damage was observed in the infected silkworms. Hematoxylin-eosin staining and observed under a microscope (200 × magnification) was showed infected with *N. farcinica* TUTN006 strain (c). (1) Hemolymph. (2) Gut lumen. (3) Branching bacilli. (4) Intestinal membrane cell layer. (5) Skin. Bacteria were found in the hemolymph, and showed filamentous branching bacilli. Gram staining (1000 × magnification) was showed at 15 (d), 18 (e), 24 (f), 28 (g), and 40 (h) hours after infection showing the Gram-positive, filamentous branching bacilli and beaded structure. Bacterial cells surrounded a granule-like mass.

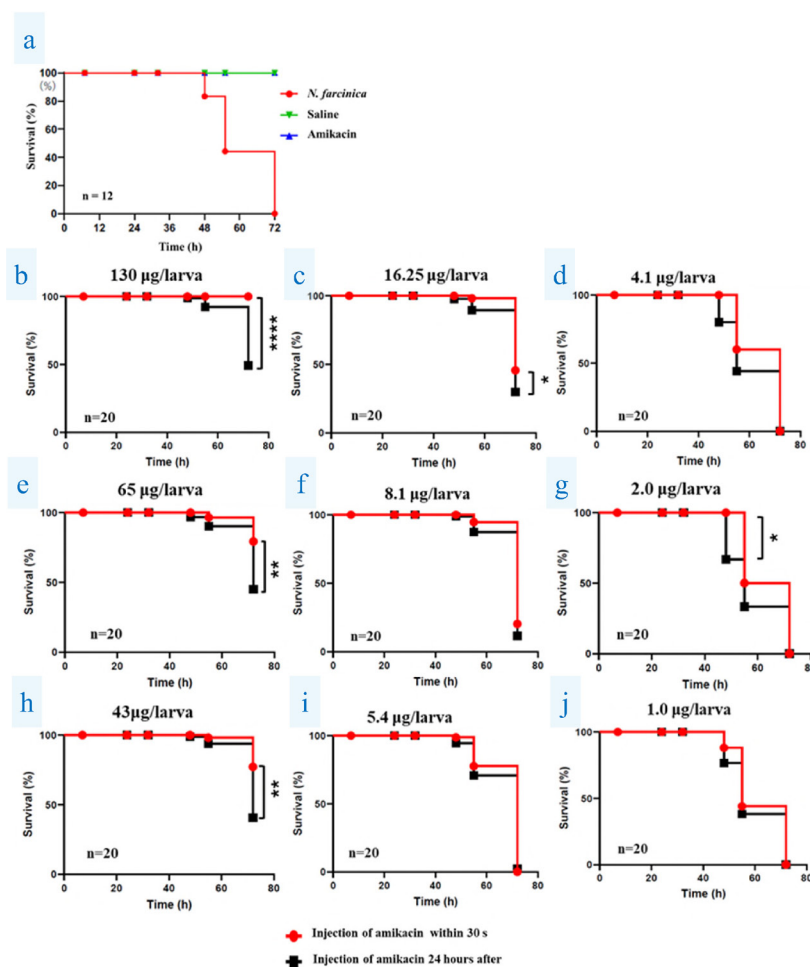


Figure 2. Evaluation of survival rates. Silkworms were injected with saline (50 µL) (control), *N. farcinica* TUTN006 strain cell suspension (1.75×10^7 cells per 50 µL) or amikacin (130 µg/larva) at 27°C, (a) The survival curves were drawn using the Kaplan-Meier method. Evaluation of survival rates. Silkworms were injected with *N. farcinica* TUTN006 cell suspension (1.75×10^7 cells per 50 µL). Amikacin at 1.0-130 µg/larva was then administered within 30 seconds or 24 hours after (b-j). The survival curves were drawn using the Kaplan-Meier method. Each symbol indicates the following: * $P < 0.05$; ** $P < 0.01$; *** $P < 0.001$; **** $P < 0.0001$.

3.3. ED₅₀ values in the infected silkworms to amikacin inoculation at two points time

We evaluated ED₅₀ values by inoculating infected silkworms with amikacin 30 seconds and 24 hours after infection. The ED₅₀ values of inoculation within 30 seconds and 24 hours of amikacin were 4.1 µg/larva and 5.6 µg/larva, respectively. These results are consistent with our previously reported results (22) and are reproducible.

4. Discussion

In this study, our histopathological analyses demonstrated that *N. farcinica* develops filamentous forms *in vivo* in the silkworm *Nocardia* infection model. To our knowledge, this study is the first report to demonstrate the filamentous forms of *Nocardia* species *in vivo* in the silkworm. It was found in the present study that the coccoid form of *Nocardia* is transformed into a

filamentous form during the growth process. This is one of the characteristics of *Nocardia* transformation (25,26). *N. farcinica* is often observed as branched bacterial filaments by Gram staining in clinical specimens from patients with nocardiosis (27,28). The study using a mouse model similarly developed a filamentous form (29). Therefore, the growth process of *Nocardia* in the silkworm infection model was consistent with that reported in the mouse model. The form of coccid and filament in *Nocardia* has been shown to undergo both complex structural and chemical modification (30). These changes in structure have significant effects on nocardial virulence and host-parasite interactions. Virulence and toxicity in the filamentous form were consistently stronger than the coccoid cells in the study using the infected mouse model (31-33).

In this study, silkworms started to die after 48 hours when the filament morphology of the organism becomes larger. This finding suggests that the growth of filamentation may contribute to survival in the silkworm

infection model. The silkworm *Nocardia* infection model may be a useful alternative to the mouse model for studying the pathogenicity *in vivo* form during the growth process of *Nocardia*. However, the tissue damage in silkworms, unlike a murine model, was quite limited in the present study, suggesting that silkworms may secrete protective agents or maintain their immune system against *Nocardia* infection, which may be elucidated by further molecular analysis.

The morphology of the organism at the lesion site in patients with *N. farcinica* infection is a filamentous form (27,34-36). Therefore, antimicrobial therapy in many cases is directed against filamentous forms of the organism. However, no quantitative evaluation of the effectiveness of antimicrobials against filamented organisms has been reported to date. Also, no studies were identified that evaluated the therapeutic effects of antimicrobial agents against filamentous forms of *Nocardia* in mice. Thus, this study demonstrated that the silkworm *Nocardia* infection model is able to quantitatively evaluate the therapeutic effect of amikacin against filamentous forms. In addition, the evaluation of the therapeutic effect of amikacin by differences in morphology of the coccoid forms and filamentous form of *Nocardia* was consistent. This trend in humans was consistent with that reported in Nocardiosis in Japan (37). Therefore, the silkworm model is useful for evaluating the therapeutic effectiveness of antimicrobial agents adapted to various morphological changes in *Nocardia* infections. Furthermore, the survival rate of silkworms in the high-concentration amikacin-only inoculation group was the same as that in the sterile saline-only group, and it maintained a high survival rate of silkworms. Therefore, high concentrations of amikacin are not toxic to silkworms. However, we found that groups of silkworms inoculated with high concentrations of amikacin after 24 hours in the infected silkworms had significantly higher mortality rates. These findings raised the following possibilities: the administration of high concentrations of amikacin is effective in the early stages of *Nocardia* infection, but it may weaken the host's resistance to infection once the infection has progressed. The establishment of a silkworm model for the purpose of screening for the side effects of antibiotics will be an important future research topic.

The present study was able to reproduce the bacterial morphology of *N. farcinica* in the silkworm *Nocardia* infection model over time. We further speculated that this model has the potential for a more clinical assessment of antimicrobial efficacy against morphological changes of *Nocardia* in antimicrobial susceptibility testing.

Funding: HW is supported by Kobayashi Foundation.

Conflict of Interest: The authors have no conflicts of interest to disclose.

References

1. Brown-Elliott BA, Brown JM, Conville PS, Wallace Jr RJ. Clinical and laboratory features of the *Nocardia* spp. based on current molecular taxonomy. Clin Microbiol Rev. 2006; 19:259-282.
2. Budzik JM, Hosseini M, Mackinnon Jr AC, Taxy JB. Disseminated *Nocardia farcinica*: literature review and fatal outcome in an immunocompetent patient. Surg Infect (Larchmt). 2012; 13:163-170.
3. Torres OH, Domingo P, Pericas R, Boiron P, Montiel JA, Vázquez G. Infection caused by *Nocardia farcinica*: case report and review. Eur J Clin Microbiol Infect Dis. 2000; 19:205-212.
4. Tamarit M, Poveda P, Barón M, Del Pozo JM. Four cases of nocardial brain abscess. Surg Neurol Int. 2012; 3:88.
5. Lerner PI. Nocardiosis. Clin Infect Dis. 1996; 22:891-905.
6. Lee EK, Kim J, Park DH, Lee CK, Kim SB, Sohn JW, Yoon YK. Disseminated nocardiosis caused by *Nocardia farcinica* in a patient with colon cancer: a case report and literature review. Medicine (Baltimore). 2021; 100:e26682.
7. Koenig S, Mehlich AM, Ackermann D, Hamid ME, Saeed NS, Mukhtar M, El Hassan M. Homologous housekeeping proteins in *Nocardia*--the NoDaMS proteomic database. Front Biosci. 2008; 13:842-855.
8. Ishikawa J, Yamashita A, Mikami Y, Hoshino Y, Kurita H, Hotta K, Shiba T, Hattori M. The complete genomic sequence of *Nocardia farcinica* IFM 10152. Proc Natl Acad Sci U S A. 2004; 101:14925-14930.
9. Nathar S, Rajmichael R, Jeyaraj Pandian C, Nagarajan H, Mathimaran A, Kingsley JD, Jeyaraman J. Exploring *Nocardia*'s ecological spectrum and novel therapeutic frontiers through whole-genome sequencing: unraveling drug resistance and virulence factors. Arch Microbiol. 2024; 206:76.
10. Desmond EP, Flores M. Mouse pathogenicity studies of *Nocardia asteroides* complex species and clinical correlation with human isolates. FEMS Microbiol Lett. 1993; 110:281-284.
11. McTaggart LR, Doucet J, Witkowska M, Richardson SE. Antimicrobial susceptibility among clinical *Nocardia* species identified by multilocus sequence analysis. Antimicrob Agents Chemother. 2015; 59:269-275.
12. Goodwin FK. From the alcohol, drug abuse, and mental health administration. JAMA. 1991; 266:1056.
13. Kaito C, Murakami K, Imai L, Furuta K. Animal infection models using non-mammals. Microbiol Immunol. 2020; 64:585-592.
14. Cheluvappa R, Scowen P, Eri R. Ethics of animal research in human disease remediation, its institutional teaching; and alternatives to animal experimentation. Pharmacol Res Perspect. 2017; 5:e00332.
15. Ahlawat S, Sharma KK. Lepidopteran insects: emerging model organisms to study infection by enteropathogens. Folia Microbiol (Praha). 2023; 68:181-196.
16. Ménard G, Rouillon A, Cattoir V, Donnio PY. *Galleria mellonella* as a suitable model of bacterial infection: past, present and future. Front Cell Infect Microbiol. 2021; 11:782733.
17. Panthee S, Paudel A, Hamamoto H, Sekimizu K. Advantages of the silkworm as an animal model for developing novel antimicrobial agents. Front Microbiol. 2017; 8:373.

18. Matsumoto Y, Fukano H, Hasegawa N, Hoshino Y, Sugita T. Quantitative evaluation of *Mycobacterium abscessus* clinical isolate virulence using a silkworm infection model. PLoS One. 2022; 17:e0278773.
19. Paudel A, Furuta Y, Higashi H. Silkworm model for *Bacillus anthracis* infection and virulence determination. Virulence. 2021; 12:2285-2295.
20. Majima H, Arai T, Kamei K, Watanabe A. *In vivo* efficacy of pitavastatin combined with itraconazole against *Aspergillus fumigatus* in silkworm models. Microbiol Spectr. 2023; 11:e0266623.
21. Ishii M, Matsumoto Y, Sekimizu K. Usefulness of silkworm as a host animal for understanding pathogenicity of *Cryptococcus neoformans*. Drug Discov Ther. 2016; 10:9-13.
22. Mikami K, Sonobe K, Ishino K, Noda T, Kato M, Hanao M, Hamamoto H, Sekimizu K, Okazaki M. Evaluation of pathogenicity and therapeutic effectiveness of antibiotics using silkworm *Nocardia* infection model. Drug Discov Ther. 2021; 15:73-77.
23. Suehiro Y, Nomura R, Matayoshi S, Otsugu M, Iwashita N, Nakano K. Evaluation of the collagen-binding properties and virulence of killed *Streptococcus mutans* in a silkworm model. Sci Rep. 2022; 12:2800.
24. Matsumoto Y, Fukano H, Katano H, Hoshino Y, Sugita T. Histopathological analysis revealed that *Mycobacterium abscessus* proliferates in the fat bodies of silkworms. Drug Discov Ther. 2023; 17:139-143.
25. Beaman BL. Structural and biochemical alterations of *Nocardia asteroides* cell walls during its growth cycle. J Bacteriol. 1975; 123:1235-1253.
26. Beaman BL, Shankel DM. Ultrastructure of *Nocardia* cell growth and development on defined and complex agar media. J Bacteriol. 1969; 99:876-884.
27. Audenaert E, Almafragi A, Vuylsteke M, Verdonck C, Verdonck R. *Nocardia farcinica* arthritis of the knee. A case report. Acta Orthop Belg. 2004; 70:386-388.
28. Thakur A, Eapen J, Cherian SS. Septic arthritis by *Nocardia farcinica*: case report and literature review. IDCases. 2022; 31:e01668.
29. Han L, Ji X, Liu X, Xu S, Li F, Che Y, Qiu X, Sun L, Li Z. Estradiol aggravate *Nocardia farcinica* infections in mice. Front Immunol. 2022; 13:858609.
30. Beaman BL, Beaman L. *Nocardia* species: host-parasite relationships. Clin Microbiol Rev. 1994; 7:213-264.
31. Beaman BL. Interaction of *Nocardia asteroides* at different phases of growth with *in vitro*-maintained macrophages obtained from the lungs of normal and immunized rabbits. Infect Immun. 1979; 26:355-361.
32. Beaman BL, Maslan S. Virulence of *Nocardia asteroides* during its growth cycle. Infect Immun. 1978; 20:290-295.
33. Beaman BL, Sugar AM. *Nocardia* in naturally acquired and experimental infections in animals. J Hyg (Lond). 1983; 91:393-419.
34. Thakur A, Eapen J, Cherian SS. Septic arthritis by *Nocardia farcinica*: case report and literature review. IDCases. 2022; 31:e01668.
35. Gao S, Liu Q, Zhou X, Dai X, He H. Primary cutaneous nocardiosis due to *Nocardia farcinica*: a case report of an often overlooked infection. Infect Drug Resist. 2021; 14:1435-1440.
36. Bittar F, Stremmer N, Audié JP, Dubus JC, Sarles J, Raoult D, Rolain JM. *Nocardia farcinica* lung infection in a patient with cystic fibrosis: a case report. J Med Case Rep. 2010; 4:84.
37. Takamatsu A, Yaguchi T, Tagashira Y, Watanabe A, Honda H; Japan Nocardia Study Group. Nocardiosis in Japan: a multicentric retrospective cohort study. Antimicrob Agent Chemother. 2022; 15:e0189021.

Received September 2, 2024; Revised October 2, 2024; Accepted October 20, 2024.

*Address correspondence to:

Mitsuhiro Okazaki, Department of Medical Technology, School of Health Sciences, Tokyo University of Technology, 5-23-22, Nishikamata, Ota-ku, Tokyo 144-8535, Japan.
E-mail: okazakimthr@stf.teu.ac.jp

Released online in J-STAGE as advance publication October 24, 2024.

Astaxanthin compound nutrient improved insulin resistance, hormone levels, embryo quality and pregnancy outcomes in polycystic ovary syndrome patients undergoing *in vitro* fertilization/intracytoplasmic sperm injection

Xiayan Fu^{1,§}, Wenli Cao^{1,§}, Feijun Ye¹, Jialu Bei¹, Yan Du^{2,3,*}, Ling Wang^{3,4,5,*}

¹Reproductive Medicine Center, Zhoushan Maternal and Child Health Care Hospital, Zhoushan, Zhejiang, China;

²Clinical Research Unit, Obstetrics and Gynecology Hospital of Fudan University, Shanghai, China;

³Laboratory for Reproductive Immunology, Obstetrics and Gynecology Hospital of Fudan University, Shanghai, China;

⁴The Academy of Integrative Medicine, Fudan University, Shanghai, China;

⁵Shanghai Key Laboratory of Female Reproductive Endocrine-related Diseases, Shanghai, China.

SUMMARY This study aimed to evaluate the effect of astaxanthin compound nutrient (ACN) complementary therapy on pregnancy outcomes in polycystic ovary syndrome (PCOS) patients undergoing *in vitro* fertilization/intracytoplasmic sperm injection (IVF/ICSI). This study enrolled 92 patients with PCOS who were continuously supplemented with ACN for three months prior to IVF/ICSI treatment from 2021 to 2023, and selected 92 patients who did not receive the treatment during the same period as controls. Baseline characteristics, ovulation induction outcomes, and pregnancy outcomes were compared between the two groups. In addition, the body mass index (BMI), anti-Müllerian hormone (AMH), antral follicle counting (AFC), fasting blood glucose (FBG), fasting insulin (FINS), homeostasis model assessment of insulin resistant (HOME-IR), and basal sex hormones of the supplementary group patients before and after treatment were compared. The results showed that there were no significant differences in the patient's duration of stimulation, total gonadotropin dose, peak E2 levels, and number of retrieved oocytes between the two groups. However, the number of 2 pronucleus (PN) fertilization, transferable embryos, and high-quality embryos was significantly higher in the ACN group compared with the control group. For both fresh and frozen embryo transplantation, positive pregnancy outcomes increased in PCOS patients who received supplementation of ACN for 3 months. In addition, after 3 months of supplementing with ACN, the patient's BMI, AMH, fasting insulin, HOME-IR, basal luteinising hormone (bLH), and basal testosterone (bT) decreased compared to before treatment. This study suggested that ACN improved insulin resistance, hormone levels, embryo quality and pregnancy outcomes in PCOS patients.

Keywords polycystic ovary syndrome, insulin resistance, oocyte quality, pregnancy outcomes

1. Introduction

Polycystic ovary syndrome (PCOS) is a highly heterogeneous disease featured by ovulation dysfunction, polycystic ovary morphology, and hyperandrogenism, often accompanied by endocrine disorders such as obesity and disorders of glucose and lipid metabolism. Seventy-five percent of underweight and 95% of overweight women with PCOS have insulin resistance (IR) (1). IR is not only related to ovulation disorders and hyperandrogenicity in PCOS patients, but also increases the risk of cardiovascular and other metabolic diseases in PCOS patients (2). In recent years, research

has found that up to 80% of PCOS patients suffer from serious damage to their endocrine and reproductive health, leading to infertility as well as a younger age of occurrence (3), which has become a challenge in the reproductive field. Due to the complexity of the etiology and the diversity of symptoms, the cure of PCOS is relatively difficult. One of the treatment strategies recommended in the 2023 International Evidence-based Guideline of PCOS is healthy lifestyle, including diet and exercise interventions (4). Women with PCOS often lack some common vitamins, vitamin nutrients, and minerals. Supplementation of individual nutrients may improve the symptoms and severity of PCOS patients by influencing

key pathways, such as insulin signaling, IR, and lipid metabolism. Therefore, nutritional supplementation as an adjunct to traditional lifestyle treatments for PCOS can provide additional benefits (5).

Astaxanthin compound nutrient (ACN, Yunlike[®]) is a complex dietary supplement that contains D-chiro inositol (DCI), astaxanthin, L-carnitine, inulin, and α -linolenic acid (ALA). It is suitable for women with infertility, undergoing *in vitro* fertilization, or women of advanced maternal age preparing for pregnancy. Previous studies have shown the beneficial effects in improving PCOS condition of each ingredient (6-13). Our own practice also suggested that ACN is effective in improving insulin resistance, ovarian function, and oocyte quality. However, the clinical efficacy of ACN lacks the support of evidence-based medicine. Therefore, we conducted a single center study to evaluate the clinical efficacy of ACN supplementation in PCOS patients prior to IVF/ICSI (Figure 1).

2. Materials and Methods

2.1. Study population

PCOS patients who met the new diagnostic criteria of Rotterdam (4) and underwent IVF/ICSI-ET at Zhoushan Maternal and Child Health Hospital from 2021 to 2023 were screened. Patients with combined chromosomal abnormalities and those who have already taken other medications to treat PCOS, such as oral contraceptives, liver and kidney dysfunction, thyroid dysfunction, hyperprolactinemia, and any other endocrine disorder causing increased androgen were excluded from the study.

We enrolled 94 patients with PCOS who received

ACN supplementation for 3 months prior to IVF/ICSI treatment as the supplement group, 2 of whom were lost to follow-up. For the control group, 92 patients with PCOS who did not receive any drug supplementation prior to IVF/ICSI treatment during the same period were selected. The study was approved by the Institutional Review Board of Zhoushan Maternal and Child Health Hospital and followed the guidelines established in the Declaration of Helsinki 2013 for research involving human participants (Reference No. 2024024).

2.2. Ovarian stimulation and oocyte retrieval

All enrolled patients were treated with an antagonist regimen for superovulation induction. Starting from the 3rd day of the menstrual cycle, gonadotropin (Gn, uniformly selected recombinant human follicle stimulating hormone injection, 450 IU/tube, Merck Serrano, Sweden) 150-225 IU was injected to stimulate ovulation. On the 6th to 8th day of the menstrual cycle or when serum LH > 5IU/L, GnRH-A (uniformly selected injection of cetuximab acetate, 0.25mg/tube, Merck Serrano, Sweden) 0.25 mg was injected. Regular monitoring of B-ultrasound and serum sex hormone levels were applied to adjust Gn dosage. When B-ultrasound detected 2 or more follicles with a diameter > 18mm, stop using Gn and inject HCG 5,000-10,000 U trigger. After 36.5 hours, puncture was performed for oocyte retrieval.

2.3. Embryo transfer plan

After oocyte retrieval, fertilization was performed through IVF or ICSI, depending on the patient's conditions (*e.g.* whether there was ovarian

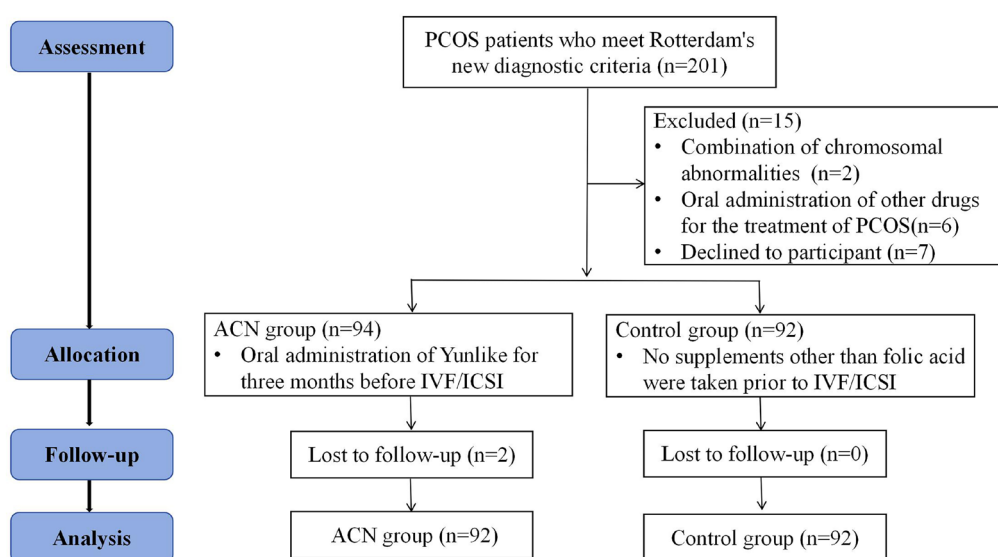


Figure 1. Study flowchart. A total of 201 patients met the diagnostic criteria of PCOS, of which 15 patients were excluded. Among included patients, 94 PCOS patients received continuous ACN supplementation for 3 months before IVF/ICSI treatment, of whom 2 patients were lost to follow-up. For the control group, 92 PCOS patients who did not supplement any nutrients except folic acid were included, and no one was lost to follow-up.

hyperstimulation syndrome, infection, hydrosalpinx, etc.). If transplanted, intramuscular injection of 60 mg/day progesterone injection was started after oocyte retrieval, and continued for three days to provide corpus luteum support. On the third day, two high-quality embryos were routinely selected and transplanted into the patient's uterine cavity. Luteal support was performed after transplantation.

If frozen embryo transfer was performed, hormone replacement regimen would be used to prepare the endometrium. Starting from the 3rd to 5th day of menstruation, 4 mg/day of estradiol valerate tablets (Bayer, Germany) were given for 5 consecutive days. From the 6th day onwards, the dosage was changed to 6 mg/day, and subsequently adjusted according to the patient's endometrial and blood hormone levels. When the thickness of the endometrium reached 8 mm, intramuscular injection of progesterone 60 mg/day was performed to transform the endometrium. After three consecutive days, two high-quality embryos were taken and transplanted into the patient's uterine cavity. Luteal support was performed post transplantation.

Urine pregnancy test or blood hCG quantification test was conducted 12 days after transplantation. For hCG positive patients, the first vaginal ultrasound examination should be performed 21 days after transplantation to rule out ectopic pregnancy. After 28 days of transplantation, ultrasound examination should be performed again to assess the number and development of embryos.

2.4. Data collection

Basic information, including age, height, weight, years of infertility, type of infertility, baseline sex hormones, AMH, AFC, FBG, and FINS levels was collected. The following variables were also collected after 3 months of ACN supplement: body weight, basal hormone levels, AMH, AFC, FBG, and FINS levels. BMI was calculated as weight (kg)/height (m)². HOME-IR was calculated as FBG (mmol/L) × FINS (μU/mL)/22.5.

The following variables of assisted reproductive technology (ART) were collected: Gn dosage, Gn days, total number of retrieved oocytes, 2PN fertilization rate, the number of transferable embryos, and the number of high-quality embryos. Pregnancy outcomes of patients undergoing frozen embryo transfer or fresh embryo transfer were followed-up.

2.5. Statistical analysis

Continuous variables conforming to the normal distribution were expressed in mean ± standard deviation and student *t*-test was used for comparison. Categorical variables were represented as numbers and percentages, and compared with chi-square tests. In addition, BMI, AMH, AFC, FBG, FINS, HOME-IR, and basal sex hormones of the experimental group patients after

3-months of ACN supplementation were compared using paired Student *t*-test. All data were analyzed by using SPSS 28.0 version, and the threshold of significance was bilateral $P < 0.05$.

3. Results

3.1. Participant characteristics

The 184 PCOS patients ranged in age from 24 to 42 years, and BMI ranged from 17.06 kg/m² to 32.27 kg/m². The ACN and control groups each contained 92 PCOS patients. In general, the baseline characteristics are comparable between the two groups ($P > 0.05$ for all), as presented in Table 1.

3.2. ART outcomes

As for the ART outcomes, the duration of stimulation, total gonadotropin dose, Peak E2 levels and the number of retrieved oocytes showed no significant differences between the two groups ($P > 0.05$ for all, Table 2). However, compared to the control group, the number of 2PN fertilization (10.85 ± 3.77 vs. 9.07 ± 3.06, $P = 0.04$), transplantable embryos (7.96 ± 2.88 vs. 6.01 ± 1.98, $P = 0.02$), and high-quality embryos (4.34 ± 2.51 vs. 3.16 ± 1.87, $P < 0.001$) were significant increased in the ACN group, as shown in Table 2.

3.3. Pregnancy outcomes

The pregnancy outcomes between the two groups are shown in Table 3. There were 25 cases in the ACN group underwent fresh embryo transfer, 67 cases underwent frozen embryo transfer; while the control group had 23 cases and 69 cases underwent fresh and frozen embryo transplantation, respectively. There was no significant difference in biochemical pregnancy, miscarriage, and ectopic pregnancy rates between the two groups, regardless of the embryo transfer methods. However, the positive pregnancy outcome was significantly higher than that in the control group (fresh embryo transfer, 44.00% vs. 34.78%, $P = 0.03$; frozen embryo transfer, 49.25% vs. 43.48%, $P = 0.04$).

3.4. Comparison of indicators in the supplementary group after 3 months of ACN supplement

After 3 months of ACN supplementation, the general indicators of the patients are compared, as shown in Table 4. Compared with before supplementation, there was no significant difference in AFC, FBG, bFSH, bE2, and bP among patients treated with ACN for 3 months. However, after 3 months of ACN supplementation, the patient's BMI (22.83 ± 3.11 kg/m² vs. 20.09 ± 3.13 kg/m², $P = 0.03$), AMH (7.13 ± 3.11 ng/mL vs. 5.88 ± 2.97 ng/mL, $P = 0.02$), fasting insulin (15.09 ± 5.84 μU/

Table 1. Clinical characteristics

Characteristics	ACN group (n = 92)	Control group (n = 92)	P value
Age, years	31.51 ± 3.03	31.79 ± 3.39	0.62
Years of infertility, years	3.17 ± 2.47	2.95 ± 2.53	0.61
Infertility type, n (%)			
Primary infertility	54 (58.7%)	61 (66.30%)	0.38
Secondary infertility	38 (41.3%)	31 (33.70%)	
BMI, kg/m ²	22.83 ± 3.11	22.37 ± 2.62	0.35
AMH, ng/mL	7.13 ± 3.11	7.80 ± 3.68	0.25
AFC, n	13.02 ± 2.01	13.43 ± 1.98	0.57
FBG, mmol/L	5.96 ± 1.87	5.88 ± 1.63	0.63
FINS, μU/mL	15.09 ± 5.84	16.55 ± 6.09	0.27
HOME-IR	2.71 ± 2.01	3.68 ± 2.43	0.16
bFSH, IU/L	5.67 ± 1.73	5.83 ± 1.49	0.36
bLH, IU/L	9.93 ± 2.08	10.06 ± 2.15	0.73
bE2, pg/mL	34.05 ± 7.95	32.60 ± 8.39	0.47
bT, nmol/L	2.81 ± 0.98	2.69 ± 1.08	0.18
bP, pmol/L	1.09 ± 0.58	0.96 ± 0.78	0.23

BMI: body mass index; AMH: anti-Müllerian hormone; AFC: antral follicle count; FBG: fasting blood glucose; FINS: fasting insulin; HOME-IR: homeostasis model assessment of insulin resistant; bFSH: basal follicle-stimulating hormone; bLH: basal luteinising hormone; bE2: basal estradiol; bT: basal testosterone; bP: basal progesterone.

Table 2. Assisted reproductive technology (ART) outcomes

Parameters	ACN group (n = 92)	Control group (n = 92)	P value
Duration of stimulation, days	9.09 ± 2.60	9.73 ± 2.78	0.39
Total gonadotropin dose, IU	2179.15 ± 455.16	2236.97 ± 540.65	0.18
Peak E2 levels, pg/mL	4383.29 ± 899.17	4199.16 ± 815.67	0.14
Number of retrieved oocytes	14.88 ± 5.31	14.60 ± 5.38	0.71
Number of 2PN fertilization	10.85 ± 3.77	9.07 ± 3.06	0.04
Number of transferable embryos	7.96 ± 2.88	6.01 ± 1.98	0.02
Number of high-quality embryos	4.34 ± 2.51	3.16 ± 1.87	< 0.001

Table 3. Pregnancy outcomes

Pregnancy outcome	ACN group (n = 92)	Control group (n = 92)	P value
Fresh embryo transfer, n (%)	25 (27.17%)	23 (25.00%)	0.77
Biochemical pregnancy, n (%)	1 (4.00%)	1 (4.35%)	0.81
Positive pregnancy outcome, n (%)	11 (44.00%)	8 (34.78%)	0.03
Miscarriage, n (%)	1 (4.00%)	1 (4.35%)	0.81
Ectopic pregnancy, n (%)	1 (4.00%)	1 (4.35%)	0.81
Frozen embryo transfer, n (%)	67 (72.82%)	69 (75%)	0.77
Biochemical pregnancy, n (%)	4 (5.97%)	5 (7.25%)	0.08
Positive pregnancy outcome, n (%)	33 (49.25%)	30 (43.48%)	0.04
Miscarriage, n (%)	2 (3.00%)	3 (4.35%)	0.38
Ectopic pregnancy, n (%)	2 (3.00%)	2 (2.90%)	0.89

mL vs. 12.01 ± 4.13 μU/mL, $P = 0.01$), and HOME-IR (2.71 ± 2.01 vs. 1.91 ± 1.09 μU/mL, $P = 0.02$) decreased significantly. At the same time, after supplementation with ACN, the patient's basal LH (9.93 ± 2.08 IU/L vs. 7.14 ± 1.97 IU/L, $P = 0.03$) and basal T (2.81 ± 0.98 nmol/L vs. 1.84 ± 0.86 nmol/L, $P = 0.01$) levels were significantly decreased.

4. Discussion

As one of the main causes of female infertility, about 10% of PCOS patients seek ART treatment to aid in pregnancy (3). In this study, we retrospectively collected

92 PCOS patients who received ACN supplementation for 3 months prior to IVF/ICSI treatment, and selected 92 PCOS patients who did not receive any supplementation as controls. Our results showed that after complementary treatment with ACN, the number of 2PN fertilization, high-quality embryos, and transferable embryos significantly increased, and the positive pregnancy outcomes of fresh and frozen embryo transplantation also improved.

The etiology of PCOS is complex. Research has shown that excessive androgen, IR combined with hypothalamic pituitary dysfunction leading to ovarian dysfunction and ovulation disorders are the main

Table 4. Comparison of indicators in the supplementary group after 3 months of ACN supplementation

Parameters	Before treatment (n = 92)	After treatment (n = 92)	P value
BMI, kg/m ²	22.83 ± 3.11	20.09 ± 3.13	0.03
AMH, ng/mL	7.13 ± 3.11	5.88 ± 2.97	0.02
AFC, n	13.02 ± 2.01	12.86 ± 1.95	0.21
FBG, mmol/L	5.96 ± 1.87	5.04 ± 1.67	0.48
FINS, μU/mL	15.09 ± 5.84	12.01 ± 4.13	0.01
HOME-IR	2.71 ± 2.01	1.91 ± 1.09	0.02
bFSH, IU/L	5.67 ± 1.73	5.02 ± 2.11	0.45
bLH, IU/L	9.93 ± 2.08	7.14 ± 1.97	0.03
bE2, pg/mL	34.05 ± 7.95	32.79 ± 6.93	0.29
bT, nmol/L	2.81 ± 0.98	1.84 ± 0.86	0.01
bP, pmol/L	1.09 ± 0.58	0.99 ± 0.47	0.22

BMI: body mass index; AMH: anti-Müllerian hormone; AFC: antral follicle count; FBG: fasting blood glucose; FINS: fasting insulin; HOME-IR: homeostasis model assessment of insulin resistant; bFSH: basal follicle-stimulating hormone; bLH: basal luteinising hormone; bE2: basal estradiol; bT: basal testosterone; bP: basal progesterone.

mechanisms of infertility in PCOS patients (14). Previous studies have shown that supplementation of multiple nutrients can improve IR in PCOS patients (5,15). However, it is not clear whether the composite components are beneficial for superovulation and pregnancy outcomes in PCOS patients. To the best of our knowledge, our study is the first of its kind to investigate the synergistic effects of different nutrients (ACN) on PCOS patients.

ACN contains active ingredients which have been respectively proven to be beneficial in PCOS patients receiving ART. It was observed that decreased availability of DCI in plasma or increased excretion of DCI in urine was associated with IR, supporting the role of DCI as an insulin sensitizer (16). An early study about DCI on PCOS patients showed that the DCI group (n = 22) had increased insulin sensitivity, decreased free testosterone levels, and significantly higher ovulation rates than the placebo group (n = 22) (86% vs. 27%, P < 0.05 for all) (7). Astaxanthin is a ketocarotenoid, super antioxidant molecule (8). It has various biological activities such as clearing free radicals, antioxidation, enhancing immunity, and anti-aging. In animal experiments, astaxanthin can inactivate the Wnt/β-Catenin signal by upregulating Klotho and activate the MEK/ERK signal, thereby preventing inflammatory reactions, improving hormone levels in PCOS rats, and improving symptoms of obesity and polycystic ovary morphology (9). An *in vitro* experiment on primary culture of human granulosa cells showed that DCI can reduce the expression of cytochrome P450 family 19 subfamily A member 1 (CYP19A1), P450Side-chain cleavage (P450scc), and insulin-like growth factor-1R (IGF-1R), indicating that DCI can reduce the production of steroidogenic enzymes by antagonizing the action of insulin (17). A randomized clinical trial showed that after taking astaxanthin for 8 weeks, FBG,

insulin, and HOMA-IR levels in PCOS patients were significantly reduced (18). It is reported that thin women with PCOS had lower levels of L-carnitine, which was mainly related to hyperandrogenism and IR (19). After supplementing PCOS patients with L-carnitine, their insulin sensitivity and glucose tolerance tests were significantly improved (11). Different aggregation levels of inulin can improve metabolic outcomes, androgen status, and clinical manifestations in PCOS patients by reducing total testosterone, free androgen index, BMI, fasting insulin, and HOMA-IR levels (20). Animal experiments have shown that supplementing with inulin can improve the estrus cycle and ovarian morphology of PCOS mice, reduce luteinizing hormone levels, increase serum levels of FSH and interleukin (IL)-22, and regulate gut microbiota and bile acid profile (21). Flaxseed oil rich in ALA improved the estrus cycle, ovarian morphology, steroid hormone imbalance, weight, lipid abnormalities, and IR in mice (22). It also improved plasma and ovarian inflammatory IL-1β, IL-6, IL-10, IL-17A, monocyte chemoattractant protein-1 and tumor necrosis factor (TNF)-α (22). Consistent with previous findings, our study confirmed that after taking ACN for 3 months, BMI, AMH, fasting insulin, and HOME-IR improved significantly, while basal LH and T also decreased significantly compared to before the treatment.

Previous studies have also suggested that nutrients were beneficial for improving ART outcomes in PCOS patients. A study of seven oocyte quality markers in patients with PCOS receiving ICSI showed that high-dose DCI helped improve oocyte quality (23). It is speculated that DCI participates in oocyte activation and increases granulosa cell activity through phosphatidylinositol-3-kinase. Another study showed that supplementation with astaxanthin in PCOS significantly increased the expression of oxidative stress factors such as Nrf2, HO-1, and NQ-1 in its granulosa cells. In addition, the rates of metaphase II oocytes and high-quality embryos significantly increased, while there was no significant intergroup difference in biochemical pregnancy and clinical pregnancy rates (24). In a PCOS rat model, after adjuvant treatment with astaxanthin, the expression levels of IL-6, TNF-α and NF-κ in ovarian tissue decreased, as well as the malondialdehyde level, while the level of superoxide dismutase increased (25). Therefore, it is speculated that astaxanthin can protect ovary from oxidative stress damage. A study of 214 infertile women receiving oral L-carnitine during IVF cycles reported that the total number of oocytes retrieved, oocyte maturation rate, and fertilization rate before and after supplementing with L-carnitine showed no significant differences, but the embryo quality significantly improved (26). However, our results were slightly different. It is possible that the high number of 2PN insemination in our experimental group may be due to other components in pregnancy. Some studies have shown that antioxidant properties of L-carnitine can

improve and maintain mitochondrial activity in oocytes, obtain high-quality oocytes with high developmental ability, thus improving embryo quality (27).

In conclusion, ACN, a complex dietary supplement, can improve IR, hormone levels, embryo quality and pregnancy outcomes in PCOS patients. It is recommended that PCOS patients receive ACN supplementation for 3 months before entering the IVF/ICSI cycle to improve their pregnancy outcomes.

Acknowledgements

We thank Yanmei Zhou for her assistance in the collection of data for this article.

Funding: This work was supported by a grant from Medical and Health Technology Plan Project of Zhoushan City, Zhejiang Province (grant No. 2023YB04 to Cao W), a project of Zhoushan Medical and Health Technology Plan (grant No. 2023RC04 to Bei J) and a project of National Natural Science Foundation of China (grant No. 82374243 to Wang L).

Conflict of Interest: The authors have no conflicts of interest to disclose.

References

- Stepito NK, Cassar S, Joham AE, Hutchison SK, Harrison CL, Goldstein RF, Teede HJ. Women with polycystic ovary syndrome have intrinsic insulin resistance on euglycaemic-hyperinsulinaemic clamp. *Hum Reprod.* 2013; 28:777-784.
- Ding H, Zhang J, Zhang F, Zhang S, Chen X, Liang W, Xie Q. Resistance to the insulin and elevated level of androgen: A major cause of polycystic ovary syndrome. *Front Endocrinol (Lausanne).* 2021; 12:741764.
- Joham AE, Norman RJ, Stener-Victorin E, Legro RS, Franks S, Moran LJ, Boyle J, Teede HJ. Polycystic ovary syndrome. *Lancet Diabetes Endocrinol.* 2022; 10:668-680.
- Teede HJ, Tay CT, Laven JJE, Dokras A, Moran LJ, Piltonen TT, Costello MF, Boivin J, Redman LM, Boyle JA, Norman RJ, Mousa A, Joham AE. Recommendations from the 2023 international evidence-based guideline for the assessment and management of polycystic ovary syndrome. *J Clin Endocrinol Metab.* 2023; 108:2447-2469.
- Rodriguez Paris V, Solon-Biet SM, Senior AM, Edwards MC, Desai R, Tedla N, Cox MJ, Ledger WL, Gilchrist RB, Simpson SJ, Handelsman DJ, Walters KA. Defining the impact of dietary macronutrient balance on PCOS traits. *Nat Commun.* 2020; 11:5262.
- Unfer V, Nestler JE, Kamenov ZA, Prapas N, Facchinetti F. Effects of inositol(s) in women with PCOS: A systematic review of randomized controlled trials. *Int J Endocrinol.* 2016; 2016:1849162.
- Nestler JE, Jakubowicz DJ, Reamer P, Gunn RD, Allan G. Ovulatory and metabolic effects of D-chiro-inositol in the polycystic ovary syndrome. *N Engl J Med.* 1999; 340:1314-20.
- Kumar S, Kumar R, Diksha, Kumari A, Panwar A. Astaxanthin: A super antioxidant from microalgae and its therapeutic potential. *J Basic Microbiol.* 2022; 62:1064-1082.
- Song Yu, Zhu Zhengyan, Huang Huan, Li Chun, Lu Jingquan, Liu Heyu, Hu Lina. Astaxanthin regulates Klotho expression and Wnt/ β - The improvement effect of the Catenin signaling pathway on polycystic ovary syndrome in rats. *Tianjin Pharmaceutical.* 2023; 51:1098-1103. (in Chinese)
- Mohd Shukri MF, Norhayati MN, Badrin S, Abdul Kadir A. Effects of L-carnitine supplementation for women with polycystic ovary syndrome: A systematic review and meta-analysis. *PeerJ.* 2022; 10:e13992.
- Tauqir S, Israr M, Rauf B, Malik MO, Habib SH, Shah FA, Usman M, Raza MA, Shah I, Badshah H, Ehtesham E, Shah M. Acetyl-L-Carnitine ameliorates metabolic and endocrine alterations in women with PCOS: A double-blind randomized clinical trial. *Adv Ther.* 2021; 38:3842-3856.
- Xue J, Li X, Liu P, Li K, Sha L, Yang X, Zhu L, Wang Z, Dong Y, Zhang L, Lei H, Zhang X, Dong X, Wang H. Inulin and metformin ameliorate polycystic ovary syndrome *via* anti-inflammation and modulating gut microbiota in mice. *Endocr J.* 2019; 66:859-870.
- Sun Lijun, Hu Jijun, Guan Yichun, Wu Wenbin, Ma Xiaojuan, Song Na, Qi Ruofan. The effect of α -linolenic acid on *in vitro* maturation of human immature oocytes. *China Maternal and Child Health.* 2015; 30:5002-5005.
- Collée J, Mawet M, Tebache L, Nisolle M, Brichant G. Polycystic ovarian syndrome and infertility: Overview and insights of the putative treatments. *Gynecol Endocrinol.* 2021; 37:869-874.
- Szczuko M, Kikut J, Szczuko U, Szydłowska I, Nawrocka-Rutkowska J, Ziętek M, Verbanac D, Saso L. Nutrition strategy and life style in polycystic ovary syndrome-narrative review. *Nutrients.* 2021; 13:2452.
- Baillargeon JP, Nestler JE, Ostlund RE, Apridonidze T, Diamanti-Kandarakis E. Greek hyperinsulinemic women, with or without polycystic ovary syndrome, display altered inositols metabolism. *Hum Reprod.* 2008; 23:1439-1446.
- Sacchi S, Marinaro F, Tondelli D, Lui J, Xella S, Marsella T, Tagliasacchi D, Argento C, Tirelli A, Giulini S, La Marca A. Modulation of gonadotrophin induced steroidogenic enzymes in granulosa cells by d-chiroinositol. *Reprod Biol Endocrinol.* 2016; 14:52.
- Jabarpour M, Aleyasin A, Shabani Nashtaei M, Amidi F. Astaxanthin supplementation impact on insulin resistance, lipid profile, blood pressure, and oxidative stress in polycystic ovary syndrome patients: A triple-blind randomized clinical trial. *Phytother Res.* 2024; 38:321-330.
- Fenkci SM, Fenkci V, Oztekin O, Rota S, Karagenc N. Serum total L-carnitine levels in non-obese women with polycystic ovary syndrome. *Hum Reprod.* 2008; 23:1602-1606.
- Ziaei R, Shahshahan Z, Ghasemi-Tehrani H, Heidari Z, Nehls MS, Ghiasvand R. Inulin-type fructans with different degrees of polymerization improve insulin resistance, metabolic parameters, and hormonal status in overweight and obese women with polycystic ovary syndrome: A randomized double-blind, placebo-controlled clinical trial. *Food Sci Nutr.* 2023; 12:2016-2028.
- Li T, Zhang Y, Song J, Chen L, Du M, Mao X. Yogurt enriched with inulin ameliorated reproductive functions and regulated gut microbiota in dehydroepiandrosterone-

- induced polycystic ovary syndrome mice. *Nutrients*. 2022; 14:279.
22. Wang T, Sha L, Li Y, Zhu L, Wang Z, Li K, Lu H, Bao T, Guo L, Zhang X, Wang H. Dietary α -linolenic acid-rich faxseed oil exerts beneficial effects on polycystic ovary syndrome through sex steroid hormones-microbiota-inflammation axis in rats. *Front Endocrinol (Lausanne)*. 2020; 11:284.
23. Mendoza N, Galan MI, Molina C, Mendoza-Tesarik R, Conde C, Mazheika M, Diaz-Roperio MP, Fonolla J, Tesarik J, Olivares M. High dose of d-chiro-inositol improves oocyte quality in women with polycystic ovary syndrome undergoing ICSI: a randomized controlled trial. *Gynecol Endocrinol*. 2020; 36:398-401.
24. Gharaei R, Alyasin A, Mahdavinezhad F, Samadian E, Ashrafnezhad Z, Amidi F. Randomized controlled trial of astaxanthin impacts on antioxidant status and assisted reproductive technology outcomes in women with polycystic ovarian syndrome. *J Assist Reprod Genet*. 2022; 39:995-1008.
25. Toktay E, Selli J, Gurbuz MA, Alaca R. Investigation of the effects of astaxanthin in experimental polycystic ovary syndrome (PCOS) in rats. *Iran J Basic Med Sci*. 2023; 26:1155-1161.
26. Kitano Y, Hashimoto S, Matsumoto H, Yamochi T, Yamanaka M, Nakaoka Y, Fukuda A, Inoue M, Ikeda T, Morimoto Y. Oral administration of l-carnitine improves the clinical outcome of fertility in patients with IVF treatment. *Gynecol Endocrinol*. 2018; 34:684-688.
27. Sheida A, Davar R, Tabibnejad N, Eftekhar M. The effect of adding L-carnitine to the GnRH-antagonist protocol on assisted reproductive technology outcome in women with polycystic ovarian syndrome: A randomized clinical trial. *Gynecol Endocrinol*. 2023; 39:1878135.

Received May 29, 2024; Revised September 19, 2024; Accepted October 7, 2024.

§These authors contributed equally to this work.

*Address correspondence to:

Ling Wang, Laboratory for Reproductive Immunology, Obstetrics and Gynecology Hospital of Fudan University, 419 Fangxie Road, Shanghai, China 200011. China.
E-mail: dr.wangling@fudan.edu.cn

Yan Du, Clinical Research Unit, Obstetrics and Gynecology Hospital of Fudan University, No. 128 Shenyang Road, Shanghai, China 200090.
E-mail: sophiedu_61@163.com

Released online in J-STAGE as advance publication October 18, 2024.

Electrolytic-reduction ion water protects keratinocytes from hydrogen peroxide through radical scavenging activity and induction of AQP3 expression

Hiroyuki Yamamoto^{1,2,*}, Tokuko Takajo³, Ami Tsuchibuchi², Kaho Makuta², Toshiyuki Yamada², Mitsuo Ikeda⁴, Yoshinao Okajima^{4,5}, Masahiro Okajima^{4,5}

¹Department of Health and Nutritional Sciences, Faculty of Food and Health Sciences, Aichi Shukutoku University, Aichi, Japan;

²Department of Microbiology and Molecular Cell Biology, Nihon Pharmaceutical University, Saitama, Japan;

³Division of Physical and Analytical Chemistry, Faculty of Pharmaceutical Sciences, Nihon Pharmaceutical University, Saitama, Japan;

⁴A.I.System Products Corp., Aichi, Japan;

⁵Department of Pharmaceutical Sciences, Meiji Pharmaceutical University, Tokyo, Japan.

SUMMARY Skin exposed to ultraviolet light produces hydrogen peroxide (H₂O₂) and reactive oxygen species (ROS) that cause protein denaturation and other disorders. We investigated whether electrolytic-reduction ion water (ERI), which has reducing properties and has been reported to protect skin, exhibits antioxidant activity in skin keratinocytes. The antioxidant activity of ERI was first examined using DPPH assay and Electron Spin Resonance to test for radicals, and using the Amplex Red method to test for H₂O₂. Concentration-dependent scavenging of hydroxyl radical but no H₂O₂ depletion were detected. An investigation of the expression of heme oxygenase-1, which is upregulated by oxidative response in cells, showed an increase through H₂O₂ oxidation, which was inhibited by ERI in a concentration-dependent manner. This suggests that ERI directly removes ROS. Quantitative real-time polymerase chain reaction analysis was performed to determine whether ERI regulates the expression of aquaporin 3 (AQP3), a known H₂O₂ transporter. This analysis revealed that ERI enhances AQP3 expression in a concentration-dependent manner and is involved in the transport of intracellular H₂O₂ to the extracellular space. In addition, ERI inhibited H₂O₂-induced cytotoxicity in a concentration-dependent manner. These results suggest that ERI protects keratinocytes from ROS by directly scavenging them and indirectly by eliminating them through the promotion of the efflux of intracellular H₂O₂.

Keywords antioxidant, electrolytic-reduction ion water, Electron Spin Resonance, heme oxygenase-1, aquaporin 3

1. Introduction

The epidermal layer of the skin plays a fundamental role in the defense against environmental pathogens. In addition, moisture is essential for organisms, and they must have a mechanism to prevent moisture loss from the epidermis. Keratinocytes, which constitute the predominant cell type of the stratum corneum, produce protective factors such as ceramide (1) and hyaluronic acid (2) to protect against invasion of external substances and moisture loss. Ultraviolet (UV) radiation comprises wavelengths present in sunlight that may cause substantial damage to organisms (3) by inducing the generation of H₂O₂ and reactive oxygen species (ROS) (4). ROS cause lipid oxidation, protein

denaturation, and DNA damage. UV radiation also causes disorders of the skin's defensive system, as well as wrinkle formation and skin hyperpigmentation. Because wrinkling, pigmentation, and sagging are signs of skin aging, UV-induced skin modifications are also referred to as photoaging. Suppressing excessive ROS production in the epidermis to protect the body from UV radiation and other damages is a crucial skin-metabolic function.

Electrolytic-reduction ion water (ERI) contains 0.3% mineral salts, such as sodium, potassium, calcium, magnesium, chlorine, silicon and phosphorus, and has a weak basicity and high reducing properties. Studies have reported beneficial effects of ERI such as improvement in skin burns (5-7) and atopic dermatitis (8). While

clarifying the mechanism through which ERI improves dermatitis, we reported that ERI enhances the expression of CerS3 (ceramide synthase 3) and ELOVL7 (very long chain fatty acid elongase 7), enzymes involved in ceramide synthesis (9). The observed anti-inflammatory effects were believed to be due to the increase in skin ceramide content, which enhances the protective function of the skin. ROS scavenging is also expected to be involved in the skin's protective function, but antioxidant effects of ERI on cells have not yet been reported.

The Nrf2-Keap1 system is a mechanism of biological response of cells to oxidative stress and is responsible for maintaining cellular homeostasis (10). In the absence of oxidative stress, Nrf2 is retained in the cytoplasm by the inhibitor Keap1, which inhibits its nuclear translocation, thereby suppressing gene expression. In oxidative stress-exposed cells, the Nrf2-inhibitory mechanism of Keap1 is unlocked and the nucleus-translocated Nrf2 induces the expression of oxidative stress response genes such as glutathione synthetase and heme oxygenase-1 (HO-1) (11). Therefore, genes induced by the Nrf2-Keap1 system can be used as indicators of cellular oxidative stress. In the present study, we sought to clarify whether ERI can exert its antioxidant effect on cells by evaluating the expression of HO-1, which is regulated by Nrf2-Keap1, as an indicator of this direct antioxidant effect. In addition, we examined the effect of ERI on the expression of aquaporin 3 (AQP3), a known transporter of H₂O₂, as an indirect mechanism of antioxidant effect.

2. Materials and Methods

2.1. Materials

ERI was obtained from AI System Products (Aichi, Japan). Normal human epidermal keratinocytes (NHEKs) were purchased from PromoCell (Heidelberg, Germany). All other chemicals were of reagent grade. The NHEKs were cultured in Keratinocyte Growth Medium 2 (PromoCell) under humidified air containing 5% CO₂ at 37°C.

2.2. DPPH antioxidant assay

The antioxidant activity of ERI was measured *via* DPPH assay. ERI was mixed with the DPPH (1,1-diphenyl-2-picrylhydrazyl radical; 2,2-diphenyl-1-picrylhydrazyl; Dojindo, Kumamoto, Japan) solution, and the mixture was incubated in the dark at 25°C for 30 min. The antioxidant activity was measured at 520 nm using a microplate reader (VersaMAX, Molecular Devices, San Jose, CA, USA).

2.3. Measurement of hydroxyl radical

Fenton reaction was employed to generate hydroxyl

radical ([•]OH) by mixing 1.8 mM DMPO (5,5-Dimethyl-1-pyrroline-N-oxide; Labotec Co. Ltd., Tokyo, Japan), 0.8 mM H₂O₂, various concentrations of ERI and 0.08 mM Fe²⁺. The mixture solution was transferred to a quartz flat cell and X-band ESR spectra were recorded using a JES-FA 100 ESR spectrometer (JEOL Ltd., Tokyo, Japan). Mn²⁺ was used as the external standard.

2.4. Measurement of hydrogen peroxide

Amplex Red (N-acetyl-3,7-dihydroxyphenoxazine; Chemodex Ltd., St. Gallen, Switzerland) was prepared in DMSO and stored at -20°C. Immediately before use, the thawed stock solution was diluted in 50 mM Tris-HCl buffer, pH7.4. H₂O₂ solution was mixed with various concentrations of ERI, and after respectively 2 and 24 h, the reaction solution containing Amplex Red at 10 μM and 1 U/mL HRP was incubated at room temperature for 10 min. Subsequently, the fluorescence intensity (ex. 563 nm, em. 587 nm) was measured using a spectrofluorophotometer (RF-5300PC; Shimadzu, Kyoto, Japan).

2.5. MTT assay

A 3-(4,5-dimethylthiazol-2-yl)-2,5-diphenyltetrazolium bromide (MTT; Dojindo) assay was used to evaluate the effect of ERI on the cellular activity of keratinocytes and the inhibitory effect of ERI on H₂O₂ injury. To this end, NHEKs were cultured in Keratinocyte Growth Medium 2 (PromoCell) under humidified air with 5% CO₂ at 37 °C. The cells were subsequently seeded into a 96-well plate (10⁴ cells/well) and cultured overnight. For the effect of ERI on keratinocytes, we prepared the cells by incubating them for 24 h with various concentrations of ERI. For the inhibitory effect of ERI on H₂O₂ injury, we cultured keratinocytes with 0.1% H₂O₂ and/or various concentrations of ERI. The cells were subsequently treated with 110 μL of Dulbecco's modified Eagle's medium containing 0.5 mg/mL MTT and incubated at 37°C for 4 h. Thereafter, the formazan crystals that formed in metabolically active cells were dissolved with 100 μL of 10% sodium dodecyl sulfate in 10 mM hydrochloric acid. Spectrophotometric absorbance was determined at 560 nm, using a microplate reader, and expressed as a percentage of cellular activity.

2.6. Quantitative real-time polymerase chain reaction

Cell oxidation was assessed by evaluating HO-1 mRNA expression through real-time polymerase chain reaction (RT-PCR). Keratinocytes (10⁵ cells/well) were seeded into a 6-well tissue culture plate and incubated overnight. The cells were cultured in media containing 0.03% H₂O₂ and/or various ERI concentrations for 24 h. Total RNA was extracted from the keratinocytes

using Isogen (Nippon Gene, Tokyo, Japan). cDNA was synthesized from the extracted RNA using ReverTra Ace (Toyobo, Osaka, Japan) according to the manufacturer's instructions. Specific primers were designed to amplify human HO-1 (5'-CTTTCAGAAGGGCCAGGTGA-3' and 5'-TCCTCCAGGGCCACATAGAT-3'), human AQP3 (5'-CACTCTGGGCATCCTCATCG-3' and 5'-GCCGGTCTGGTCAAAGAAG-3'), and human β -actin (5'-AGTCCTGTGGCATCCACGAAAC-3' and 5'-GCAGTGATCTCCTTCTGCATCC-3'). RT-PCR was performed using the StepOne system (Applied Biosystems, Foster City, CA, USA) or Thermal Cycler Dice Real-Time System III (Takara bio, Tokyo, Japan). Specificity of the PCR products was verified on the basis of the melt curve. Ct values of the samples were normalized to that of β -actin, and the relative expression was calculated using the comparative Ct method.

2.7. Statistical analysis

Data are presented as the mean \pm standard deviation (SD). The results were analyzed using the Tukey–Kramer test performed in R (R Development Core Team), and a P -value < 0.05 was considered statistically significant.

3. Results and Discussion

Skin keratinocytes were used in this study to evaluate the antioxidant effect of ERI on intracellular oxidation in the presence of H_2O_2 .

First, radical-scavenging activity was evaluated using the DPPH method (Figure 1A) and hydroxyl radical was detected using the ESR spin trapping technique (Figure 1B). These are among the common methods for determining the free radical-scavenging capacity of substances. The results revealed that ERI scavenged DPPH radicals and hydroxyl radical in a concentration-dependent manner, with an IC_{50} of respectively 3.37% (v/v) and 6.81% (v/v). We also evaluated the scavenging capacity of H_2O_2 when mixed with ERI. No decrease in H_2O_2 was present in the ERI even when reacted at concentrations of 50% (v/v) ERI for up to 24 h (Figure 1C).

Next, we evaluated the intracellular antioxidant activity of ERI by way of keratinocytes. To determine the required concentration of ERI, the cytotoxic potential of ERI on keratinocytes was evaluated using the MTT test. ERI exhibited no cytotoxicity up to a 5% (v/v) concentration (Figure 2A), and this value was therefore used as a maximum concentration in subsequent experiments. To assess intracellular antioxidant activity, we used HO-1, the expression of which is upregulated by the Nrf2-Keap1 system, as an indicator of cellular oxidative stress. We used 0.03% H_2O_2 as an ROS donor. As shown in Figure 2B, stimulation with 0.03% (w/v) H_2O_2 increased HO-1 mRNA expression by

approximately 2.57-fold. ERI decreased this expression in a concentration-dependent manner.

Because AQP3 expressed in keratinocytes uses water, glycerol, and H_2O_2 as substrates (12), AQP3 plays a role in skin moisturization and suppresses intracellular antioxidant activity to efflux intracellular excess H_2O_2 . Therefore, we examined whether ERI exerts a cytoprotective effect against indirect oxidative stress through AQP3 expression (Figure 2C). H_2O_2 did not affect AQP3 mRNA expression, but ERI enhanced the expression of AQP3 in a concentration-dependent manner. This result suggests that ERI exhibits a cytoprotective function that is mediated by AQP3. Unlike HO-1 expression, gene expression is not affected by intracellular oxidation induced by H_2O_2 treatment, which suggests that a different mechanism is involved; however, this mechanism remains unknown to date. AQP3 in keratinocytes is upregulated by retinoic acid, and AQP3 expression is believed to be enhanced through

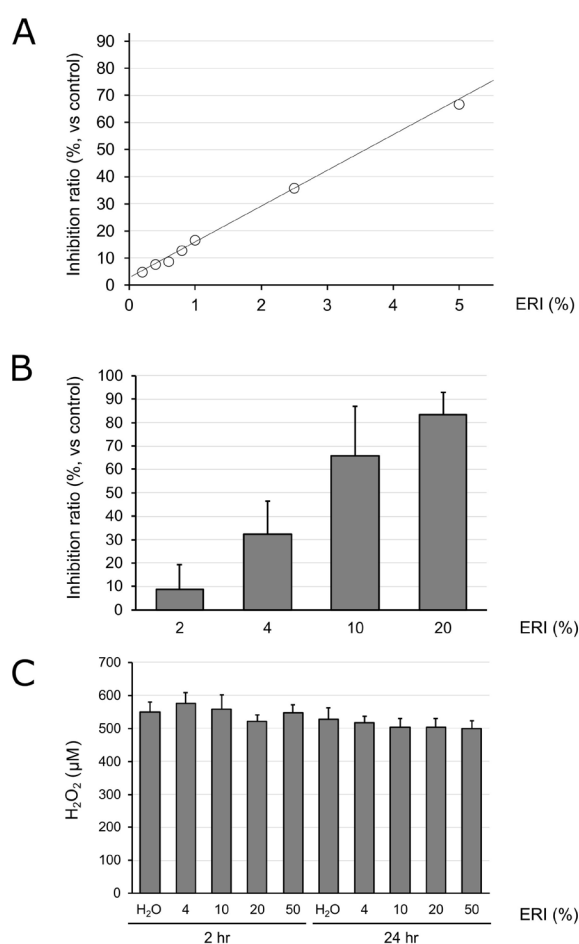


Figure 1. Scavenging activity of ERI on free radicals and hydroxy peroxide. The scavenging properties of ERI for radicals were measured using DPPH radicals (A) and hydroxyl radicals (B), vs. ERI non-additive as control (implied 100%). Data are shown as the mean \pm SD ($n = 3-4$). To assess the decrement activity of hydroxy peroxide of ERI, concentrations of hydroxy peroxide were measured with Amplex Red (C). Data are shown as the mean \pm SD ($n = 4-6$).

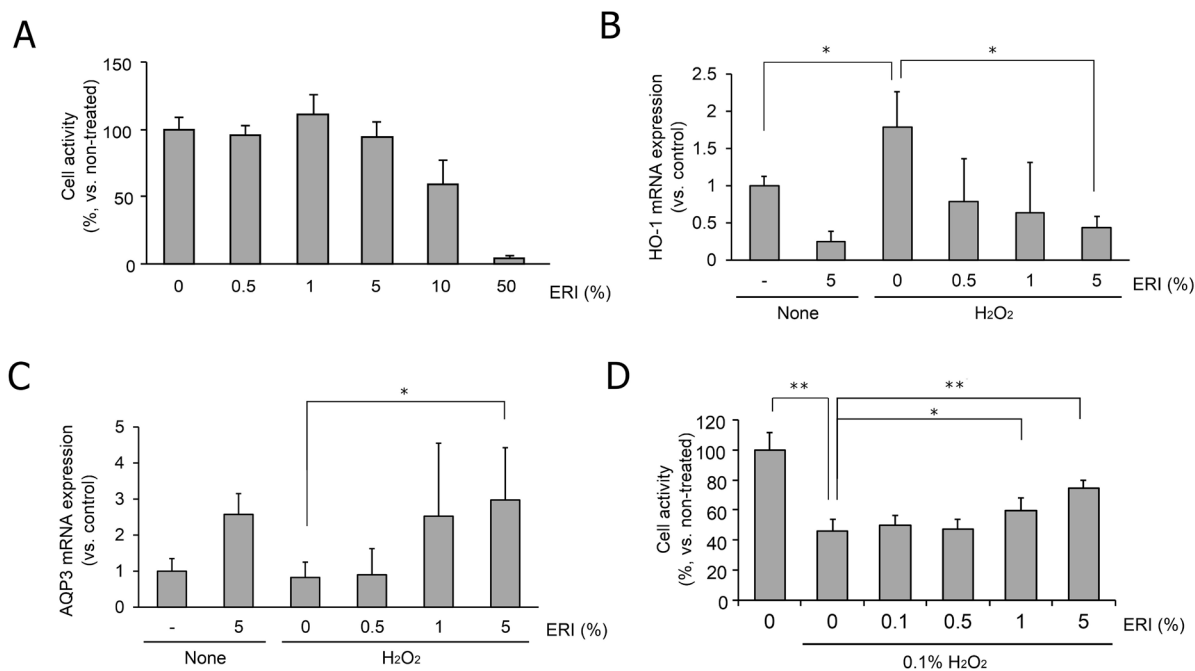


Figure 2 Activity of ERI on normal skin keratinocytes. The effect of ERI on keratinocytes was measured using an MTT assay (A). Data are shown as the mean \pm SD of eight biological replicates. "100%" indicates an untreated control. HO-1 (B) and AQP3 (C) mRNA expression levels. mRNA was extracted from NHEKs treated with 0.5%, 1%, or 5% ERI and/or 0.03% H₂O₂ added to the cell culture medium for 24 h. mRNA expression was determined *via* RT-PCR. The expression levels were normalized to that of β -actin. Data are shown as the mean \pm SD of three biological replicates. * $P < 0.05$. The inhibitory effect of ERI on 0.1% H₂O₂-induced injury of keratinocytes was measured using an MTT assay (D). Data are shown as the mean \pm SD of eight biological replicates. "100%" indicates an untreated control. *: $P < 0.05$, **: $P < 0.01$.

the retinoic acid receptor (RAR) (13). Therefore, ERI can be assumed to enhance AQP3 expression through RAR. Further verification is required to validate this conclusion.

Finally, the inhibitory effect of ERI on 0.1% H₂O₂-induced keratinocyte injury was evaluated *via* an MTT assay. ERI inhibited cell injury caused by H₂O₂ in a concentration-dependent manner (Figure 2D). This result suggests that ERI may reach the keratinocytes in the epidermal layer and protect the skin when the stratum corneum is damaged by UV exposure, atopic dermatitis, burns, and factors such as H₂O₂ and ROS generated by inflammation. In addition, ERI has been used to deliver drugs through the skin, and dissolving drugs in ERI reportedly enhances their absorption efficiency without damaging the skin (14). Although the mechanism of skin-permeability enhancement by ERI has not been fully clarified, ERI holds promise as a vehicle with the ability to scavenge H₂O₂ and ROS.

In summary, our results indicate that ERI exerts its protective effect on keratinocytes by reducing oxidative stress through two pathways: one pathway in which ERI acts directly on intracellular oxidants and electrophiles to reduce oxidative damage, and another pathway in which intracellular H₂O₂ is eliminated through AQP3.

Funding: None.

Conflict of Interest: MI, YO, and MO are employees of

A.I. System Products Corp.

References

- Madison KC, Wertz PW, Strauss JS, Downing DT. Lipid composition of cultured murine keratinocytes. *J Invest Dermatol.* 1986; 87:253-259.
- Brown KW, Parkinson EK. Glycoproteins and glycosaminoglycans of cultured normal human epidermal keratinocytes. *J Cell Sci.* 1983; 61:325-338.
- Claesson S, Juhlin L, Wettermark G. The reciprocity law of Uv-irradiation effects; damage on mouse skin exposed to Uv-light varied over a 107-fold intensity range. *Acta Derm Venereol.* 1958; 38:123-136.
- Parat MO, Richard MJ, Leccia MT, Amblard P, Favier A, Beani JC. Does manganese protect cultured human skin fibroblasts against oxidative injury by UVA, diethanolol and hydrogen peroxide? *Free Radic Res.* 1995; 23:339-351.
- Okajima M, Shimokawa K, Ishii F. The healing effect of electrolytic-reduction ion water on burn wounds. *Biosci Trends.* 2010; 4:31-36.
- Shu T, Okajima M, Shimokawa K, Ishii F. The treatment effect of the burn wound healing by electrolyticreduction ion water lotion. *Biosci Trends.* 2010; 4:1-3.
- Shu T, Okajima M, Wada Y, Shimokawa K, Ishii F. The treatment effect of the burn wound healing by electrolytic-reduction ion water lotion combination therapy. Part 2: Two degree burn of forearm to the dorsum of the hand. *Biosci Trends.* 2010; 4:213-217.
- Shu T, Okajima M, Wada Y, Shimokawa K, Ishii F. The treatment effect of the atopic dermatitis by electrolytic-reduction ion water lotion. *Drug Discov Ther.* 2010;

- 4:499-503.
9. Yamamoto H, Ikeda M, Okajima Y, Okajima M. Electrolytic-reduction ion water induces ceramide synthesis in human skin keratinocytes. *Drug Discov Ther.* 2021; 15:248-253.
 10. Jaiswal AK. Nrf2 signaling in coordinated activation of antioxidant gene expression. *Free Radic Biol Med.* 2004; 36:1199-1207.
 11. Alam J, Stewart D, Touchard C, Boinapally S, Choi AM, Cook JL. Nrf2, a Cap'n'Collar transcription factor, regulates induction of the heme oxygenase-1 gene. *J Biol Chem.* 1999; 274:26071-26078.
 12. Miller EW, Dickinson BC, Chang CJ. Aquaporin-3 mediates hydrogen peroxide uptake to regulate downstream intracellular signaling. *Proc Natl Acad Sci U S A.* 2010; 107:15681-15686.
 13. Bellemère G, Von Stetten O, Oddos T. Retinoic acid increases aquaporin 3 expression in normal human skin. *J Invest Dermatol.* 2008; 128:542-548.
 14. Kitamura T, Todo H, Sugibayashi K. Effect of several electrolyzed waters on the skin permeation of lidocaine, benzoic acid, and isosorbide mononitrate. *Drug Dev Ind Pharm.* 2009; 35:145-153.
- Received July 15, 2024; Revised October 1, 2024; Accepted October 7, 2024.
- *Address correspondence to:*
Hiroyuki Yamamoto, Department of Health and Nutritional Sciences, Faculty of Food and Health Sciences, Aichi Shukutoku University, 2-9 Katahira, Nagakute City, Aichi, 480-1197, Japan.
E-mail: yamahiro@asu.aasa.ac.jp
- Released online in J-STAGE as advance publication October 18, 2024.

Panax notoginseng root extract induces nuclear translocation of CRTC1 and *Bdnf* mRNA expression in cortical neurons

Shunsuke Shimizu^{1,§}, Aoi Nakano^{1,§}, Daisuke Ihara¹, Hironori Nakayama¹, Michiko Jo², Kazufumi Toume³, Katsuko Komatsu³, Naotoshi Shibahara⁴, Masaaki Tsuda¹, Mamoru Fukuchi^{5,*}, Akiko Tabuchi^{1,*}

¹Laboratory of Molecular Neurobiology, Graduate School of Medicine and Pharmaceutical Sciences, University of Toyama, Toyama, Japan;

²Department of Medicinal Resources Management, Institute of Natural Medicine, University of Toyama, Toyama, Japan;

³Division of Pharmacognosy, Institute of Natural Medicine, University of Toyama, Toyama, Japan;

⁴Kampo Education and Training Center, Institute of Natural Medicine, University of Toyama, Toyama, Japan;

⁵Laboratory of Molecular Neuroscience, Faculty of Pharmacy, Takasaki University of Health and Welfare, Gunma, Japan.

SUMMARY Brain-derived neurotrophic factor (BDNF), a member of the neurotrophin family, is deeply involved in the development and higher function of the nervous system, including learning and memory. By contrast, a reduction in BDNF levels is associated with various neurological disorders such as dementia and depression. Therefore, the inducers of *Bdnf* expression might be valuable in ameliorating or protecting against a decline in brain functions. We previously reported that, through high-throughput screening to identify inducers of *Bdnf* expression in *Bdnf-luciferase* transgenic mice, several herbal extracts induced *Bdnf* expression in cortical neurons. In the present study, we found that Panax notoginseng root extract (PNRE) potently induced *Bdnf* expression in primary cultured cortical neurons primarily *via* the L-type voltage-dependent Ca²⁺ channel (L-VDCC) and calcineurin. PNRE promoted nuclear translocation of cAMP-responsive element-binding protein-regulated transcription coactivator 1 (CRTC1). These findings suggest that PNRE activates the L-VDCC/calcineurin/CRTC1 axis, which is the primary signaling pathway involved in the neuronal activity-dependent expression of *Bdnf*. Moreover, we demonstrated that PNRE increased the dendritic complexity of cortical neurons *in vitro*. Thus, by upregulating *Bdnf* expression, PNRE is a potential candidate for improving cognitive impairment seen in several kinds of dementia.

Keywords Panax notoginseng root extract, BDNF, CRTC1, calcineurin, L-VDCC

1. Introduction

Overcoming dementia, including Alzheimer disease, is an urgent global health issue, and many strategies for developing treatments have been proposed. Brain-derived neurotrophic factor (BDNF) is a member of the neurotrophin protein family and plays roles in memory and in the survival and differentiation of neurons (1). The level of BDNF mRNA is decreased in patients with Alzheimer disease (2,3). By contrast, antidepressant drugs may increase BDNF levels (4,5), and high expression of BDNF in the brain may delay the decline in cognitive function caused by aging (6). Therefore, upregulating *Bdnf* expression is a potential therapeutic target for the treatment of dementia.

Previously, we established a high-throughput screening method to identify inducers of *Bdnf* expression using primary cortical cell cultures derived from *Bdnf-*

luciferase (alias *Bdnf-luc*) transgenic mice (7). We screened 120 herbal extracts and found that several extracts, including those from Panax notoginseng root (8), contained *Bdnf* inducers (7). The roots of *Panax notoginseng* (Burkill) F. H. Chen are traditionally used in the Chinese medicine and known for its various effects on the immune and cardiovascular systems and for its antitumor and antiatherosclerotic effects (9). A flavonol glycoside from the root of *P. notoginseng* decreases A β -mediated neurotoxicity (10). However, little is known about the effect of Panax notoginseng root extract (PNRE) on the nervous system, including its effect on regulating gene expression for neurotrophic factors, such as BDNF. In the present study, we found that PNRE induces *Bdnf* transcription *via* the L-type voltage-dependent calcium channel (L-VDCC) and calcineurin. PNRE is also a potent inducer of nuclear translocation of the cAMP-responsive element-binding protein (CREB)-

regulated transcription coactivator 1 (CRTC1), which is known as a substrate of calcineurin and a regulator of *Bdnf*. Furthermore, PNRE promoted dendritic complexity of cortical neurons.

Administration of the Panax notoginseng root saponin ginsenoside Rg1 to rats ameliorated $A\beta_{1-42}$ -induced deficits in learning and memory by downregulating $A\beta_{1-42}$ production and promoting $A\beta_{1-42}$ degradation (11). In addition, *P. notoginseng* root saponins upregulated neurogenesis in the hippocampus, attenuated the reduction in BDNF protein levels caused by cerebral ischemia, activated the mTOR pathway, and ameliorated neurological deficits (12). Therefore, PNRE in this study might contribute to novel drug designs to improve cognitive impairment.

2. Materials and Methods

2.1. Animals

Pregnant female Sprague Dawley rats were purchased from Japan SLC (Hamamatsu, Shizuoka, Japan). All experiments were performed in accordance with the ARRIVE guidelines and the requirements of the Animal Care and Experimentation Committee of the University of Toyama, Sugitani Campus. The Committee approved the protocols with permit Nos. A2022PHA-6, A2022PHA-7, A2019PHA-7, A2019PHA-10, and A2016PHA-8. Every effort was made to minimize animal suffering and the number of animals used.

2.2. Cell culture

Primary cultured cortical cells were prepared and maintained as described previously (7). Plastic dishes (35 mm diameter, AGC Techno Glass, Shizuoka, Japan) were coated with poly-L-lysine (P9155, Sigma, St. Louis, MO, USA) and used for real-time quantitative PCR experiments. Cortical cells were seeded at 1.8×10^6 cells/dish. For immunostaining, coverslips (83-0233, Matsunami, Osaka, Japan) were coated with poly-D-lysine (P6407, Sigma) and placed into a well in 12-well plates. Cortical cells were seeded at 7.0×10^5 cells/well in 12-well plates. Half of the medium was exchanged for fresh medium every 3 days.

2.3. Reagents

PNRE was prepared by extracting Panax notoginseng root (purchased from Tochimoto Tenkaido (lot No. 029716001, Osaka, Japan) in autoclaved Milli-Q water (10 \times the volume of herbal medicine) at 100°C for 50 min, after which the infusion mixture was filtered. Then, the extract was freeze-dried to obtain a powder. The powdered extract was redissolved in autoclaved Milli-Q water before use. The PNRE was characterized using LC-IT-TOF ME ESJ (Shimadzu), and the results are shown

in the Traditional Medical & Pharmaceutical Database of the University of Toyama at the following URL (https://dentomed.toyama-wakan.net/en/information_on_experimental_crude_drug_extracts/Panax%20Notoginseng%20Root-T/EXC278004). DL-APV (A5282), nifedipine (N7510) and FK506 (F4679) were obtained from Sigma. STO609 (570250, Calbiochem, La Jolla, CA, USA) and KN93 (AG-CR1-0065, AdipoGen Life Sciences, San Diego, USA) were used.

2.4. RNA isolation and quantitative (q)PCR

Total RNA isolation and the complementary DNA synthesis were performed as described previously (7). To detect *Bdnf* and *glyceraldehyde-3-phosphate dehydrogenase* gene (*Gapdh*) at the mRNA level, PCR was performed in 20 μ L of 1 \times SYBR Select Master Mix (4472908, Thermo Fisher Scientific) containing 2 μ L of cDNA solution and 0.2 μ M of each primer. The primer sequences and PCR program is provided in the Supplementary material (<https://www.ddtjournal.com/action/getSupplementalData.php?ID=217>). The value indicating relative expression was obtained by the ratio of *Bdnf* mRNA level/*Gapdh* mRNA level, and was indicated as the fold change, where the vehicle control value was regarded as "1".

2.5. Plasmids and antibodies

Enhanced green fluorescent protein (pEGFP-C1) vector was purchased from Takara Bio USA (San Jose, CA, USA). The following primary goat antibodies were used: CF594-conjugated anti-mouse IgG (20110, Biotium, Fremont, CA, USA; 1:1,000) and CF488A-conjugated anti-rabbit IgG (20019, Biotium; 1:1,000). Polyclonal rabbit antibodies were used as follows: anti-GFP (598, Medical & Biological Laboratories, Tokyo, Japan; 1:1,000) and anti-transducer of CREB protein 1 (TORC1) (#A300-769A, Bethyl Lab, Montgomery, Texas, USA; 1:500) for detecting CRTC1. A mouse monoclonal antibody raised against microtubule-associated protein 2 (MAP2) (M4403, 1:1,000) was purchased from Sigma.

2.6. DNA transfection

Four-day primary cultured cortical cells were transfected using a previously described calcium phosphate precipitation method (13). The vector expressing EGFP (4 μ g/well) was transfected.

2.7. Immunostaining

We used an existing method for immunostaining (13) with only minor modifications. 4',6-diamidino-2-phenylindole (DAPI) was used for nuclear staining. MAP2-positive cells were regarded as neurons.

2.8. Localization of CRTC1

Immunofluorescence images of immunostained cells were acquired using an LSM 700 confocal microscope (Zeiss). Fluorescence intensities with nuclear or cytoplasmic localization were evaluated using ImageJ software (National Institutes of Health, <https://imagej.nih.gov/ij/>) by investigators blinded to the various treatments. The fluorescent area within the DAPI-positive area was regarded as the nuclear, and the area within the MAP2-positive area was regarded as cytoplasmic. At least 50 cells were examined in each of three independent experiments.

2.9. Morphological analysis

Sholl analysis was used to evaluate dendritic morphology (13). The immunofluorescence images were obtained using a fluorescence microscope (BX50-34LFA-1, Olympus). MAP2-positive cell processes were regarded as dendrites. The number of GFP and MAP2 double-positive dendrites crossing circles drawn at the center of the cell body (at 20, 40, and 60 μm radii) was counted and totaled to obtain the number of crossings.

2.10. Statistical analysis

Data sets were compared using a one-way ANOVA followed by a Scheffe F test, or by paired or Welch t tests. Differences were considered significant when $P < 0.05/x$ (where x was the number of tests). Microsoft Excel 2013 [version 15.0.5127.1000] was used for all statistical analyses.

3. Results and Discussion

We had identified PNRE as an inducer of *Bdnf* expression using high-throughput screening (7). We initially examined whether PNRE induces endogenous *Bdnf* mRNA expression *via* activity-dependent Ca^{2+} channels in primary cultured rat cortical cells. PNRE increased *Bdnf* mRNA expression, and an NMDA receptor antagonist, APV, inhibited this increase slightly (Figure 1A). By contrast, the PNRE-induced increase in *Bdnf* mRNA expression was strongly inhibited by nicardipine, an inhibitor of L-VDCC (Figure 1B). These findings suggest that PNRE might activate primarily *via* L-VDCC and subsequent Ca^{2+} signaling in cortical neurons. Elevated Ca^{2+} levels in neurons *via* the L-VDCC propagate multiple signals, thereby regulating

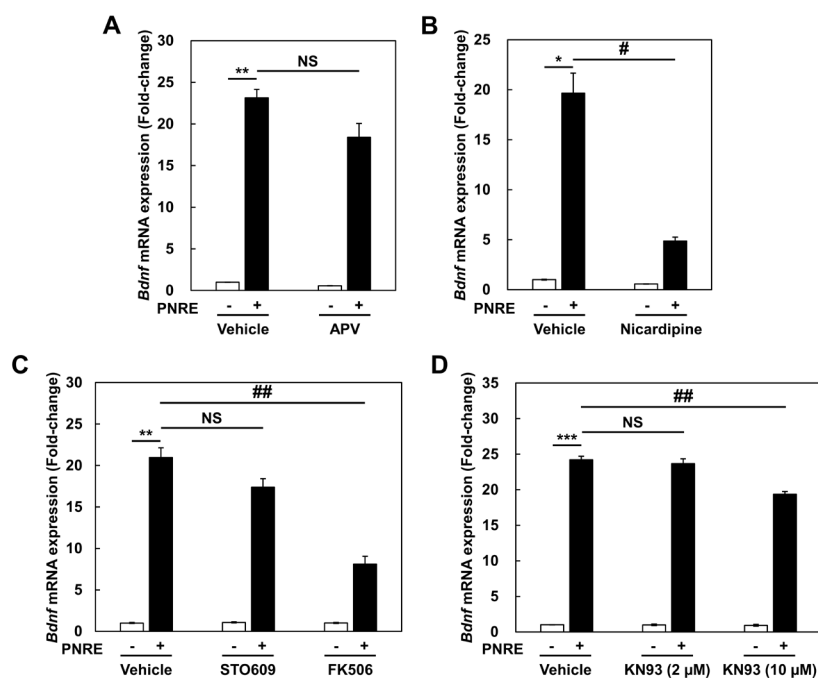


Figure 1. PNRE induces *Bdnf* mRNA expression in primary cultured cortical cells and the effects of signaling inhibitors on this induction. (A–D) Influence of signaling inhibitors on PNRE-induced *Bdnf* mRNA expression [days *in vitro* (DIV)13]. Inhibitors were added 10 min before administering PNRE (500 $\mu\text{g}/\text{mL}$). Three hours later, total RNA was extracted and subjected to qPCR. (A) APV (200 μM) partially inhibited *Bdnf* mRNA expression. The bars represent the means \pm SEMs ($n = 3-6$). Differences between treatment outcomes were analyzed using a Welch t test with post hoc Bonferroni correction ($^{**}P < 0.01/2$; NS, not significant). (B) Nicardipine (5 μM) significantly inhibited *Bdnf* mRNA expression. Bars represent the means \pm SEMs ($n = 3$). Differences between treatment outcomes were analyzed using a Welch t test with post hoc Bonferroni correction ($^{*}P < 0.05/2$; $^{#}P < 0.05/2$). (C) FK506 (5 μM), but not STO609, significantly inhibited *Bdnf* mRNA expression. Bars represent the means \pm SEMs ($n = 3-4$). Differences between treatment outcomes were analyzed using one-way ANOVA with a post hoc Scheffe F test ($^{##}P < 0.01$; NS, not significant) or a Welch t test with post hoc Bonferroni correction ($^{**}P < 0.01/3$). (D) KN93 (10 μM) partially inhibited *Bdnf* mRNA expression. The bars represent the means \pm SEMs ($n = 4$). Differences between treatment outcomes were analyzed using one-way ANOVA with a post hoc Scheffe F test ($^{##}P < 0.01$; NS, not significant) or a Welch t test with a post hoc Bonferroni correction ($^{***}P < 0.001/3$).

neuronal activity-dependent gene expression (14). Therefore, we next determined the main Ca^{2+} signaling pathway downstream of Ca^{2+} channels. STO609, a Ca^{2+} /calmodulin-dependent protein kinase kinase (CaMKK) inhibitor, tended to inhibit the induction of *Bdnf*, but the effect was not significant (Figure 1C). A Ca^{2+} /calmodulin-dependent protein kinase (CaMK) inhibitor (KN93) appeared to inhibit the induction of *Bdnf* slightly at 10 μM , but not at 2 μM (Figure 1D), indicating that CaMK pathways, such as the CaMKIV–CREB axis, but not CaMKII, might also contribute to PNRE-induced *Bdnf* transcription, at least in part. Subsequently, we focused on calcineurin, a Ca^{2+} /calmodulin-dependent serine–threonine phosphatase. FK506, a calcineurin inhibitor, strongly inhibited PNRE-induced *Bdnf* mRNA expression (Figure 1C). These experiments suggested that L-VDCC/calcineurin signaling might be the primary pathway that mediates PNRE-induced *Bdnf*.

CREB and its cofactor, CRTCI, are transcription factors involved in *Bdnf* induction (15). CRTCI is

dephosphorylated by calcineurin, thereby translocating into the nucleus (15). As described above, our findings suggest that calcineurin is involved in PNRE-induced *Bdnf* (Figure 1). Therefore, we next investigated whether PNRE induces the nuclear translocation of CRTCI in cortical neurons. Immunostaining of CRTCI in cortical neurons with and without PNRE-treatment revealed that the extract strongly promoted nuclear translocation of CRTCI (Figure 2A). PNRE increased the nuclear/cytoplasmic ratio of CRTCI, suggesting that the extract significantly induced the nuclear translocation of CRTCI in cortical neurons (Figure 2B). Among the herbal and Kampo extracts we screened, ginseng extracts and the Kampo formula daikenchuto were identified as *Bdnf* inducers via L-VDCC and calcineurin activation (7,16). The ginseng extract induces CREB phosphorylation and the translocation of CRTCI into the nucleus in cortical neurons (7). Our screening method is considered appropriate for identifying *Bdnf* inducers mediated by the L-VDCC/calcineurin/CRTCI axis, which is the primary

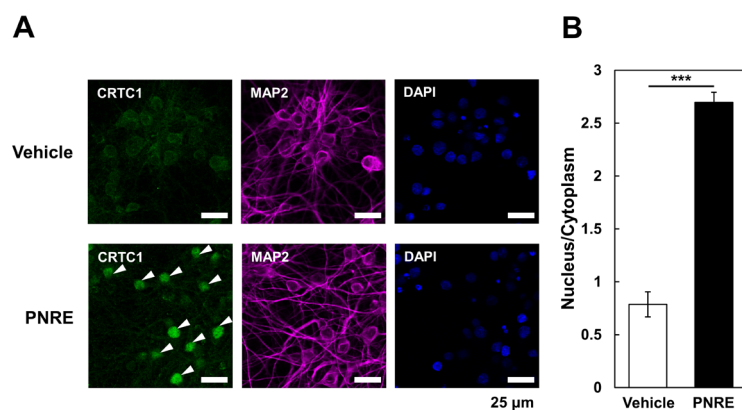


Figure 2. PNRE promotes the translocation of CRTCI into the nucleus in cortical neurons. (A) Representative images showing the localization of CRTCI (white arrowheads). Primary cultured rat cortical cells (DIV13) were stimulated with PNRE (500 $\mu\text{g}/\text{mL}$) for 15 min and immunostained. The cells were stained with an anti-CRTCI antibody (left), an anti-MAP2 antibody (middle), and DAPI (right). Scale bars, 25 μm . (B) Bar graphs showing the nuclear/cytoplasmic ratio of CRTCI under the experimental conditions shown in A. The bars represent the means \pm SEMs ($n = 3$). Intensities of the fluorescence immunostaining were quantified using ImageJ software (National Institutes of Health). Differences in treatment outcomes were analyzed using a paired t test ($***P < 0.001$).

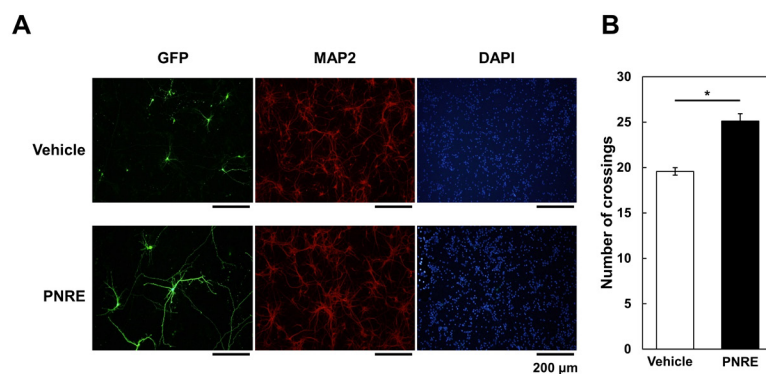


Figure 3. Dendritic complexity is increased by PNRE. (A) Primary cultured cortical cells (DIV4) were transfected with a green fluorescent protein (GFP) vector. Cells were stimulated with PNRE (500 $\mu\text{g}/\text{mL}$) 48 h posttransfection and incubated for 24 h. Then, the cells were immunostained with anti-GFP (left), anti-microtubule-associated protein 2 (MAP2) monoclonal antibodies (middle), and 4',6-diamidino-2-phenylindole (DAPI) (right). Scale bars, 200 μm . (B) Bar graphs showing the total number of dendritic crossings of circles drawn around soma (at 20, 40, and 60 μm radii) as a proxy for dendritic complexity under the experimental conditions described for A. The bars represent the means \pm SEMs ($n = 3$). Differences between treatment outcomes were analyzed using a paired t test ($P < 0.05$).

pathway involved in *BDNF* expression.

The activity-dependent expression of *Bdnf* may contribute to neurite outgrowth (17). As described above, we found that PNRE increased *Bdnf* induction in cortical neurons. These findings prompted us to investigate whether PNRE promotes the dendritic complexity of cortical neurons. Compared with vehicle control, PNRE induced greater dendritic complexity in GFP- and MAP2-double-positive neurons (Figure 3A). Sholl analysis to quantify dendritic morphology revealed that the total number of dendritic crossings across circles drawn around cell bodies increased significantly in response to treatment of cortical neurons with PNRE (Figure 3B), suggesting that PNRE had a neurotrophin-like effect on dendritic morphology. Daikenchuto, which includes the ginseng, induces *Bdnf* and promotes dendritic complexity (16). Additionally, we identified deltamethrin as an inducer of *Bdnf*, which mediates dendritic complexity in cortical neurons through endogenously expressed BDNF (17). Therefore, the dendritic complexity observed in the present study may be due to endogenous BDNF expression induced by PNRE.

Panax notoginseng root may be valuable for treating neurological disorders (11,12,18). The Panax notoginseng root saponin ginsenoside Rg1 may be a promising compound which induces *Bdnf* gene in our study because of identification of the Rg1 for ameliorating A β ₁₋₄₂-induced deficits in learning and memory (11). The protection of Panax notoginseng root against traumatic brain injury is associated with inhibiting autophagic events *via* the mTOR pathway (18). Natural products, such as polygalasaponin XXXII (19), P7C3 (20), and Glehnia Root and Rhizome extract (21), reverse scopolamine-induced BDNF reduction and memory impairment. To our knowledge, the present study is the first to demonstrate that PNRE induces *Bdnf* expression at the mRNA level and to elucidate the mechanisms by which Ca²⁺ signaling *via* the L-VDCC enhances the calcineurin/CRTC1 axis-mediated activation of *Bdnf* expression. This study on PNRE potentially contributes to the development of therapeutic strategies to upregulate *BDNF* expression for patients with neurological disorders associated with dysfunction of higher brain functions.

Acknowledgements

We are grateful that the Institute of Natural Medicine, University of Toyama provided us with a library of herbal extracts. This work was conducted using the Traditional Medical & Pharmaceutical Database, Institute of Natural Medicine, University of Toyama (<https://dentomed.toyama-wakan.net/index/en>). We thank Robin James Storer, PhD, from Edanz (<https://jp.edanz.com/ac>), for editing a draft of this manuscript.

Funding: This study was funded in part by the Mochida

Memorial Foundation for Medical and Pharmaceutical Research (to M.F.), the Takeda Science Foundation (to M.F.), the Discretionary Funds of the President of the University of Toyama [Project leader: Prof. Chihiro Tohda (Section of Neuromedical Science, Division of Bioscience, Institute of Natural Medicine, University of Toyama)], a grant-in-aid for the Cooperative Research Project from the Institute of Natural Medicine at the University of Toyama in 2015 and 2016 (to M.F.), the JSPS KAKENHI grant Nos. JP25870256 [Grant-in-Aid for Young Scientists (B) to M.F.], 16H05275 [Grant-in-Aid for Scientific Research (B) to M.F.], 22K11859 [Grant-in-Aid for Scientific Research (C) to M.F.], and 23H03305, 23K27995 [Grant-in-Aid for Scientific Research (B) to A.T.] .

Conflict of Interest: The authors have no conflicts of interest to disclose.

References

1. Park H, Poo MM. Neurotrophin regulation of neural circuit development and function. *Nat Rev Neurosci*. 2013; 14:7-23.
2. Ferrer I, Marin C, Rey MJ, Ribalta T, Goutan E, Blanco R, Tolosa E, Marti E. BDNF and full-length and truncated TrkB expression in Alzheimer disease. Implications in therapeutic strategies. *J Neuropathol Exp Neurol*. 1999; 58:729-739.
3. Forlenza OV, Diniz BS, Teixeira AL, Radanovic M, Talib LL, Rocha NP, Gattaz WF. Lower cerebrospinal fluid concentration of brain-derived neurotrophic factor predicts progression from mild cognitive impairment to Alzheimer's Disease. *Neuromolecular Med*. 2015; 17:326-332.
4. Chen B, Dowlatshahi D, MacQueen GM, Wang JF, Young LT. Increased hippocampal BDNF immunoreactivity in subjects treated with antidepressant medication. *Biol Psychiatry*. 2001; 50:260-265.
5. Molendijk ML, Bus BA, Spinhoven P, Penninx BW, Kenis G, Prickaerts J, Voshaar RC, Elzinga BM. Serum levels of brain-derived neurotrophic factor in major depressive disorder: state-trait issues, clinical features and pharmacological treatment. *Mol Psychiatry*. 2011; 16:1088-1095.
6. Buchman AS, Yu L, Boyle PA, Schneider JA, De Jager PL, Bennett DA. Higher brain BDNF gene expression is associated with slower cognitive decline in older adults. *Neurology*. 2016; 86:735-741.
7. Fukuchi M, Okuno Y, Nakayama H, Nakano A, Mori H, Mitazaki S, Nakano Y, Toume K, Jo M, Takasaki I, Watanabe K, Shibahara N, Komatsu K, Tabuchi A, Tsuda M. Screening inducers of neuronal BDNF gene transcription using primary cortical cell cultures from BDNF-luciferase transgenic mice. *Sci Rep*. 2019; 9:11833.
8. The Ministry of Health, Labour, and Welfare (2022) The Japanese standards for non-Pharmacopoeial crude drugs 2022 (English version), Monograph, pp49-51, Tokyo. (<https://www.mhlw.go.jp/content/11120000/001010074.pdf>) (accessed 13 May 2024)
9. Wang T, Guo R, Zhou G, Zhou X, Kou Z, Sui F, Li C, Tang L, Wang Z. Traditional uses, botany, phytochemistry,

- pharmacology and toxicology of *Panax notoginseng* (Burk.) F.H. Chen: A review. *J Ethnopharmacol.* 2016; 188:234-258.
10. Choi RC, Zhu JT, Leung KW, Chu GK, Xie HQ, Chen VP, Zheng KY, Lau DT, Dong TT, Chow PC, Han YF, Wang ZT, Tsim KW. A flavonol glycoside, isolated from roots of *Panax notoginseng*, reduces amyloid-beta-induced neurotoxicity in cultured neurons: signaling transduction and drug development for Alzheimer's disease. *J Alzheimers Dis.* 2010; 19:795-811.
 11. Liu SZ, Cheng W, Shao JW, Gu YF, Zhu YY, Dong QJ, Bai SY, Wang P, Lin L. Notoginseng saponin Rg1 prevents cognitive impairment through modulating APP processing in Aβ(1-42)-injected rats. *Curr Med Sci.* 2019; 39:196-203.
 12. Gao J, Liu J, Yao M, Zhang W, Yang B, Wang G. *Panax notoginseng* saponins stimulates neurogenesis and neurological restoration after microsphere-induced cerebral embolism in rats partially *via* mTOR signaling. *Front Pharmacol.* 2022; 13:889404.
 13. Ishikawa M, Nishijima N, Shiota J, Sakagami H, Tsuchida K, Mizukoshi M, Fukuchi M, Tsuda M, Tabuchi A. Involvement of the serum response factor coactivator megakaryoblastic leukemia (MKL) in the activin-regulated dendritic complexity of rat cortical neurons. *J Biol Chem.* 2010; 285:32734-32743.
 14. Greer PL, Greenberg ME. From synapse to nucleus: calcium-dependent gene transcription in the control of synapse development and function. *Neuron.* 2008; 59:846-860.
 15. Nonaka M, Kim R, Fukushima H, Sasaki K, Suzuki K, Okamura M, Ishii Y, Kawashima T, Kamijo S, Takemoto-Kimura S, Okuno H, Kida S, Bito H. Region-specific activation of CRTCL1-CREB signaling mediates long-term fear memory. *Neuron.* 2014; 84:92-106.
 16. Nakayama H, Ihara D, Fukuchi M, Toume K, Yuri C, Tsuda M, Shibahara N, Tabuchi A. The extract based on the Kampo formula daikenchuto (Da Jian Zhong Tang) induces *Bdnf* expression and has neurotrophic effects in cultured cortical neurons. *J Nat Med.* 2023; 77:584-595.
 17. Ihara D, Fukuchi M, Honma D, Takasaki I, Ishikawa M, Tabuchi A, Tsuda M. Deltamethrin, a type II pyrethroid insecticide, has neurotrophic effects on neurons with continuous activation of the *Bdnf* promoter. *Neuropharmacology.* 2012; 62:1091-1098.
 18. Shi Y, Zhou X, Yang R, Ying S, Wang L. *Panax notoginseng* protects the rat brain function from traumatic brain injury by inhibiting autophagy *via* mammalian targeting of rapamycin. *Aging (Albany NY).* 2021; 13:11207-11217.
 19. Xue W, Hu JF, Yuan YH, Sun JD, Li BY, Zhang DM, Li CJ, Chen NH. Polygalasaponin XXXII from *Polygala tenuifolia* root improves hippocampal-dependent learning and memory. *Acta Pharmacol Sin.* 2009; 30:1211-1219.
 20. Jiang B, Song L, Huang C, Zhang W. P7C3 attenuates the scopolamine-induced memory impairments in C57BL/6J mice. *Neurochem Res.* 2016; 41:1010-1019.
 21. Balakrishnan R, Kim YS, Kim GW, Kim WJ, Hong SM, Kim CG, Choi DK. Standardized extract of *Glehnia littoralis* abrogates memory impairment and neuroinflammation by regulation of CREB/BDNF and NF-κB/MAPK signaling in scopolamine-induced amnesic mice model. *Biomed Pharmacother.* 2023; 165:115106.
- Received August 9, 2024; Revised October 1, 2024; Accepted October 17, 2024.
- §These authors contributed equally to this work.
*Address correspondence to:
Akiko Tabuchi, Laboratory of Molecular Neurobiology, Graduate School of Medicine and Pharmaceutical Sciences, University of Toyama, 2630 Sugitani, Toyama 930-0194, Japan.
E-mail: atabuchi@pha.u-toyama.ac.jp
- Mamoru Fukuchi, Laboratory of Molecular Neuroscience, Faculty of Pharmacy, Takasaki University of Health and Welfare, 60 Nakaorui-machi, Takasaki, Gunma 370-0033, Japan.
E-mail: fukuchi@takasaki-u.ac.jp
- Released online in J-STAGE as advance publication October 24, 2024.

Padding the seat of a wheelchair reduces ischial pressure and improves sitting comfort

Yoshiyuki Yoshikawa^{1,*}, Kiyo Sasaki¹, Kyoko Nagayoshi², Kenta Nagai², Yuki Aoyama³, Shuto Takita⁴, Teppei Wada⁵, Yoshinori Kitade⁶

¹Naragakuen University Graduate School of Rehabilitation Sciences, Nara, Japan;

²Visiting Nurse Station Mich, Avanzar Inc., Akashi, Japan;

³Department of Rehabilitation, Heisei Memorial Hospital, Nara, Japan;

⁴Department of Rehabilitation, Gakkentoshi Hospital, Kyoto, Japan;

⁵Department of Rehabilitation, Naramachi Rehabilitation Hospital, Nara, Japan;

⁶Department of Rehabilitation, Seiyu Memorial Hospital, Wakayama, Japan.

SUMMARY In this study, we aimed to examine whether a wheelchair cushion placed directly atop a sling seat or deflection of the sling seat compensated by a pad along with the placement of a wheelchair cushion changed sitting pressure. Additionally, we examined whether these additions changed sitting comfort. For twenty healthy adults who consented to participate, measurements were taken for three types of cushions, each with and without padding, under six conditions. The cushion types tested included air (cushion A), urethane foam (cushion U), and three-dimensional thermoplastic elastomer (cushion T). A pressure distribution measurement equipment was used for the measurements. Following the measurement, the comfort of the wheelchair cushion was measured. The ischial area pressure of the cushion A pad was significantly lower than that without the pad. Cushions U and T were for ischial area pressure with a pad, resulting in a decreasing trend in ischial area pressure with a pad compared to that without a pad; however, the difference was insignificant. For all cushions, sitting comfort was significantly better in all groups with padding than in those without. In conclusion, ischial pressure can be dispersed by placing a pad on the seat surface of a wheelchair cushion, and pads were suggested to improve sitting comfort for all cushions.

Keywords wheelchair cushion, pressure redistribution, sling seat

1. Introduction

Pressure ulcers occur when soft tissues are compressed between the bony prominence and external surface for a prolonged period or when blood flow is obstructed by external forces such as misalignment (1). Although some studies have posited pressure ulcers as preventable, their incidence remains high (2-4). In addition, when pressure ulcers develop, long-term treatment is required before healing, resulting in significant medical and economic losses (5-7).

Pressure ulcers are more common in wheelchair users who are at long-term risk of developing these sores (8). When an individual sits in a wheelchair, external forces are concentrated on the bony prominences of the ischium and tailbone, increasing the risk of pressure ulcers (8). Thus, wheelchair users should remove external forces every 15-30 min (9); however, individuals of advanced age have difficulty removing external forces

by themselves. Therefore, the pressure ulcer prevention guidelines recommend the use of wheelchair cushions for pressure ulcer prevention (1,10). We have previously reported that the use of wheelchair cushions enables pressure dispersion (11).

However, because the seat of a wheelchair is a sling, deflection of its surface is prone to occur, contributing to pelvic tilt, which in turn increases local pressure and leads to pressure ulcers (12). In addition, because the level of seat deflection of a wheelchair varies from model to model, wheelchair cushions cannot accommodate all deflections, and the effect of seat pressure dispersion of the wheelchair cushion is reduced by half. In our previous study, the pressure dispersion effect of wheelchair cushions with padding to compensate for deflection was high (11). Another study evaluated the insertion of a pad under the wheelchair cushion, referred to as the "pelvic well pad" study (13). In that study, researchers created and inserted a pad with

the ischial area cut off and reported a decrease in the mean and peak pressures and an increase in the contact area in the buttocks and thighs. These results suggest that inserting a pad that compensates for the deflection under a wheelchair cushion can increase sciatic pressure and contribute to the prevention of pressure ulcers.

Therefore, in this study, we aimed to examine whether sitting pressure changes when a wheelchair cushion is placed directly on top of a sling seat or when a pad and a wheelchair cushion compensate the deflection of the sling seat is placed on top of the sling seat. Additionally, we examined whether there was a change in sitting comfort with and without a pad.

2. Materials and Methods

2.1. Participants

The number of participants in this study was calculated using the G Power software. Based on a previous study (11), with an effect size of 0.7, an alpha error of 0.05, and a power of 0.8, the required sample size was 19. Therefore, 20 participants were included in this study, after excluding those who withdrew consent and those with missing data. The inclusion criteria for this study were a sitting girdle width of 34–40 cm and a sitting base length of 41–49 cm. In contrast, the exclusion criteria were a sitting girdle width of ≥ 41 cm and ≤ 33 cm, sitting base length of ≥ 50 cm and ≤ 40 cm, and the presence of back or lower limb disease. The final sample included 20 healthy adults (10 male and 10 female).

2.2. Ethics

This study was conducted in accordance with the Declaration of Helsinki. Its purpose and significance were fully explained to all participants, who all provided their signatures on a consent form before the study. This study was approved by the Ethics Committee of Naragakuen University (approval number/ID 3-R003).

2.3. Devices and equipment used

A CONFORMat (Nitta Corp., Osaka, Japan) was used

to measure body pressure, which is a sensor mat with previous testing for reliability and validity (11,14-16). The specifications of the sensor sheet were as follows: depth, 471 mm \times width, 471 mm; 1024 sensors (32 rows \times 32 columns); thickness of 1.8 mm, and a resolution of 14.7 mm. A standard wheelchair (MATSUNAGA MANUFACTORY Co., Ltd., Tokyo, Japan) was used. Three types of cushions were tested: an air material (ROHO; Permobil Co., Ltd., Västernorrland Sweden: single-valve low-profile air material, 40.5 \times 43 \times 5.5 cm: cushion A), urethane foam material (Moderate cushion; LAC Healthcare Ltd., Osaka, Japan: special urethane material, 40 \times 40 \times 6 cm: cushion U), and a three-dimensional (3D) thermoplastic elastomer material (Geltron; Pacific wave Co., Ltd., Japan: 3D thermoplastic elastomer material, 38 \times 38 \times 3.5 cm: cushion T). The seat deflection was measured beforehand, and urethane foam pads were prepared to match the deflection.

2.4. Measurements

Measurements were taken for the three cushion types, each with and without padding, under six conditions. After the participant's seated lower leg length was measured and foot support was adjusted, they were assessed for 5 min without a wheelchair cushion to determine the reference value. The order of the six conditions was randomly assigned using the envelope method. The participants then sat in a wheelchair in the assigned order, and the position of the ischial region was identified. The measurement position was taken with the pelvis positioned as far back in the seat as possible, and the seat and thighs were positioned horizontally. The feet were placed on footrests, and both upper limbs were positioned on the thighs instead of the arm supports. Measurements were taken after the sitting pressure stabilized (after approximately 5 min) for 10 min. After the measurement, the sitting comfort of the wheelchair cushion was measured using a numerical rating scale (NRS). Using the NRS, the participants were then instructed to rate their sitting comfort on a scale of 10, with 10 being "very poor" and 0 being "very good and comfortable." When the state of sitting comfort without the standard cushion was set to 10 (very poor), the



Figure 1. Measuring and padding wheelchair seat deflection. (A) Measurement of wheelchair seat deflection. Wheelchair (B) with deflection compensation pad and (C) without deflection compensation pad.

participants were instructed to indicate how comfortable they felt in the target group. The wheelchair cushion and pad were replaced after the NRS score assessment, and a 5-min break was allowed between measurements.

2.5. Analyses

For assessing pressure at the ischium, the mean value of the four sensors around the maximum pressure area (peak pressure index) was calculated for each condition. Sciatic pressure and NRS scores with and without deflection correction in each condition were compared using a paired *t*-test. In addition, 95% confidence intervals and effect sizes were calculated. Effect sizes were calculated using Field's *r* to measure the standardized mean difference between the two groups, calculated as $r = \sqrt{t^2 / (t^2 + df)}$ (17). All analyses were performed using the R (version 4.0.3, R Foundation) for Windows. Statistical significance was set at a Bonferroni-corrected $P < 0.015$.

3. Results and Discussion

The ischial area pressures of cushion A were 34.2 ± 6.2 mmHg without a pad and 31.0 ± 7.1 mmHg with a pad. The ischial area pressure with a pad was significantly lower than that without a pad ($P = 0.0021$), and the effect size was large ($r = 0.63$). The ischial area pressures of cushion U were 26.4 ± 4.4 mmHg without a pad and 24.2 ± 5.1 mmHg with a pad, showing a decreasing trend in ischial area pressure with a pad compared to that without a pad. However, the difference was not significant ($P = 0.018$). However, the effect size was large ($r = 0.51$). The ischial area pressures of cushion T were 37.9 ± 8.4 mmHg without a pad and 33.4 ± 8.3 mmHg with a pad, showing a decreasing trend in ischial area pressure with a pad compared to that without a pad, but without significant difference ($P = 0.031$). The effect size was moderate ($r = 0.47$) (Table 1). As the use

of wheelchair cushions for wheelchair users decreases sciatic pressure ulcers and reduces the risk of pressure ulcers (1,10), these devices should be used to reduce and prevent ischial pressure ulcers. However, as the seat surface of a wheelchair is a sling, deflection occurs and is believed to reduce the performance of the wheelchair cushion. In a previous study, Shin *et al.* reported that padding the seat surface reduces peak pressure (13). However, adding a seat surface increases ischial pressure (18). Therefore, unlike the previous study, this research was conducted with a pad placed on the seat surface of a wheelchair following the deflection of the seat surface. Consequently, ischial pressure was significantly reduced when the wheelchair cushion was used with padding compared with when it was used without padding; however, no significant reduction was observed in cushions U and T, the effect sizes were high (cushion U), and medium (cushion T) and ischial pressure tended to decrease. In our previous wheelchair cushion study, a hybrid-type wheelchair cushion was padded, resulting in lower ischial pressure (11). Although the ischial pressure was shown to increase in a study by Kamegaya *et al.* (18), this may have been due to different materials. Wood was used in their study, whereas urethane was used in ours. It is possible that the urethane foam material dispersed the pressure while compensating for the deflection as it is a porous material used for cushions (19). Based on the aforementioned findings, placing a pad on the seat surface of a wheelchair when using a wheelchair cushion can reduce the ischial pressure ulcer pressure and contribute to the prevention of pressure ulcers.

Regarding seating comfort, the three cushions had the following values: cushion U (without pad, 5.0 ± 1.1 ; with pad, 4.1 ± 0.9), cushion T (without pad, 5.1 ± 0.9 ; with pad, 4.0 ± 0.6), and cushion A (without pad, 5.5 ± 1.0 ; with pad, 4.5 ± 0.8). The sitting comfort was significantly better in all groups with padding than in those without padding ($P < 0.015$; cushion U: $r = 0.66$, effect size,

Table 1. Comparison of ischial area pressure with and without a pad

Cushions	Without pad	With pad	<i>P</i> value	Effect size: <i>r</i>
U	26.4 ± 4.4 (24.3–28.5)	24.2 ± 5.1 (21.3–26.6)	0.018	0.51
T	37.9 ± 8.4 (34.0–41.8)	33.4 ± 8.3 (29.5–37.3)	0.031	0.47
A	34.2 ± 6.2 (31.3–37.1)	31.0 ± 7.1 (27.7–34.3)	< 0.015	0.63

Values are expressed as means±standard deviations (95% confidence intervals). Abbreviations: U, urethane foam material; T, three-dimensional thermoplastic elastomer material; A, air material.

Table 2. Comparison of seating comfort with and without a pad

Cushions	Without pad	With pad	<i>P</i> value	Effect size: <i>r</i>
U	5.0 ± 1.1 (4.5–5.5)	4.1 ± 0.9 (3.7–4.5)	< 0.015	0.66
T	5.1 ± 0.9 (4.7–5.5)	4.0 ± 0.6 (3.7–4.2)	< 0.015	0.88
A	5.5 ± 1.0 (5.0–6.0)	4.5 ± 0.8 (4.1–4.9)	< 0.015	0.83

Values are expressed as means±standard deviations (95% confidence intervals). Abbreviations: U, urethane foam material; T, three-dimensional thermoplastic elastomer material; A, air material.

large; cushion T: $r = 0.88$, effect size, large; cushion A: $r = 0.83$, effect size, large) (Table 2). This result confirmed the comfort of the wheelchair seating position using pads. Regarding wheelchair seating comfort, Harms reported that wheelchair sling seats promoted a kyphotic posture and caused neck and back discomfort in able-bodied and disabled participants (20). Wheelchair sitting in a sling seat also promotes scoliosis and poor posture (21), which can contribute to deformities (22) and increase the risk of neck and back pain due to muscle strain (23,24). Therefore, sitting comfort is important. This study showed that padding compensated for the deflection and increased the contact area of the buttocks to maintain a stable posture, resulting in significantly better seating comfort for all cushions. This suggests using pads to compensate for the deflection and improve sitting comfort.

Nevertheless, this study has some limitations. First, the participants were healthy. Therefore, in the future, we would like to conduct studies on older individuals with atrophied gluteal muscles and patients with spinal injuries to confirm the prevention of pressure ulcers. Second, the sitting time was approximately 10 min. Wheelchair users are forced to sit for long periods. Therefore, it is necessary to observe changes in ischial pressure and sitting comfort when sitting for long periods. Third, only ischial pressure was measured as an external force in this study. Because the external force can be misaligned, we believe that verifying misalignment is also necessary in the future. In conclusion, ischial pressure can be dispersed by placing a pad on the seat surface of the air material. Although no significant pressure-reducing effect was observed for the urethane and 3D thermoplastic elastomer material cushions, a pressure-reducing effect was confirmed. In addition, the pads improved the sitting comfort of all the cushions.

Acknowledgements

The authors would like to thank the participants who participated in the measurements of this study.

Funding: This research was funded by JSPS KAKENHI (grant number, JP21K18107).

Conflict of Interest: The authors have no conflicts of interest to disclose.

Informed Consent Statement: Written informed consent has been obtained from all participants to publish this paper.

References

1. European Pressure Ulcer Advisory Panel, National Pressure Injury Advisory Panel and Pan Pacific Pressure Injury Alliance, Emily Haesler (Ed). Prevention and treatment of pressure ulcers/injuries: clinical practice

- guideline. <https://internationalguideline.com/2019>; Third edition:1-405. (accessed 25 August 2024)
2. Chaboyer W, Bucknall T, Webster, J, McInnes E, Gillespie MB, Banks M, Whitty JA, Thalib L, Roberts S, Tallott M, Cullum N, Wallis M. The effect of a patient centred care bundle intervention on pressure ulcer incidence (INTACT): a cluster randomised trial. *Int J Nurs Stud.* 2016; 64:63-71.
3. McInnes E, Jammali-Blasi A, Bell-Syer SE, Dumville JC, Middleton V, Cullum N. Support surfaces for pressure ulcer prevention. *Cochrane Database Syst Rev.* 2015; 2015:CD001735.
4. Webster J, Coleman K, Mudge A, Marquart L, Gardner G, Stankiewicz M, Kirby J, Vellacott C, Horton-Breshears M, McClymont A. Pressure ulcers: effectiveness of risk-assessment tools. A randomised controlled trial (the ULCER trial). *BMJ Qual Saf.* 2011; 20:297-306.
5. Nguyen KH, Chaboyer WP, Whitty JA. Pressure injury in Australian public hospitals: a cost-of-illness study. *Aust Health Rev.* 2015; 39:329-336.
6. Dealey C, Posnett J, Walker A. The cost of pressure ulcers in the United Kingdom. *J Wound Care.* 2012; 21:261-262.
7. Moore ZE, van Etten MT, Dumville JC. Bed rest for pressure ulcer healing in wheelchair users. *Cochrane Database Syst Rev.* 2016; 10:CD011999.
8. Stockton L, Parker D. Pressure relief behaviour and the prevention of pressure ulcers in wheelchair users in the community. *J Tissue Viability.* 2002; 12:84-99.
9. Schofield R, Porter-Armstrong A, Stinson M. Reviewing the literature on the effectiveness of pressure relieving movements. *Nurs Res Pract.* 2013; 2013:124095.
10. Japanese Society of Pressure Ulcers Guideline Revision Committee. JSPU guidelines for the prevention and management of pressure ulcers (4th Ed.). *Jpn J PU.* 2016; 18:455-544. (in Japanese)
11. Yoshikawa Y, Nagayoshi K, Maeshige N, Yamaguchi A, Aoyama Y, Takita S, Wada T, Tanaka M, Terashi H, Sonoda Y. Stability of ischial pressure with 3D thermoplastic elastomer cushion and the characteristics of four types of cushions in pressure redistribution. *Drug Discov Ther.* 2024; 18:188-193.
12. Kinose T, Hirose H. Modular wheelchair for the elderly. *J Jpn Phys Ther Assoc.* 2001; 28:173-176. (in Japanese).
13. Shin H, Kim J, Kim JJ, Kim HR, Lee HJ, Lee BS, Han ZA. Pressure relieving effect of adding a pelvic well pad to a wheelchair cushion in individuals with spinal cord injury. *Ann Rehabil Med.* 2018; 42:270-276.
14. Nakagami G, Sanada H, Sugama J. Development and evaluation of a self-regulating alternating pressure air cushion. *Disabil Rehabil Assist Technol.* 2015; 10:165-169.
15. Hori J, Ohara H, Inayoshi S. Control of speed and direction of electric wheelchair using seat pressure mapping. *Biocybern Biomed Eng.* 2018; 38:624-633.
16. Matsuo J, Sugama J, Sanada H, Okuwa M, Nakatani T, Konya C, Sakamoto J. Development and validity of a new model for assessing pressure redistribution properties of support surfaces. *J Tissue Viability.* 2011; 20:55-66.
17. Field A. *Discovering Statistics Using SPSS* (2nd ed.), London: Sage Publications, United Kingdom, 2005.
18. Kamegaya T, Yamazaki M, Onaka Y, Jingu Y, Tanaka Y. Effects of using insert panels to improve wheelchair seat deflection. *J Gunma Assoc Occup Ther.* 2018; 20:11-15. (in Japanese).
19. Suleman S, Khan SM, Gull N, Aleem W, Shafiq M, Jamil T.

- A comprehensive short review on polyurethane foam. *Int J Innov Sci Res.* 2014; 12:165-169.
20. Harms M. Effect of wheelchair design on posture and comfort of users. *Physiotherapy.* 1990; 76:266-271.
 21. Holden JM, Fernie G, Lunau K. Chairs for the elderly-design considerations. *Appl Ergon.* 1988; 19:281-288.
 22. Hey HWD, Wong CG, Lau ET, Tan KA, Lau LL, Liu KG, Wong HK. Differences in erect sitting and natural sitting spinal alignment-insights into a new paradigm and implications in deformity correction. *Spine J.* 2017; 17:183-189.
 23. Nimbarte AD, Zreiqat M, Ning X. Impact of shoulder position and fatigue on the flexion-relaxation response in cervical spine. *Clin Biomech (Bristol, Avon).* 2014; 29:277-282.
 24. Stewart DM, Gregory DE. The use of intermittent trunk flexion to alleviate low back pain during prolonged standing. *J Electromyogr Kinesiol.* 2016; 27:46-51.

Received September 2, 2024; Revised October 12, 2024; Accepted October 23, 2024.

**Address correspondence to:*

Yoshiyuki Yoshikawa, Naragakuen University Graduate School of Rehabilitation Sciences, 3-15-1, Nakatomigaoka, Nara-city, Nara 631-8524, Japan.

E-mail: y-yoshi@naragakuen-u.jp

Released online in J-STAGE as advance publication October 27, 2024.

A stroke patient with persistently intermittent fever treated with gabapentin: A clinical case

Jingjie Huang^{1,2,§}, Bangqi Wu^{2,§,*}, Yupei Cheng^{1,2}, Chaoran Wang^{1,2}

¹Degree: Postgraduate student, Tianjin University of Traditional Chinese Medicine, Tianjin, China;

²National Clinical Research Center for Chinese Medicine Acupuncture and Moxibustion, First Teaching Hospital of Tianjin University of Traditional Chinese Medicine, Tianjin, China.

SUMMARY Fever is one of the most common complications in stroke patients and can generally be classified as either infectious or non-infectious. Infectious fevers are commonly caused by pulmonary infections, urinary tract infections, and secondary infections associated with medical interventions such as endotracheal intubation, urinary catheterization, and nasogastric tubes. Non-infectious fevers primarily manifest as central fevers, although in rare cases, they may also result from drug-induced causes. Existing research indicates that the most common cause of central fever is brainstem hemorrhage, followed by hemorrhage in the basal ganglia and thalamus, then cerebellar hemorrhage, large cortical infarction, and basilar artery occlusion, with intraventricular hemorrhage being relatively rare. Stroke patients' body temperatures can rise to 39°C within 12 hours after onset and peak within 24 hours. In this case, a stroke patient with acute cerebral infarction and secondary thalamic hemorrhage developed new sensory abnormalities in the left limbs and intermittent fever during hospitalization. Despite the use of antibiotics targeting a pulmonary infection, the patient's fever did not show significant improvement. Gabapentin was added to the treatment regimen to address the sensory abnormalities. Surprisingly, within four hours of gabapentin administration, the patient's body temperature normalized and remained stable during subsequent monitoring. This observation led us to hypothesize that gabapentin may have a potential role in alleviating central fever.

Keywords stroke, infection, thalamic fever, gabapentin, central fever

Letter to the Editor,

The typical manifestation of central fever is a significant fluctuation in body temperature over a short period, characterized by a rapid rise followed by a gradual decline, and is often associated with high mortality rates (1,2). Additionally, studies have suggested that dysphagia may also be linked to fever (3,4). Paroxysmal sympathetic hyperactivity can also cause fever, with clinical symptoms including paroxysmal hyperthermia, tachycardia, rapid breathing, hypertension, and generalized muscle rigidity (5,6). Common treatments for such fevers include acetaminophen and nonsteroidal anti-inflammatory drugs (NSAIDs) (7-9). Traditional pharmacological interventions, such as diclofenac sodium, are widely used, while bromocriptine and dantrolene are frequently prescribed for patients with malignant hyperthermia (10). Furthermore, the literature mentions the adjunctive use of non-pharmacological therapies and physical cooling methods, such as warm compresses, ice packs,

and alcohol wipes (11,12).

The thalamus not only functions as the brain's primary sensory relay center but also plays a critical role in temperature regulation, as the hypothalamus, which is responsible for thermoregulation, is closely linked to central fever symptoms (13). Central fever is not uncommon in clinical practice, particularly among stroke patients. A review of the literature and case reports reveals that treatment for central fever primarily focuses on anti-infective and anti-inflammatory therapies. However, to date, no reports have documented the use of gabapentin for treating central fever following a stroke.

Here, we report a novel case: A 70-year-old patient initially presented with persistent dizziness, vomiting, and urinary incontinence, without any clear cause. Upon admission, her symptoms included drowsiness, slowed responses, cognitive impairment, poor speech fluency, and reduced motor function in both limbs, with more pronounced symptoms on the right side, including

sensory deficits in the right lower limb. Muscle strength assessment revealed 2/5 in the right upper and lower limbs, 4/5 in the left upper limb, and 3/5 in the left lower limb.

An initial evaluation at the local hospital included a brain MRI, which showed medullary infarction. Due to the severity and complexity of her condition, the patient was transferred to our hospital for further evaluation and treatment. Upon admission, we developed a comprehensive treatment plan to address her medical issues. According to stroke management guidelines, the patient received dual antiplatelet therapy with aspirin and clopidogrel to prevent stroke recurrence. In addition, atorvastatin was prescribed to regulate lipid levels and stabilize plaques. Butylphthalide was introduced to improve cerebral circulation and metabolism. Urokinase was used to promote collateral circulation, and betahistine was administered to prevent vertigo episodes. Fibrinolytic was also used to manage the patient's hypercoagulable state.

During hospitalization, the patient developed additional complications, including signs of upper gastrointestinal bleeding, prompting the introduction

of omeprazole to protect the gastric mucosa. The patient also experienced intermittent fever, leading to immediate laboratory tests and imaging studies. Subsequent imaging revealed a hematoma in the right thalamus with rupture into the ventricle. A chest CT also showed patchy shadows in the right upper lobe and left lower lobe, suggestive of pulmonary inflammation. Based on these findings, standard antibiotic therapy was initiated with cefoperazone-sulbactam. However, despite treatment, the patient's temperature continued to rise, and infection markers did not improve as expected. Cefoperazone-sulbactam was then combined with linezolid, but the results remained unsatisfactory. Antibiotic therapy was escalated to meropenem, and after detecting *Legionella*, moxifloxacin was added for targeted treatment. Despite these anti-infective interventions and improvement in infection markers, the patient's intermittent fever persisted, and her clinical condition remained complex and challenging (Figures 1 and 2).

When we were struggling to control the patient's fever, the patient's family reported the recent onset of pain in the left limbs. Given that the patient's pain likely

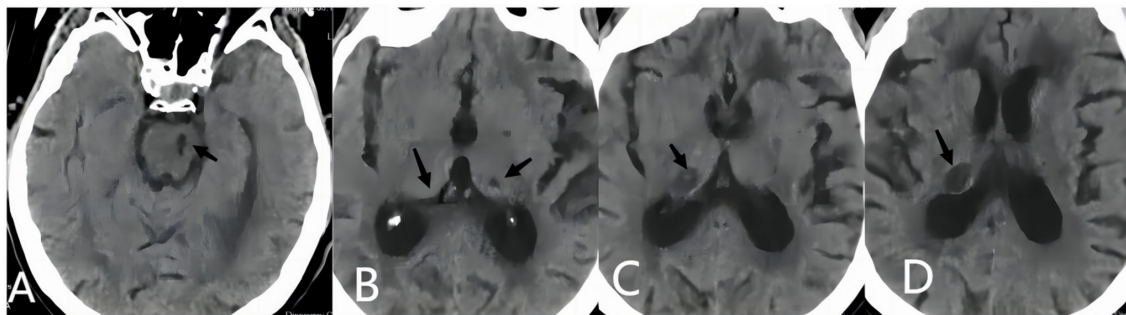


Figure 1. Clinical imaging of stroke indicators at initial presentation. (A and B) Suspected areas of ischemia and infarction are observed in both the basal ganglia, frontal and parietal lobes, the left thalamic region, and the brainstem, with associated softening. (C and D) A slightly hypodense area is visible in the right thalamic region.

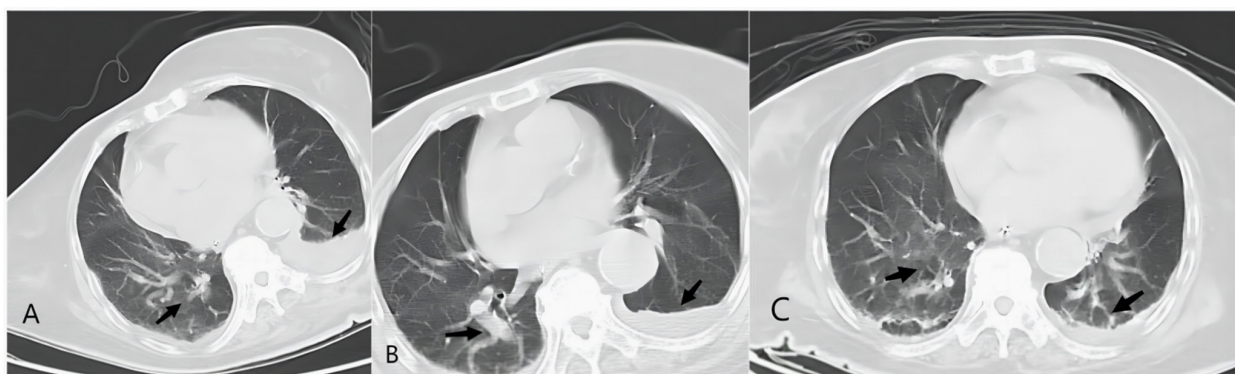


Figure 2. Imaging examinations on days 13, 17, and 25 of hospitalization. (A) Infectious lesions are considered in both lungs, with left pleural effusion and partial left lung collapse. (B) Inflammatory changes in both lungs, with partial absorption compared to the previous scan. Both pleurae are thickened, with left pleural effusion and partial left lung collapse or consolidation. (C) Inflammatory changes in both lungs. Both pleurae remain thickened, with left pleural effusion and partial left lung collapse or consolidation, showing slight improvement compared to the previous scan.

Table 1. Temperature variations following medication use during hospitalization

Pre-medication temperature (°C)	Post-medication temperature (°C)	Drugs
38-39	37.5-38.5 (+5d*)	sulperazone
	37-38.9 (+3d)	Sulperazone + linezolid
	36.5-38.5 (+5d)	Sulperazone + linezolid + azithromycin
	36.2-38.4 (+4d)	meropenem
	36.4-37.9 (+5d)	Meropenem + moxifloxacin
	36.4-38.1 (+2d)	Sulperazone + aspirin-dl-lysine
	36-36.8 (+5d)	Sulperazone + gabapentin
	36-36.9 (+10d)	Sulperazone + gabapentin + tigecycline + fluconazole
	36.1-36.8 (+8d)	Gabapentin + tigecycline + fluconazole + meropenem
	36-36.6 (+2d)	Gabapentin + tigecycline + meropenem
	36.2-36.6 (+2d)	Gabapentin + meropenem

*d: days

originated from thalamic lesion stimulation, we decided to administer gabapentin to target the neuropathic pain. The patient was initially given 0.3 g of gabapentin *via* a nasogastric tube. Unexpectedly, by 2 p.m., the patient's body temperature had dropped to 36.3°C, without the use of any other medications during this time. Over the next 29 days of treatment, gabapentin was continued to manage the patient's neuropathic pain. On the second day, the patient received 0.3 g of gabapentin twice daily *via* the nasogastric tube, and from the third day onward, the dosage was increased to 0.3 g three times daily. Encouragingly, not only did the patient's neuropathic pain improve, but her body temperature also remained consistently between 36°C and 36.9°C, with no recurrence of intermittent fever (Table 1).

In clinical practice, managing post-stroke fever involves not only providing antipyretic treatment when necessary but also collecting laboratory and imaging data to assess for the presence of infection or inflammation, as infectious fever is the most common cause in such cases. If infection is confirmed, targeted antibiotic therapy should be administered. However, if the patient's condition does not improve after the use of appropriate antibiotics, other potential causes of fever, such as drug-induced or central fever, should be considered. Central fever, primarily caused by lesions or injury to the central nervous system, can be particularly challenging to manage. In this case, despite the use of broad-spectrum antibiotics and the fact that laboratory indicators and imaging results suggested that the infection was under control, the patient's fever did not significantly improve. This led us to suspect that while the initial fever may have been related to infection, the persistent intermittent fever that followed was likely due to central factors affecting thermoregulation. Considering the location of the patient's lesion and the concurrent thalamic hemorrhage during fever episodes, we hypothesized that the primary cause of the ongoing intermittent fever was not infection or inflammation, but central fever (14-16).

Body temperature regulation is primarily managed

by the hypothalamus and brainstem, with the hypothalamus playing a central role (13). Thalamic fever refers to fever originating from thalamic lesions, as the thalamus is involved in various sensory and motor functions, as well as temperature regulation. Reviewing the patient's medical history, we suspected that the left-sided brainstem infarction may have disrupted the thermoregulatory pathways. Furthermore, the later-stage right thalamic hematoma, which extended into the ventricle, may have stimulated specific areas of the thalamus. The combined influence of these two factors likely increased neuronal excitability, enhancing the sensitivity of the thermoregulatory center to inflammatory stimuli. This heightened sensitivity could lead to significant increases in body temperature, even in response to mild external or internal stimuli.

Gabapentin, an anticonvulsant, is also used to manage neuropathic pain and certain neurological conditions. It works by modulating neural signals in the central nervous system, helping to alleviate abnormal neuronal excitability. In cases of central fever, gabapentin may help stabilize body temperature by reducing the abnormal electrical excitability in the thermoregulatory center triggered by thalamic lesions (Figure 3).

In this case, we observed that gabapentin may have potential efficacy in intervening against central or thalamic fever induced by abnormal neuronal excitation. This suggests that gabapentin could be considered as an alternative treatment when traditional antipyretic therapies fail. Although more scientific research is needed to establish a definitive link, this case highlights the importance of considering central fever in the differential diagnosis of fever in stroke patients, particularly those with complex or severe conditions, and paying close attention to lesion locations.

Funding: None.

Conflict of Interest: The authors have no conflicts of interest to disclose.

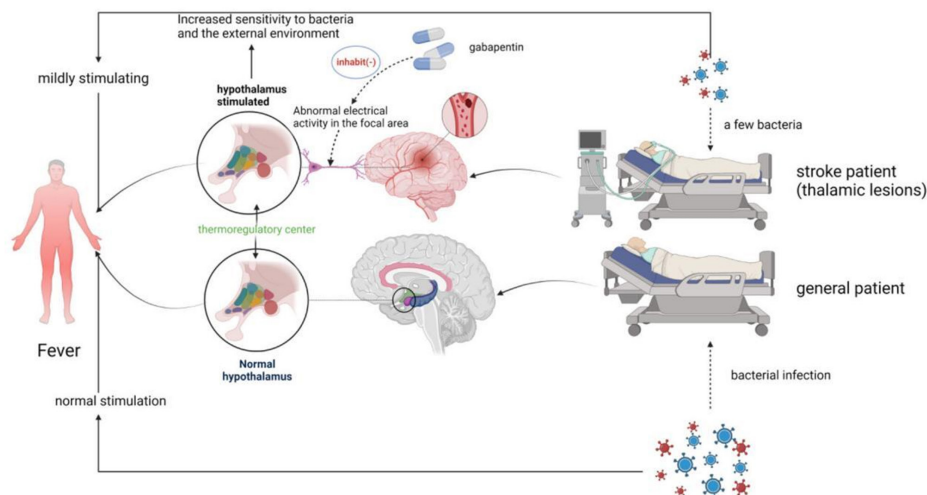


Figure 3. Central fever potential mechanisms and treatment strategies diagram.

References

- Sung CY, Lee TH, Chu NS. Central hyperthermia in acute stroke. *Eur Neurol.* 2009; 62:86-92.
- Middleton S, McElduff P, Ward J, Grimshaw JM, Dale S, D'Este C, Drury P, Griffiths R, Cheung NW, Quinn C, Evans M, Cadilhac D, Levi C. Implementation of evidence-based treatment protocols to manage fever, hyperglycaemia, and swallowing dysfunction in acute stroke (QASC): a cluster randomised controlled trial. *Lancet.* 2011; 378:1699-706.
- Stösser S, Gotthardt M, Lindner-Pfleghar B, Jüttler E, Kassubek R, Neugebauer H. Severe dysphagia predicts poststroke fever. *Stroke.* 2021; 52:2284-2289.
- Ruborg R, Gunnarsson K, Ström JO. Predictors of post-stroke body temperature elevation. *BMC Neurol.* 2017; 17:218.
- Scott RA, Rabinstein AA. Paroxysmal sympathetic hyperactivity. *Semin Neurol.* 2020; 40:485-491.
- Kim HS, Kim NY, Kim YW. Successful intrathecal baclofen therapy for intractable paroxysmal sympathetic hyperactivity in patient with pontine hemorrhage: A case report. *Clin Neuropharmacol.* 2018; 41:138-141.
- D'Eramo RE, Nadpara PA, Sandler M, Taylor PD, Brophy GM. Intravenous versus oral acetaminophen use in febrile neurocritical care patients. *Ther Hypothermia Temp Manag.* 2022; 12:155-158.
- Giaccari LG, Pace MC, Passavanti MB, Sansone P, Esposito V, Aurilio C, Pota V. Continuous intravenous low-dose diclofenac sodium to control a central fever after ischemic stroke in the intensive care unit: a case report and review of the literature. *J Med Case Rep.* 2019; 13:373.
- de Ridder IR, den Hertog HM, van Gemert HM, *et al.* PAIS 2 (Paracetamol [acetaminophen] in stroke 2): Results of a randomized, double-blind placebo-controlled clinical trial. *Stroke.* 2017; 48:977-982.
- Samudra N, Figueroa S. Intractable central hyperthermia in the setting of brainstem hemorrhage. *Ther Hypothermia Temp Manag.* 2016; 6:98-101.
- Wrotek SE, Kozak WE, Hess DC, Fagan SC. Treatment of fever after stroke: conflicting evidence. *Pharmacotherapy.* 2011; 31:1085-1091.
- Jang SH, Seo YS. Neurogenic fever due to injury of the hypothalamus in a stroke patient: Case report. *Medicine.* 2021; 100:e24053.
- Meier K, Lee K. Neurogenic fever. *J Intensive Care Med.* 2017; 32:124-129.
- Li G, Xu XY, Wang Y, Gu XB, Xue YY, Zuo L, Yu JM. Mild-to-moderate neurogenic pyrexia in acute cerebral infarction. *Eur Neurol.* 2011; 65:94-98.
- Georgilis K, Plomaritoglou A, Dafni U, Bassiakos Y, Vemmos K. Aetiology of fever in patients with acute stroke. *J Intern Med.* 1999; 246:203-209.
- Morales-Ortiz A, Jiménez-Pascual M, Pérez-Vicente JA, Monge-Arguiles A, Bautista-Prados J. Fever of central origin during stroke. *Rev Neurol.* 2001; 32:1111-1114.

Received August 1, 2024; Revised October 9, 2024; Accepted October 24, 2024.

§These authors contributed equally to this work.

*Address correspondence to:

Bangqi Wu, National Clinical Research Center for Chinese Medicine Acupuncture and Moxibustion, First Teaching Hospital of Tianjin University of Traditional Chinese Medicine, Tianjin, 300381, China.
E-mail: wbqwbq1980@outlook.com

Released online in J-STAGE as advance publication October 28, 2024.

Effect of switching from dulaglutide to tirzepatide on blood glucose and renal function

Atsushi Ishimura^{1,*}, Hiroyoshi Kumakura²

¹Division of Practical Pharmacy, Nihon Pharmaceutical University, Saitama, Japan;

²Pharmaceutical Department, Ina Hospital, Saitama, Japan.

SUMMARY The case reports a woman in her 70s, with type 2 diabetes and chronic kidney disease in G4 stage. The patient had elevated HbA1c, and she was switched from linagliptin, a dipeptidyl peptidase 4 inhibitor, to dulaglutide, a glucagon-like peptide-1 receptor agonist (GLP-1RA). Thereafter, the HbA1c level decreased; however, since the dulaglutide supply became a problem, the patient was switched to tirzepatide, a glucose-dependent insulinotropic polypeptide (GIP)/GLP-1RA. To date, no clinical studies have evaluated the efficacy and safety of switching from GLP-1RA to GIP/GLP-1RA, but we report this case because efficacy was observed in this patient. The therapeutic effects after switching to tirzepatide included decrease in HbA1c, increase in eGFR, and decrease in BUN, when compared to when dulaglutide was used. A change from dulaglutide to tirzepatide, could inhibit renal impairment progression and improve renal function.

Keywords tirzepatide, dulaglutide, chronic kidney disease

Letter to the Editor,

Diabetes mellitus is a group of metabolic diseases characterized by chronic hyperglycemia caused by insufficient insulin action. Type 2 diabetes (T2DM), accounts for about 90% of all diabetic patients. T2DM treatment requires a stepwise approach that combines diet and exercise therapy with pharmacotherapy.

Incretin-related drugs were developed because incretin, a hormone secreted by gastrointestinal endocrine cells upon ingestion of food and other factors, plays a major role in hypoglycemic effects by stimulating insulin secretion. Incretins include glucagon-like peptide-1 (GLP-1) and glucose-dependent insulinotropic polypeptide (GIP). GLP-1 in particular, has various effects, including blood glucose lowering and weight loss effects, *via* inhibition of glucagon secretion and delayed gastric emptying (1). GLP-1 receptor agonists (GLP-1RA) are recommended in major international diabetes treatment guidelines (2). Conversely, GIP has been neglected as a target for diabetes drugs due to its lack of insulin secretagogue action and concerns over weight gain due to its fat storage effect (3). However, a chimeric peptide that has elements of both GLP-1 and GIP and can activate both receptors has been demonstrated to have remarkable weight loss and blood glucose lowering effects in obese T2DM patients (4). Tirzepatide was launched as a drug that acts on both GIP and GLP-1 receptors *via* a single molecule. There are no

reports of clinical trials evaluating the efficacy and safety of switching from GLP-1RA to GIP/GLP-1RA.

We describe our experience with a patient who switched from dulaglutide (5) to tirzepatide, the most commonly used GLP-1RA in Japan, and who exhibited improvement not only in glycemic control but also in renal function values.

The case is a woman in her 70s, with type 2 diabetes and chronic kidney disease at G4 stage. She refuses to receive nutritional guidance and does not stop eating between meals. Because of increased HbA1c and decreased renal function, she was switched from linagliptin of dipeptidyl peptidase 4 inhibitor to dulaglutide. The HbA1c level decreased; however, due to dulaglutide supply challenges, the patient was switched to tirzepatide. Figure 1 shows the changes in HbA1c, eGFR, and BUN from the start of dulaglutide to after change to tirzepatide. Following change to tirzepatide, HbA1c and eGFR and BUN values improved, when compared to when dulaglutide was used. After the change to tirzepatide, treatment has continued without any significant side effects. The patient's informed consent obtained and was given in writing.

Diabetes is considered a risk factor for chronic kidney disease, and diabetic nephropathy is a major cause of dialysis induction in many countries. The development of diabetic nephropathy is not only a risk factor for end-stage renal disease (ESRD) and the introduction of dialysis, but

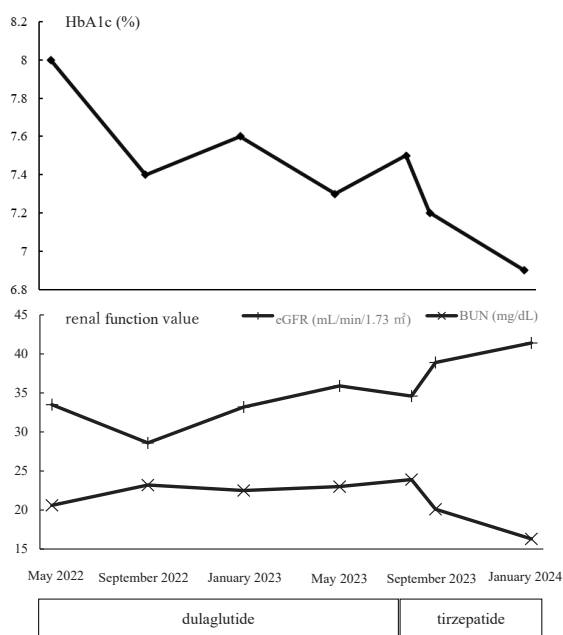


Figure 1. Course of treatment after dulaglutide initiation and change to tirzepatide.

also increases the rate of cardiovascular events and all-cause mortality due to decreased eGFR (6,7). Therefore, delaying progression to ESRD and introduction of dialysis is considered a key strategy for the maintenance of patient quality of life but also life support. Dulaglutide, a GLP-1RA, reportedly increases eGFR in addition to decreasing HbA1c and weight loss (8). However, when patients were switched to tirzepatide, a GIP/GLP-1RA, there was a further decrease in HbA1c, an increase in eGFR and a decrease in BUN compared to when dulaglutide was used. In a recent clinical trial in obese or associated overweight patients, tirzepatide was shown to reduce body weight and other cardio-renal risk factors (blood pressure, low-density lipoprotein cholesterol, glycated hemoglobin, and albuminuria) and to potentially prevent chronic kidney disease (9). However, the results were not reported when switching from GLP-1RA to GIP/GLP-1RA. The cases suggest that tirzepatide is more effective than dulaglutide in controlling blood glucose and preventing renal impairment progression or improving renal function. Dulaglutide, as a once-weekly formulation, has been reported to have a higher retention rate than the daily dosing formulation (10). Tirzepatide, similar to dulaglutide, is a once-weekly formulation; therefore, a high continuation rate can be expected. Furthermore, while changes in self-injection formulations, such as insulin and GLP-1RA, may involve issues such as operability due to changes in injectors, the injector for both dulaglutide and tirzepatide is the same, Ateos®. Therefore, there are no concerns regarding the operability of the injector for the patient following drug change.

Finally, GLP-1RA have different indications for patients with impaired renal function and should be used according to renal function as well. Although dulaglutide

has no restrictions in the package insert, its clinical results in patients with severe renal dysfunction are limited, and careful administration is advised. A change from dulaglutide to tirzepatide, could inhibit the progression of renal impairment and improve renal function.

Funding: None.

Conflict of Interest: The authors have no conflicts of interest to disclose.

References

1. Nauck MA, Quast DR, Wefers J, Meier JJ. GLP-1 receptor agonists in the treatment of type 2 diabetes - state-of-the-art. *Mol Metab.* 2021; 46:101102.
2. Kamata M, Kubota A, Shikishima T, Inoue A, Kaneshige S, Nomiyama T, Ogata K, Yanase T, Kamimura H. Evaluation of the safety and efficacy of change to dulaglutide (a once-weekly GLP-1 receptor agonist). *Jpn J Pharm Diabetes.* 2017; 6:193-200.
3. Bailey CJ. GIP analogues and the treatment of obesity-diabetes. *Peptides.* 2020; 125:170202.
4. Holst JJ, Rosenkilde MM. GIP as a therapeutic target in diabetes and obesity: Insight from incretin co-agonists. *J Clin Endocrinol Metab.* 2020; 105:e2710-2716.
5. Ishimura A, Takizawa Y. Glucagon-like peptide-1 (GLP-1) receptor agonist usage and safety study. *Apra.* 2024; 19:36-42.
6. Fox CS, Matsushita K, Woodward M, *et al.* Associations of kidney disease measures with mortality and end-stage renal disease in individuals with and without diabetes: A meta-analysis. *Lancet.* 2012; 380:1662-1673.
7. Ninomiya T, Perkovic V, de Galan BE, *et al.* Albuminuria and kidney function independently predict cardiovascular and renal outcomes in diabetes. *J Am Soc Nephrol.* 2009; 20:1813-1821.
8. Ishigo T, Kondo F, Tateishi R, Nonoyama M, Fujii S, Kimyo T, Nakata H, Noda N, Miyamoto A. Effects of dulaglutide on glucose control and renal function. *Jpn J Nephrol Pharmacother.* 2018; 7:201-209.
9. Bosch C, Carriazo S, Soler MJ, Ortiz A, Fernandez-Fernandez B. Tirzepatide and prevention of chronic kidney disease. *Clin Kidney J.* 2022; 16:797-808.
10. Alatorre C, Fernández Landó L, Yu M, Brown K, Montejano L, Juneau P, Mody R, Swindle R. Treatment patterns in patients with type 2 diabetes mellitus treated with glucagon-like peptide-1 receptor agonists: Higher adherence and persistence with dulaglutide compared with once-weekly exenatide and liraglutide. *Diabetes Obes Metab.* 2017; 19:953-961.

Received August 9, 2024; Revised September 24, 2024; Accepted October 25, 2024.

*Address correspondence to:

Atsushi Ishimura, Division of Practical Pharmacy, Nihon Pharmaceutical University, 10281, Komuro, Ina-machi, Kitaadachi-gun, Saitama 362-0806, Japan.
E-mail: atsushiishimura@nichiyaku.ac.jp

Released online in J-STAGE as advance publication October 28, 2024.



Drug Discoveries & Therapeutics

Guide for Authors

1. Scope of Articles

Drug Discoveries & Therapeutics (Print ISSN 1881-7831, Online ISSN 1881-784X) welcomes contributions in all fields of pharmaceutical and therapeutic research such as medicinal chemistry, pharmacology, pharmaceutical analysis, pharmaceuticals, pharmaceutical administration, and experimental and clinical studies of effects, mechanisms, or uses of various treatments. Studies in drug-related fields such as biology, biochemistry, physiology, microbiology, and immunology are also within the scope of this journal.

2. Submission Types

Original Articles should be well-documented, novel, and significant to the field as a whole. An Original Article should be arranged into the following sections: Title page, Abstract, Introduction, Materials and Methods, Results, Discussion, Acknowledgments, and References. Original articles should not exceed 5,000 words in length (excluding references) and should be limited to a maximum of 50 references. Articles may contain a maximum of 10 figures and/or tables. Supplementary Data are permitted but should be limited to information that is not essential to the general understanding of the research presented in the main text, such as unaltered blots and source data as well as other file types.

Brief Reports definitively documenting either experimental results or informative clinical observations will be considered for publication in this category. Brief Reports are not intended for publication of incomplete or preliminary findings. Brief Reports should not exceed 3,000 words in length (excluding references) and should be limited to a maximum of 4 figures and/or tables and 30 references. A Brief Report contains the same sections as an Original Article, but the Results and Discussion sections should be combined.

Reviews should present a full and up-to-date account of recent developments within an area of research. Normally, reviews should not exceed 8,000 words in length (excluding references) and should be limited to a maximum of 10 figures and/or tables and 100 references. Mini reviews are also accepted, which should not exceed 4,000 words in length (excluding references) and should be limited to a maximum of 5 figures and/or tables and 50 references.

Policy Forum articles discuss research and policy issues in areas related to life science such as public health, the medical care system, and social science and may address governmental issues at district, national, and international levels of discourse. Policy Forum articles should not exceed 3,000 words in length (excluding references) and should be limited to a maximum of 5 figures and/or tables and 30 references.

Case Reports should be detailed reports of the symptoms, signs, diagnosis, treatment, and follow-up of an individual patient. Case reports may contain a demographic profile of the patient but usually describe an unusual or novel occurrence. Unreported or unusual side effects or adverse interactions involving medications will also be considered. Case Reports should not exceed 3,000 words in length (excluding references).

Communications are short, timely pieces that spotlight new research findings or policy issues of interest to the field of global health and medical practice that are of immediate importance. Depending on their content, Communications will be published as "Comments" or

"Correspondence". Communications should not exceed 1,500 words in length (excluding references) and should be limited to a maximum of 2 figures and/or tables and 20 references.

Editorials are short, invited opinion pieces that discuss an issue of immediate importance to the fields of global health, medical practice, and basic science oriented for clinical application. Editorials should not exceed 1,000 words in length (excluding references) and should be limited to a maximum of 10 references. Editorials may contain one figure or table.

News articles should report the latest events in health sciences and medical research from around the world. News should not exceed 500 words in length.

Letters should present considered opinions in response to articles published in *Drug Discoveries & Therapeutics* in the last 6 months or issues of general interest. Letters should not exceed 800 words in length and may contain a maximum of 10 references. Letters may contain one figure or table.

3. Editorial Policies

For publishing and ethical standards, *Drug Discoveries & Therapeutics* follows the Recommendations for the Conduct, Reporting, Editing, and Publication of Scholarly Work in Medical Journals issued by the International Committee of Medical Journal Editors (ICMJE, <https://icmje.org/recommendations>), and the Principles of Transparency and Best Practice in Scholarly Publishing jointly issued by the Committee on Publication Ethics (COPE, <https://publicationethics.org/resources/guidelines-new/principles-transparency-and-best-practice-scholarly-publishing>), the Directory of Open Access Journals (DOAJ, <https://doaj.org/apply/transparency>), the Open Access Scholarly Publishers Association (OASPA, <https://oaspa.org/principles-of-transparency-and-best-practice-in-scholarly-publishing-4>), and the World Association of Medical Editors (WAME, <https://wame.org/principles-of-transparency-and-best-practice-in-scholarly-publishing>).

Drug Discoveries & Therapeutics will perform an especially prompt review to encourage innovative work. All original research will be subjected to a rigorous standard of peer review and will be edited by experienced copy editors to the highest standards.

Ethical Approval of Studies and Informed Consent: For all manuscripts reporting data from studies involving human participants or animals, formal review and approval, or formal review and waiver, by an appropriate institutional review board or ethics committee is required and should be described in the Methods section. When your manuscript contains any case details, personal information and/or images of patients or other individuals, authors must obtain appropriate written consent, permission and release in order to comply with all applicable laws and regulations concerning privacy and/or security of personal information. The consent form needs to comply with the relevant legal requirements of your particular jurisdiction, and please do not send signed consent form to *Drug Discoveries & Therapeutics* to respect your patient's and any other individual's privacy. Please instead describe the information clearly in the Methods (patient consent) section of your manuscript while retaining copies of the signed forms in the event they should be needed. Authors should also state that the study conformed to the provisions of the Declaration of Helsinki (as revised in 2013, <https://wma.net/what-we-do/medical-ethics/declaration-of-helsinki>). When reporting experiments on animals, authors should indicate whether the institutional and national guide for the care and use of laboratory animals was followed.

Reporting Clinical Trials: The ICMJE (<https://icmje.org/recommendations/browse/publishing-and-editorial-issues/clinical-trial-registration.html>) defines a clinical trial as any research project that prospectively assigns people or a group of people to an intervention, with or without concurrent comparison or control groups, to study the relationship between a health-related intervention and a health outcome. Registration of clinical trials in a public trial registry

at or before the time of first patient enrollment is a condition of consideration for publication in *Drug Discoveries & Therapeutics*, and the trial registration number will be published at the end of the Abstract. The registry must be independent of for-profit interest and publicly accessible. Reports of trials must conform to CONSORT 2010 guidelines (<https://consort-statement.org/consort-2010>). Articles reporting the results of randomized trials must include the CONSORT flow diagram showing the progress of patients throughout the trial.

Conflict of Interest: All authors are required to disclose any actual or potential conflict of interest including financial interests or relationships with other people or organizations that might raise questions of bias in the work reported. If no conflict of interest exists for each author, please state "There is no conflict of interest to disclose".

Submission Declaration: When a manuscript is considered for submission to *Drug Discoveries & Therapeutics*, the authors should confirm that 1) no part of this manuscript is currently under consideration for publication elsewhere; 2) this manuscript does not contain the same information in whole or in part as manuscripts that have been published, accepted, or are under review elsewhere, except in the form of an abstract, a letter to the editor, or part of a published lecture or academic thesis; 3) authorization for publication has been obtained from the authors' employer or institution; and 4) all contributing authors have agreed to submit this manuscript.

Initial Editorial Check: Immediately after submission, the journal's managing editor will perform an initial check of the manuscript. A suitable academic editor will be notified of the submission and invited to check the manuscript and recommend reviewers. Academic editors will check for plagiarism and duplicate publication at this stage. The journal has a formal recusal process in place to help manage potential conflicts of interest of editors. In the event that an editor has a conflict of interest with a submitted manuscript or with the authors, the manuscript, review, and editorial decisions are managed by another designated editor without a conflict of interest related to the manuscript.

Peer Review: *Drug Discoveries & Therapeutics* operates a single-anonymized review process, which means that reviewers know the names of the authors, but the authors do not know who reviewed their manuscript. All articles are evaluated objectively based on academic content. External peer review of research articles is performed by at least two reviewers, and sometimes the opinions of more reviewers are sought. Peer reviewers are selected based on their expertise and ability to provide quality, constructive, and fair reviews. For research manuscripts, the editors may, in addition, seek the opinion of a statistical reviewer. Every reviewer is expected to evaluate the manuscript in a timely, transparent, and ethical manner, following the COPE guidelines (https://publicationethics.org/files/cope-ethical-guidelines-peer-reviewers-v2_0.pdf). We ask authors for sufficient revisions (with a second round of peer review, when necessary) before a final decision is made. Consideration for publication is based on the article's originality, novelty, and scientific soundness, and the appropriateness of its analysis.

Suggested Reviewers: A list of up to 3 reviewers who are qualified to assess the scientific merit of the study is welcomed. Reviewer information including names, affiliations, addresses, and e-mail should be provided at the same time the manuscript is submitted online. Please do not suggest reviewers with known conflicts of interest, including participants or anyone with a stake in the proposed research; anyone from the same institution; former students, advisors, or research collaborators (within the last three years); or close personal contacts. Please note that the Editor-in-Chief may accept one or more of the proposed reviewers or may request a review by other qualified persons.

Language Editing: Manuscripts prepared by authors whose native language is not English should have their work proofread by a native English speaker before submission. If not, this might delay the publication of your manuscript in *Drug Discoveries & Therapeutics*.

The Editing Support Organization can provide English

proofreading, Japanese-English translation, and Chinese-English translation services to authors who want to publish in *Drug Discoveries & Therapeutics* and need assistance before submitting a manuscript. Authors can visit this organization directly at <https://www.iacmhr.com/iac-eso/support.php?lang=en>. IAC-ESO was established to facilitate manuscript preparation by researchers whose native language is not English and to help edit works intended for international academic journals.

Copyright and Reuse: Before a manuscript is accepted for publication in *Drug Discoveries & Therapeutics*, authors will be asked to sign a transfer of copyright agreement, which recognizes the common interest that both the journal and author(s) have in the protection of copyright. We accept that some authors (e.g., government employees in some countries) are unable to transfer copyright. A JOURNAL PUBLISHING AGREEMENT (JPA) form will be e-mailed to the authors by the Editorial Office and must be returned by the authors by mail, fax, or as a scan. Only forms with a hand-written signature from the corresponding author are accepted. This copyright will ensure the widest possible dissemination of information. Please note that the manuscript will not proceed to the next step in publication until the JPA Form is received. In addition, if excerpts from other copyrighted works are included, the author(s) must obtain written permission from the copyright owners and credit the source(s) in the article.

4. Cover Letter

The manuscript must be accompanied by a cover letter prepared by the corresponding author on behalf of all authors. The letter should indicate the basic findings of the work and their significance. The letter should also include a statement affirming that all authors concur with the submission and that the material submitted for publication has not been published previously or is not under consideration for publication elsewhere. The cover letter should be submitted in PDF format. For an example of Cover Letter, please visit: Download Centre (<https://www.ddtjournal.com/downcentre>).

5. Submission Checklist

The Submission Checklist should be submitted when submitting a manuscript through the Online Submission System. Please visit Download Centre (<https://www.ddtjournal.com/downcentre>) and download the Submission Checklist file. We recommend that authors use this checklist when preparing your manuscript to check that all the necessary information is included in your article (if applicable), especially with regard to Ethics Statements.

6. Manuscript Preparation

Manuscripts are suggested to be prepared in accordance with the "Recommendations for the Conduct, Reporting, Editing, and Publication of Scholarly Work in Medical Journals", as presented at <http://www.ICMJE.org>.

Manuscripts should be written in clear, grammatically correct English and submitted as a Microsoft Word file in a single-column format. Manuscripts must be paginated and typed in 12-point Times New Roman font with 24-point line spacing. Please do not embed figures in the text. Abbreviations should be used as little as possible and should be explained at first mention unless the term is a well-known abbreviation (e.g. DNA). Single words should not be abbreviated.

Title page: The title page must include 1) the title of the paper (Please note the title should be short, informative, and contain the major key words); 2) full name(s) and affiliation(s) of the author(s), 3) abbreviated names of the author(s), 4) full name, mailing address, telephone/fax numbers, and e-mail address of the corresponding author; 5) author contribution statements to specify the individual contributions of all authors to this manuscript, and 6) conflicts of interest (if you have an actual or potential conflict of interest to disclose, it must be included as a footnote on the title page of the manuscript; if no conflict of interest

exists for each author, please state "There is no conflict of interest to disclose").

Abstract: The abstract should briefly state the purpose of the study, methods, main findings, and conclusions. For article types including Original Article, Brief Report, Review, Policy Forum, and Case Report, a one-paragraph abstract consisting of no more than 250 words must be included in the manuscript. For Communications, Editorials, News, or Letters, a brief summary of main content in 150 words or fewer should be included in the manuscript. For articles reporting clinical trials, the trial registration number should be stated at the end of the Abstract. Abbreviations must be kept to a minimum and non-standard abbreviations explained in brackets at first mention. References should be avoided in the abstract. Three to six key words or phrases that do not occur in the title should be included in the Abstract page.

Introduction: The introduction should provide sufficient background information to make the article intelligible to readers in other disciplines and sufficient context clarifying the significance of the experimental findings.

Materials/Patients and Methods: The description should be brief but with sufficient detail to enable others to reproduce the experiments. Procedures that have been published previously should not be described in detail but appropriate references should simply be cited. Only new and significant modifications of previously published procedures require complete description. Names of products and manufacturers with their locations (city and state/country) should be given and sources of animals and cell lines should always be indicated. All clinical investigations must have been conducted in accordance with the Declaration of Helsinki (as revised in 2013, <https://wma.net/what-we-do/medical-ethics/declaration-of-helsinki>). All human and animal studies must have been approved by the appropriate institutional review board(s) and a specific declaration of approval must be made within this section.

Results: The description of the experimental results should be succinct but in sufficient detail to allow the experiments to be analyzed and interpreted by an independent reader. If necessary, subheadings may be used for an orderly presentation. All Figures and Tables should be referred to in the text in order, including those in the Supplementary Data.

Discussion: The data should be interpreted concisely without repeating material already presented in the Results section. Speculation is permissible, but it must be well-founded, and discussion of the wider implications of the findings is encouraged. Conclusions derived from the study should be included in this section.

Acknowledgments: All funding sources (including grant identification) should be credited in the Acknowledgments section. Authors should also describe the role of the study sponsor(s), if any, in study design; in the collection, analysis, and interpretation of data; in the writing of the report; and in the decision to submit the paper for publication. If the funding source had no such involvement, the authors should so state.

In addition, people who contributed to the work but who do not meet the criteria for authors should be listed along with their contributions.

References: References should be numbered in the order in which they appear in the text. Citing of unpublished results, personal communications, conference abstracts, and theses in the reference list is not recommended but these sources may be mentioned in the text. In the reference list, cite the names of all authors when there are fifteen or fewer authors; if there are sixteen or more authors, list the first three followed by *et al.* Names of journals should be abbreviated in the style used in *PubMed*. Authors are responsible for the accuracy of the references. The EndNote Style of *Drug Discoveries & Therapeutics* could be downloaded at **EndNote** (https://www.ddtjournal.com/examples/Drug_Discoveries_Therapeutics.ens).

Examples are given below:

Example 1 (Sample journal reference):

Nakata M, Tang W. Japan-China Joint Medical Workshop on Drug Discoveries and Therapeutics 2008: The need of Asian pharmaceutical researchers' cooperation. *Drug Discov Ther.* 2008; 2:262-263.

Example 2 (Sample journal reference with more than 15 authors):

Darby S, Hill D, Auvinen A, *et al.* Radon in homes and risk of lung cancer: Collaborative analysis of individual data from 13 European case-control studies. *BMJ.* 2005; 330:223.

Example 3 (Sample book reference):

Shalev AY. Post-traumatic stress disorder: Diagnosis, history and life course. In: *Post-traumatic Stress Disorder, Diagnosis, Management and Treatment* (Nutt DJ, Davidson JR, Zohar J, eds.). Martin Dunitz, London, UK, 2000; pp. 1-15.

Example 4 (Sample web page reference):

World Health Organization. The World Health Report 2008 – primary health care: Now more than ever. <https://apps.who.int/iris/handle/10665/43949> (accessed September 23, 2022).

Tables: All tables should be prepared in Microsoft Word or Excel and should be arranged at the end of the manuscript after the References section. Please note that tables should not in image format. All tables should have a concise title and should be numbered consecutively with Arabic numerals. If necessary, additional information should be given below the table.

Figure Legend: The figure legend should be typed on a separate page of the main manuscript and should include a short title and explanation. The legend should be concise but comprehensive and should be understood without referring to the text. Symbols used in figures must be explained. Any individually labeled figure parts or panels (A, B, *etc.*) should be specifically described by part name within the legend.

Figure Preparation: All figures should be clear and cited in numerical order in the text. Figures must fit a one- or two-column format on the journal page: 8.3 cm (3.3 in.) wide for a single column, 17.3 cm (6.8 in.) wide for a double column; maximum height: 24.0 cm (9.5 in.). Please make sure that artwork files are in an acceptable format (TIFF or JPEG) at minimum resolution (600 dpi for illustrations, graphs, and annotated artwork, and 300 dpi for micrographs and photographs). Please provide all figures as separate files. Please note that low-resolution images are one of the leading causes of article resubmission and schedule delays.

Units and Symbols: Units and symbols conforming to the International System of Units (SI) should be used for physicochemical quantities. Solidus notation (*e.g.* mg/kg, mg/mL, mol/mm²/min) should be used. Please refer to the SI Guide www.bipm.org/en/si/ for standard units.

Supplemental data: Supplemental data might be useful for supporting and enhancing your scientific research and *Drug Discoveries & Therapeutics* accepts the submission of these materials which will be only published online alongside the electronic version of your article. Supplemental files (figures, tables, and other text materials) should be prepared according to the above guidelines, numbered in Arabic numerals (*e.g.*, Figure S1, Figure S2, and Table S1, Table S2) and referred to in the text. All figures and tables should have titles and legends. All figure legends, tables and supplemental text materials should be placed at the end of the paper. Please note all of these supplemental data should be provided at the time of initial submission and note that the editors reserve the right to limit the size

and length of Supplemental Data.

7. Online Submission

Manuscripts should be submitted to *Drug Discoveries & Therapeutics* online at <https://www.ddtjournal.com/login>. Receipt of your manuscripts submitted online will be acknowledged by an e-mail from Editorial Office containing a reference number, which should be used in all future communications. If for any reason you are unable to submit a file online, please contact the Editorial Office by e-mail at office@ddtjournal.com

8. Accepted Manuscripts

Page Charge: Page charges will be levied on all manuscripts accepted for publication in *Drug Discoveries & Therapeutics* (Original Articles / Brief Reports / Reviews / Policy Forum / Communications: \$140 per page for black white pages, \$340 per page for color pages; News / Letters: a total cost of \$600). Under exceptional circumstances, the author(s) may apply to the editorial office for a waiver of the publication charges by stating the reason in the Cover Letter when the

manuscript online.

Misconduct: *Drug Discoveries & Therapeutics* takes seriously all allegations of potential misconduct and adhere to the ICMJE Guideline (<https://icmje.org/recommendations>) and COPE Guideline (https://publicationethics.org/files/Code_of_conduct_for_journal_editors.pdf). In cases of suspected research or publication misconduct, it may be necessary for the Editor or Publisher to contact and share submission details with third parties including authors' institutions and ethics committees. The corrections, retractions, or editorial expressions of concern will be performed in line with above guidelines.

(As of December 2022)

Drug Discoveries & Therapeutics
Editorial and Head Office
Pearl City Koishikawa 603,
2-4-5 Kasuga, Bunkyo-ku,
Tokyo 112-0003, Japan.
E-mail: office@ddtjournal.com

